

Organotin assemblies containing Sn–O bonds

Vadapalli Chandrasekhar*, Selvarajan Nagendran, Viswanathan Baskar

Department of Chemistry, Indian Institute of Technology, Kanpur 208 016, India

Received 1 October 2001; accepted 22 January 2002

Contents

Abstract	1
1. Introduction	1
2. Triorganotin derivatives	2
2.1 Discrete structures	4
2.2 Chain structures	5
3. Diorganotin derivatives	11
3.1 Diorganotin oxides $[R_2SnO]_n$ and related compounds	11
3.2 Tetraorganodistannoxanes and related systems	14
3.3 Alkyl bridged double and triple ladders	17
3.4 Triflic acid mediated synthesis of four-membered $[Sn-O]_2$ rings and related systems	20
3.5 Reaction of R_2SnO with organoboronic acids	24
3.6 Reactions of R_2SnO with carboxylic acids	26
3.6.1 $(n-Bu_2SnO_2CCl_3)_2(\mu_2-OH)(O_2CCl_3)$	29
3.6.2 $[n-Bu_2Sn(pyridine-2-phosphonate-6-carboxylate)]_2$	29
3.6.3 $\{[(PhCH_2)_2Sn(O_2P(c-Hex)_2)(c-Hex)_2PO_2H]\}$	30
3.6.4 $\{[n-Bu_2Sn(O_2P(OH)R)]_2(O_3PMe)\}$	33
3.7 Reactions of R_2SnO with salicylaldehyde	34
4. Monoorganotin derivatives	36
4.1 Hydrolysis of $RSnCl_3$	36
4.2 $(RSn)_{12}$ oxo hydroxo cages and related systems	39
4.3 Reactions of $RSn(O)OH$ with carboxylic or phosphorus based acids	39
4.4 Other stannoxanes	44
5. Conclusions	45
Acknowledgements	48
References	49

Abstract

This review deals with the recent progress in the area of organotin assemblies that contain Sn–O bonds. Various kinds of tri-, di- and monoorganotin compounds are described in terms of their preparation by methods such as hydrolysis of organotin halides, reactions of suitable organotin compounds with various kinds of substrates such as carboxylic acids, sulfonic acids, oxide transfer reagents etc. The structural characterization of these compounds by the use of ^{119}Sn -NMR, ^{119}Sn Mössbauer and X-ray crystallography is presented in considerable detail. The amazing structural diversity present in this family of compounds is discussed. © 2002 Elsevier Science B.V. All rights reserved.

Keywords: Stannoxanes; Organotin compound; Hydrolysis

1. Introduction

In recent years there has been considerable interest in organotin compounds. This is because of several reasons. Many organotin compounds are biologically

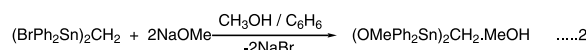
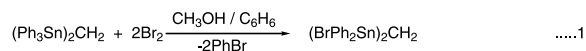
* Corresponding author

E-mail address: vc@iitk.ac.in (V. Chandrasekhar).

active [1,2]. The triorganotin compounds, R_3SnX have been known for several years as having a specific action on mitochondrial oxidative phosphorylation; the activity is independent of the X group but dependent on the R group [3]. Thus when $R = Me$, Et or n -Pr the compounds are most toxic towards mammals while when $R = n$ -octyl the compound has very low toxicity. Similarly aquatic organisms such as fish, molluscs, crustaceans or algae are sensitive to tri n -butyltin, triphenyltin and tricyclohexyltin compounds leading to the incorporation of these triorganotin units in anti-fouling paints for marine transport vessels [4]. In recent years many triorgano- and diorganotin compounds have been tested for their in vitro activity against a large variety of tumor lines and have been found to be as effective or better than traditional heavy metal anti-cancer drugs such as *cis*-platin [5–8]. In addition to their biological activity, organotin compounds have been used as reagents or catalysts in organic reactions [9–12]. Recently, several organostannoxanes have been shown to be extremely versatile catalysts for transesterification reactions [13–15]. Another important industrial use of organotin compounds is in the stabilization of PVC [4]. In addition to the aforesaid applications organotin compounds are also of interest in view of the considerable structural diversity that they possess. This aspect has been attracting the attention of a number of researchers and a multitude of structural types have been discovered [16]. This review will focus on the recent developments of this latter aspect. The emphasis will be on organotin assemblies containing Sn–O bonds. Recently, an excellent critical review has appeared on stannasiloxanes [17]. Hence these compounds are not discussed in this review. Also the phosphorus acid based organotin compounds are not discussed here in much detail since these have also been recently covered [18]. The literature on organotin chemistry has been periodically reviewed in the form of monographs or critical review articles [5,13,16–27]. All the X-ray diagrams discussed in the present review have been drawn with the DIAMOND program [28] using the fractional coordinates, which have been either published or obtained from Cambridge Crystallographic Data Base [29]. In all of these diagrams hydrogen atoms have not been included unless mentioned.

2. Triorganotin derivatives

One of the simplest ways of preparing triorganotin compounds containing Sn–O bonds is by the hydrolysis of the corresponding halides. Compounds such as Me_3SnOH , Ph_3SnOH and c -Hex $_3SnOH$ can be isolated in the hydroxy forms. Others undergo spontaneous dehydration to afford the bis(triorganotin)oxides, $R_3Sn-O-SnR_3$ [30]. X-ray structural investigations of



Scheme 1.

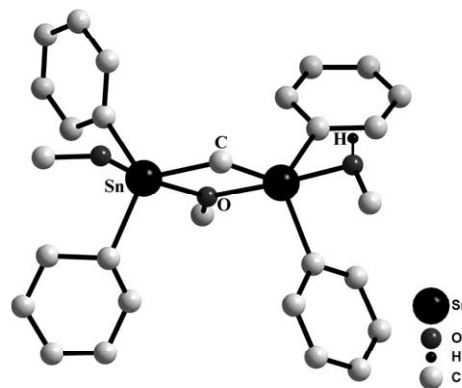
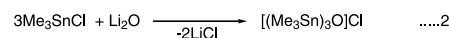
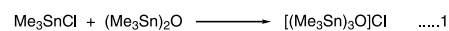


Fig. 1. The structure of $Ph_2Sn(OCH_3)(\mu-CH_2)(\mu-OCH_3)SnPh_2(CH_3OH)$ [36].

hydroxides such as Me_3SnOH [31] and Ph_3SnOH [32] show that these compounds possess polymeric structures in the solid-state with the oxygen atom functioning as a bridging ligand between neighboring triorganotin units. In such structures the local coordination environment around tin is trigonal-bipyramidal; the alkyl or aryl substituents on tin occupying the equatorial positions and the oxygen atoms taking up the axial positions. Such associated structures are also found for the corresponding alkoxides, Me_3SnOMe [33] and Ph_3SnOi -Bu [34]. A modification of this structural motif has been reported recently. Thus a methylene bridged alkoxide $H_2C(SnPh_2OMe)_2 \cdot MeOH$ has been prepared [35] (Scheme 1) and its X-ray structure solved [36]. The structure of this compound reveals the presence of two pentacoordinated tin atoms, which are linked by the methylene group and one bridging methoxy group. This leads to the formation of a four-membered Sn_2CO ring (Fig. 1). Recently, Roesky and coworkers have reported an interesting oxonium ion $[(Me_3Sn)_3O]Cl$ that can be prepared by two synthetic routes (Scheme 2) [37]. The structure of this compound consists of trigonal-planar positively charged oxygen attached to three $SnMe_3$ groups. The coordination environment around tin is distorted trigonal-bipyramidal with the three methyl substituents occupying the equatorial positions and the oxygen and a chloride ion occupying the axial positions (Fig. 2). In the crystal structure the chloride acts as



Scheme 2.

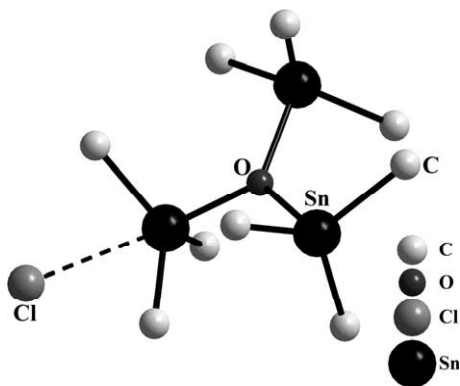


Fig. 2. The local coordination environment around tin and oxygen in $[(\text{Me}_3\text{Sn})_3\text{O}][\text{Cl}]$ showing a distorted trigonal-bipyramidal geometry around tin and a trigonal-planar geometry around oxygen [37].

bridging ligand (μ_3) being coordinated to three tin atoms to generate an infinite two-dimensional hexagonal graphite like structure; each hexagon is made up of a 12-membered $\text{Sn}_6\text{Cl}_3\text{O}_3$ ring (Fig. 3).

Among the triorganotin compounds containing Sn–O bonds the most ubiquitous are the carboxylates $\text{R}_3\text{SnO}_2\text{CR}'$ [19–21]. Examples of such compounds anchored to polymeric supports are also known [38]. Although the corresponding compounds formed in the reactions with the phosphorus-based acids, $\text{R}_2\text{P}(\text{O})(\text{OH})$ or $\text{R}_2\text{P}(\text{S})(\text{OH})$ are known these are not covered here as this aspect has been recently reviewed [18]. Also, recently a seleninic acid analogue $\text{Ph}_3\text{SnO}_2\text{SePh}$ has been reported [39]. The solid-state structure of this compound shows that the PhSeO_2 motif functions as an intermolecular bridging ligand connecting successive

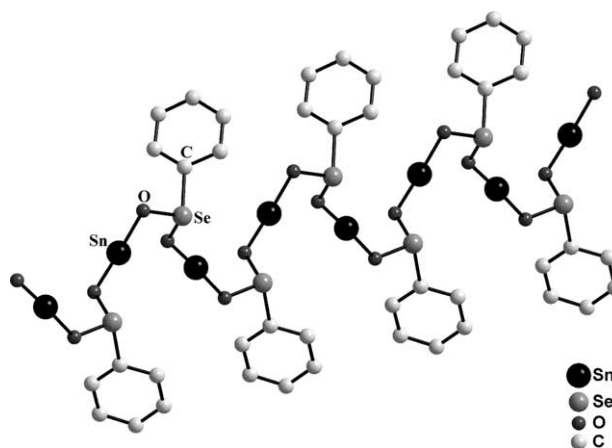
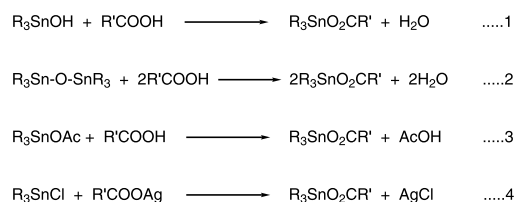


Fig. 4. The structure of $\text{Ph}_3\text{SnO}_2\text{SePh}$ showing a polymeric chain (the aryl substituents on tin have been omitted for clarity) [39].



Scheme 3.

Ph_3Sn units to afford a polymeric structure (Fig. 4) analogous to polymeric structures found for many $\text{R}_3\text{SnO}_2\text{CR}'$ (vide infra).

Triorganotin carboxylates $\text{R}_3\text{SnO}_2\text{CR}'$ are readily synthesized by several synthetic routes (Scheme 3). Several types of aliphatic and aromatic carboxylic acids

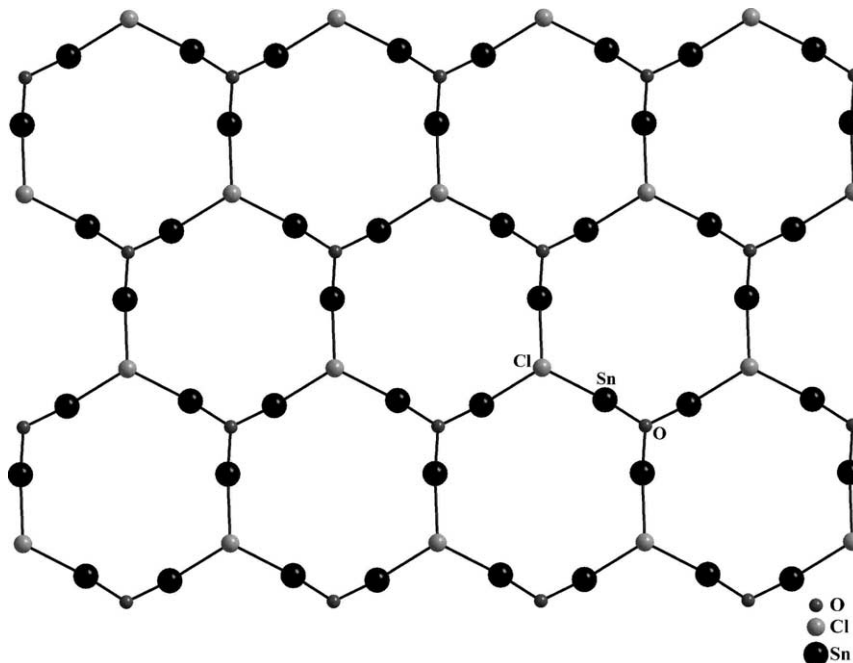


Fig. 3. The graphite like associated sheet structure of $[(\text{Me}_3\text{Sn})_3\text{O}][\text{Cl}]$ (the methyl groups on tin have been omitted for clarity) [37].

have been used and a large variety of triorganotin carboxylates have been synthesized. Indeed, the above reactions seem to be extremely general and there does not appear to be any instance where a particular carboxylic acid failed to react with the triorganotin precursor.

The X-ray crystal structures of several triorganotin carboxylates have been elucidated. This aspect has been quite exhaustively and critically dealt [20,21]. Only the important structural types will be discussed here in. Also, carboxylates obtained from dicarboxylic acids are not dealt here. An analysis of the various X-ray crystal structures of triorganotin carboxylates reveals that there are two major structural types: (a) discrete; and (b) polymeric structures (Fig. 5). For certain carboxylates such as $\text{Me}_3\text{SnO}_2\text{C}-\text{C}_6\text{H}_4-2-\text{NH}_2$ [40], $\text{Me}_3\text{SnO}_2\text{C}-\text{C}_6\text{H}_4-2-\text{NHMe}$ [40], $\text{Me}_3\text{SnO}_2\text{C}-\text{CH}_2-\text{NH}_2$ [41] and $\text{Me}_3\text{SnO}_2\text{CC}_6\text{H}_4-2-\text{OH}$ [40] although polymeric structures are formed in the solid-state, the chains are propagated as a result of interaction with the substituent on the aromatic carboxylic acid (Fig. 6). Such polymeric structures formed through O, N coordination are also found for triphenyltin carboxylates formed from pyridine carboxylic acids, $\text{Ph}_3\text{SnO}_2\text{CC}_6\text{H}_4\text{N}-4$ and $\text{Ph}_3\text{SnO}_2\text{CC}_6\text{H}_4\text{N}-3$ [21]. However, interaction with the heteroatom present on the R group of the carboxylic acid can also lead to dimeric structures as found in $[\text{Ph}_3\text{Sn}(\text{O}_2\text{CC}_6\text{H}_4-2-\text{S})\text{SnPh}_3]$ [42]. For two specific carboxylates $n\text{-Bu}_3\text{SnO}_2\text{C}-\text{C}_6\text{H}_3-2,6-\text{F}_2$ [43] and $\text{Ph}_3\text{Sn}(\text{NPG})$ ($\text{NPG} = N\text{-phthalyl glycinate}$) [44] macro-

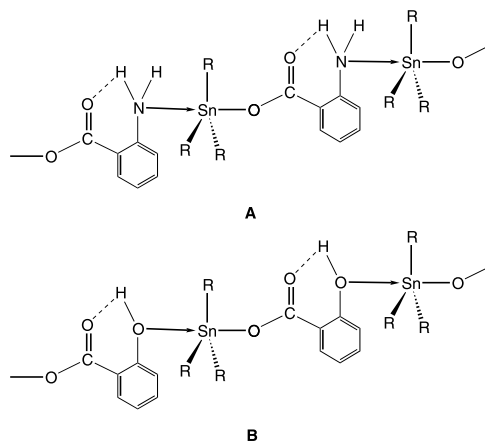


Fig. 6. Polymer formation in the solid-state structures of $\text{R}_3\text{SnO}_2\text{CR}'$ through a covalently bound Sn–O bond and a Sn←D dative bond from a donor substituent atom (D) on the carboxylic acid moiety; (A) shows Sn←N coordination while (B) shows Sn←O coordination [40,41].

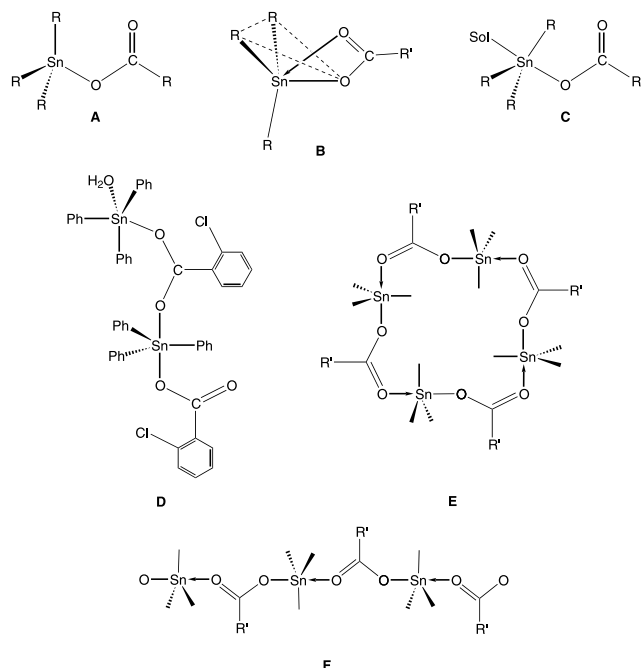


Fig. 5. The various structural forms of triorganotin carboxylates. (A) and (B) represents the discrete forms; (C) is a discrete form with a solvent molecule coordination; (D) is a dimeric form; (E) macrocyclic form; (F) polymeric form [19–21,40–69].

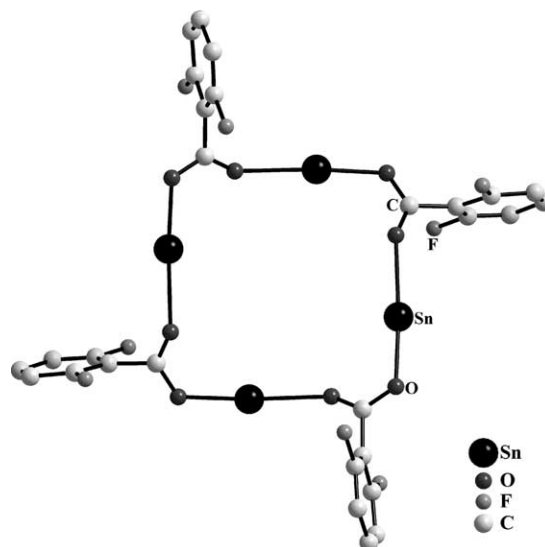


Fig. 7. The structure of $n\text{-Bu}_3\text{SnO}_2\text{CC}_6\text{H}_3-2,6-\text{F}_2$ showing a macrocyclic structure involving a tetrameric tin assembly (the alkyl groups on tin have been omitted for clarity) [43].

cyclic structures containing four and six tin atoms have been realized (Figs. 7 and 8). Interestingly, the X-ray structure of $[\text{Ph}_3\text{SnO}_2\text{P}(\text{OPh})_2]$ is also hexameric containing a 24-membered ring [45]. In contrast the compounds $\text{Me}_3\text{SnO}_2\text{PX}_2$ ($\text{X} = \text{Cl}$ or Me) and $\text{Me}_3\text{SnO}_2\text{P}(\text{OH})\text{Ph}$ consist of polymeric chains [18]. The X-ray structural data of selected triorganotin carboxylates is summarized in Table 1 [39,40,43,44,46–56].

2.1. Discrete structures

In the triorganotin carboxylates $\text{R}_3\text{SnO}_2\text{CR}'$ having discrete structures, the tin is bound covalently to three carbons and one oxygen and is present in a distorted

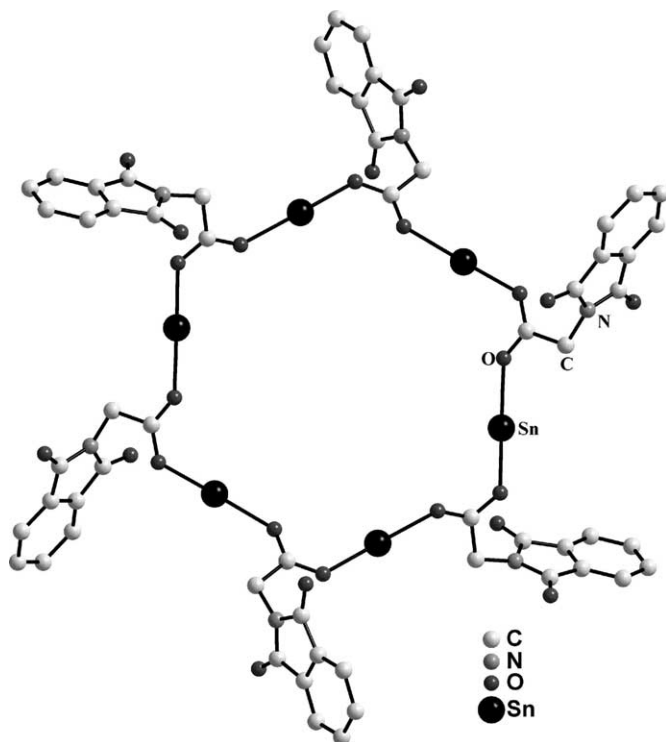


Fig. 8. The X-ray structure of $\text{Ph}_3\text{Sn}(\text{NPG})$ (NPG = *N*-phthalyl glycinate) showing a macrocyclic structure with a hexameric tin assembly (the aryl substituents on tin have been omitted for clarity) [44].

tetrahedral geometry. A representative example of this structural type is shown in Fig. 9. All of these compounds have phenyl or cyclohexyl substituents on the tin (Table 1). However, Harrison classifies the tricyclohexyltin carboxylates also as polymeric albeit with weak intermolecular interactions [57]. There are some subtle nuances in the representation of the solid-state structures of this family of compounds. It is possible to represent this in two forms as shown in Fig. 5(A and B). The issue revolves around the participation of the carbonyl oxygen in an intramolecular coordination to tin. In a pure tetrahedral form (Fig. 5A) there is no interaction. Intramolecular co-

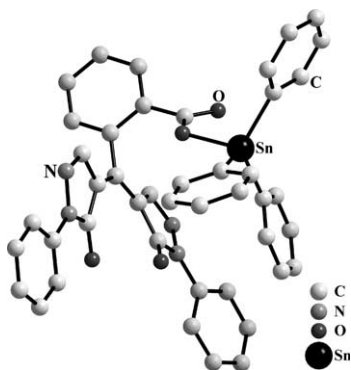


Fig. 9. The X-ray structure of $\text{Ph}_3\text{SnO}_2\text{CR}$ (Table 1, entry 32) showing the discrete structural form [54].

ordination on the other hand would lead to approximate trigonal-bipyramidal geometry around tin (Fig. 5B). Considering the X-ray structures of several triorganotin carboxylates it is possible to detect two types of Sn–O bond lengths [19–21]. While the Sn–O covalent bond distance in these molecules varies very little and is from 2.038(9) to 2.115(6) Å the Sn–O coordinate bond distance varies from 2.463(7) to 3.11(4) Å (Table 1). Although these latter sets of distances are considerably longer than the *normal* Sn–O covalent bond distance, they are smaller than the sum of the *van der Waals* radii of tin and oxygen (3.70 Å) [58]. On this basis it is possible to represent the discrete structures as shown in Fig. 5B showing that the carboxyl oxygen is involved in a weak coordinative interaction with tin along one of the tetrahedral faces. The extent of the intramolecular coordination seem to be affected by the presence of intramolecular hydrogen bonding as observed in the differences of Sn–O bond distances in $\text{Ph}_3\text{SnO}_2\text{CC}_6\text{H}_4-2\text{-NH}_2$, $\text{Ph}_3\text{SnO}_2\text{CC}_6\text{H}_4-2\text{-NMe}_2$ and $\text{Ph}_3\text{SnO}_2\text{CC}_6\text{H}_4-4\text{-NH}_2$ (Table 1). Thus the anthranilic acid derivative in which the NH_2 group is intramolecularly hydrogen bonded to the C=O has the longest Sn–O distance. The solid-state structures have an excellent correlation with ^{119}Sn Mössbauer values. Mössbauer data for selected triorganotin compounds are summarized in Table 2 [40,43,46,48,49,56,59,60]. The quadrupole splitting parameters for the discrete structures have been found to be in the range of 2.3–3.00 mm s^{-1} (Table 2). In solution the ^{119}Sn -NMR values are typical of four-coordinate tin (Table 3) [38,40,43,46–49,56,54,59–63].

2.2. Chain structures

In the chain structures the carboxylate unit functions as a bridging ligand and connects two different tin centers in an intermolecular manner. A representative X-ray structure for $n\text{-Bu}_3\text{SnO}_2\text{CCH}=\text{CHC}_6\text{F}_5$ [48] is shown in Fig. 10. The coordination polyhedron around tin is essentially a trigonal-bipyramid with the equatorial positions being taken up by the carbon substituents (sum of C–Sn–C angles average from 357 to 360°) and the axial position being occupied by the two oxygens ($\text{O}^1\text{–Sn–O}^2$ 170–175°). Importantly the Sn–O distances are non-equivalent, with the Sn–O (carboxyl) being slightly longer (Table 1). Thus the RCO_2 does not function as symmetric bridging ligand. This may be contrasted with the situation found for $\text{Ph}_3\text{SnO}_2\text{SePh}$ where in a similar polymeric structure the two Sn–O bonds are exactly same [39]. Because of the variation of the bond distances in the triorganotin carboxylates the tin is displaced from the equatorial plane towards the covalently bond oxygen by about 0.18–0.20 Å. An analysis of these polymers has shown an average repeat distance 5.185 Å which is relatively insensitive to the

Table 1

X-ray structural data for some triorganotin carboxylates

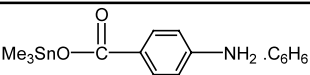
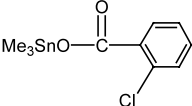
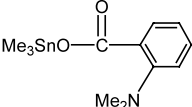
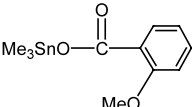
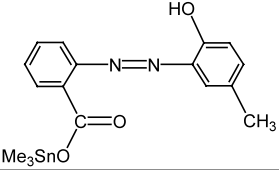
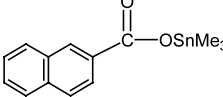
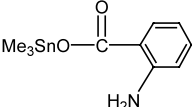
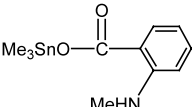
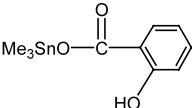
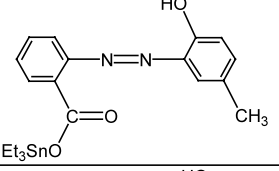
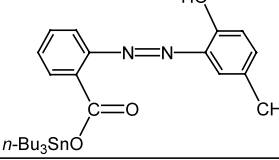
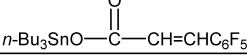
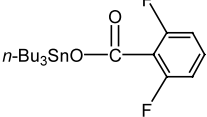
S.No.	Compound	Structure	Sn-O ¹ [Å]	Sn-O ² [Å]	Δ	Ref
1		Polymer	2.169(5) 2.168(5)	2.477(5) 2.416(6)	0.308 0.248	40
2		Polymer	2.200(3)	2.414(3)	0.214	40
3		Polymer	2.201(5)	2.426(5)	0.225	40
4		Polymer	2.208(2)	2.381(2)	0.173	40
5		Polymer	2.164(3)	2.487(3)	0.323	46
6		Polymer	2.14(1)	2.57(1)	0.43	47
7		Polymer through N	2.146(3)	2.781(5)	0.635	40
8		Polymer through N	2.128(3)	3.162(6)	1.034	40
9		Polymer through O	2.114(7)	3.08(1)	0.966	40
10		Polymer	2.200(1)	2.550(1)	0.350	46
11		Polymer	2.164(3)	2.579(4)	0.415	46
12		Polymer	2.201(3)	2.413(3)	0.212	48
13		Cyclic Tetramer	2.186(4)	2.514(4)	0.328	43

Table 1 (Continued)

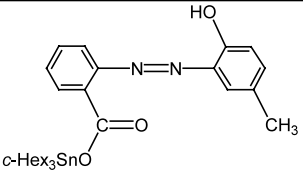
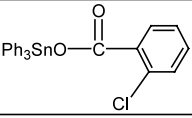
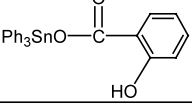
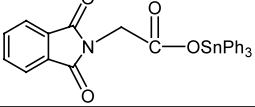
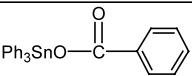
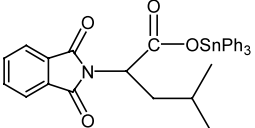
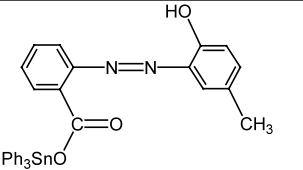
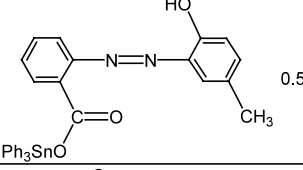
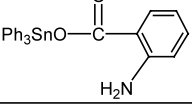
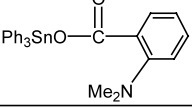
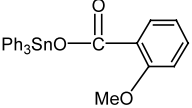
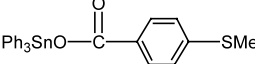
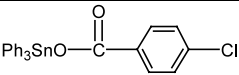
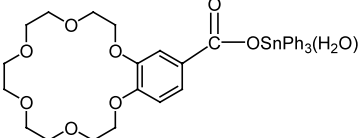
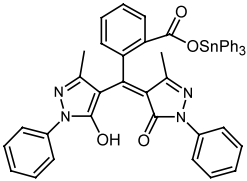
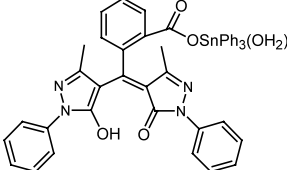
14		Discrete	2.076(3)	2.759(4)	0.683	46
15	(c-Hex) ₃ SnO ₂ CCF ₃	Discrete	2.080(4)	3.110(0)	1.030	55
16	Ph ₃ SnO ₂ SePh	Polymer	2.225(5)	2.224(2)	0.001	39
17		Polymer	2.201(3)	2.384(3)	0.183	53
18		Polymer through O	2.083(2)	3.035(2)	0.952	52
19		Cyclic Hexamer	2.191(18)	2.319(14)	0.128	44
20	Ph ₃ SnO-C(=O)-C ₁₀ H ₇ -1	Discrete	2.068(2)	2.711(2)	0.643	40
21		Discrete	2.074(4) 2.073(3)	2.695(5) 2.674(3)	0.621 0.601	40 49
22		Discrete	2.038(9)	2.91(1)	0.872	41
23		Discrete	2.070(5)	2.463(7)	0.393	50
24	 0.5(Me) ₂ C(O)	Discrete	2.079(5)	2.656(5)	0.577	46
25		Discrete	2.043(3)	2.823(3)	0.78	51
26		Discrete	2.115(6)	2.564(7)	0.449	51
27	Ph ₃ SnO-C(=O)-C6H4NH ₂ 0.5C ₆ H ₆	Discrete	2.072(2)	2.629(2)	0.557	51
28		Discrete	2.054(3)	2.781(3)	0.727	52
29		Discrete	2.060(2)	2.783(3)	0.723	52

Table 1 (Continued)

30		Discrete	2.048(4)	2.861(4)	0.813	53
31		Discrete	2.120(6)	2.937(8)	0.817	56
32		Discrete	2.075(3)	2.890(3)	0.815	54
33		Discrete	2.140(3)	2.806(3)	0.666	54

substituents on either the tin or the carboxylate group [64].

^{119}Sn Mössbauer is also diagnostic of the polymeric structures. In these the local coordination environment around tin is made up of three carbons and two oxygens. In all of these compounds the quadrupole splitting parameters observed are higher than those found for the discrete structures and are in between 3.3 and 3.9 mm s^{-1} (Table 2). In solution all the polymeric structures break down to monomeric structures (even in non-coordinating solvents such as dichloromethane) as evidenced by ^{119}Sn -NMR (Table 3), molecular weight measurements and infrared studies.

The preference for the chain structures seems to be the natural consequence of the principles of pentacoordination. In this mode the tin atom is in trigonal-bipyramidal geometry and has the least electronegative groups in the equatorial position and the electronegative oxygens in the axial position. In the discrete structure even if one assumes distorted trigonal-bipyramidal geometry to be present around tin, one of the organic groups attached to tin has to occupy an axial position. Holmes has argued that this becomes feasible if the organic group is an electronegative aryl substituent, which has comparable group electronegativity as that of oxygen [51,52]. However, the formation of chain structures for $\text{Ph}_3\text{SnO}_2\text{CC}_6\text{H}_4\text{-2-Cl}$ [53] and also for $\text{Ph}_3\text{SnO}_2\text{CCH}_3$ [20] suggests that there may be other subtle factors including the pK_a of the acid and crystal packing which may tilt the balance from one structure to the other [60]. Also, X-ray structures of triorganotin carboxylates containing a solvent molecule of crystallization have been found to show *regular* five-coordinate discrete

structures (Fig. 5C). These include $\text{Ph}_3\text{SnO}_2\text{CR}'\cdot\text{OH}_2$ ($\text{R}' = \text{benzo-15-crown-5}$) [56] (Fig. 11), $\text{Me}_3\text{Sn}(\text{O}_2\text{CC}_5\text{-H}_4\text{N-2})\cdot\text{OH}_2$ [65], $[n\text{-Bu}_3\text{Sn}(N\text{-phthaloyl glycinate})\cdot\text{OH}_2]$ [66], $\{\text{Ph}_3\text{Sn}[\text{O}_2\text{CC}_6\text{H}_4(\text{N}=\text{N}(\text{C}_6\text{H}_3\text{-4-OH-5-CHO}))\text{-o}]\cdot\text{OH}_2\}$ [67] and $\text{Ph}_3\text{Sn}(\text{O}_2\text{CCCl}_3)\cdot\text{MeOH}$ [68]. More recently a new polydentate ligand bearing carboxylic acid 2-[(5-hydroxy-1-phenyl-3-methylpyrazol-4-yl) (5-oxo-1,5-dihydro-4-phenyl-2-methyl pyrazol-4-ylidene)methyl]benzoic acid (H2QBz) has been found to form a triorganotin ester Ph_3SnHQBz possessing a discrete structure (Table 1, Fig. 9). This compound also crystallizes with a molecule of water, which coordinates to the tin [54]. In all of these compounds the tin is in trigonal-bipyramidal geometry with the equatorial positions taken up by the alkyl or aryl substituents on tin and the axial positions occupied by the oxygen of the solvent molecule and the covalently bound oxygen of the Sn-O-C bond. It may be of interest to note that the compound $[(\text{Ph}_3\text{SnO}_2\text{CC}_6\text{H}_4\text{-2-Cl})_2\cdot\text{H}_2\text{O}]$ shows a dimeric structure because the solvent of crystallization viz. H_2O blocks the fifth coordination site on the second tin preventing propagation of the polymer structure (Fig. 5C) [53]. A dimeric structure is also formed for $\text{Ph}_3\text{Sn}(\text{O}_2\text{CC}_6\text{H}_4\text{-2-S})_2\text{SnPh}_3$ [42]. In this structure the two Ph_3Sn are linked via the carboxylate residue at one end and the thiolate at the other end. Both the tins are present in distorted tetrahedral geometries. Prevention of polymeric structures is also possible by the presence of an additional anionic ligand such as Cl^- as in $\text{Ph}_3\text{Sn}(\text{O}_2\text{C}(\text{CH}_2)_2\text{PPh}_3)\text{Cl}$; this compound is monomeric and contains the tin in a five-coordinate trigonal-bipyramidal geometry with the chloride and the oxygen atoms occupying the axial positions [69].

Table 2

Mössbauer data for some triorganotin carboxylates

S.No.	Compounds	δ (mm s ⁻¹)	ϵE_Q (mm s ⁻¹)	Ref
1		1.36	3.71	40
2		1.40	3.47	40
3		1.33	3.63	40
4		1.36	3.59	40
5		1.36	3.43	40
6		1.38	3.40	40
7		1.37	3.74	40
8		1.30	3.68	40
9		1.37	3.76	46
10		1.27	3.55	59
11		1.49	3.74	46
12		1.50	3.88	43
13		1.53	3.94	43
14		1.51	3.87	43
15		1.52	3.86	43

Table 2 (Continued)

16		1.51	3.75	43
17		1.49	3.59	43
18		1.48	3.35	43
19		1.48	3.54	43
20		1.47	3.30	43
21		1.50	3.85	46
22		1.53	3.97	48
23		1.48	3.83	48
24		1.45	3.75	48
25		1.48	3.65	49
26		1.45	3.72	49
27		1.44	3.63	49
28		1.44	3.41	56
29		1.45	3.29	56
30		1.28	3.50	59
31		1.50	2.76	46
32		1.41	2.63	59

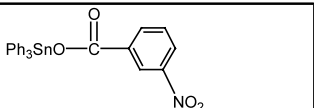
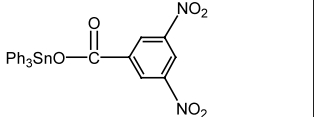
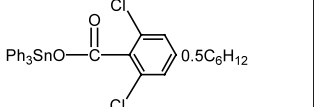
Table 2 (Continued)

33		1.28	3.36	40
34		1.24	2.39	40
35		1.34	2.97	40
36		1.23	2.33	40
37		1.25	2.37	40
38		1.34	3.71	40, 60
39		1.24	2.55	40, 60
40		1.24	2.36	40, 60
41		1.27	2.42	40, 60
42		1.21	2.44	40, 60
43		1.25	2.30	40, 60
44		1.23	2.45	46
45		1.34	3.76	48
46		1.31	3.55	48
47		1.31	3.52	48
48		1.30	3.60	49
49		1.31	3.60	49
50		1.25	2.46	49
51		1.24	2.33	56
52		1.23	2.77	56

Table 2 (Continued)

53		1.24	3.41	59
54		1.33	3.70	60
55		1.33	3.49	60
56		1.31	3.70	60
57		1.33	3.56	60
58		1.33	3.56	60
59		1.28	2.35	60
60		1.29	2.58	60
61		1.26	2.54	60
62		1.25	2.42	60
63		1.31	2.55	60
64		1.23	2.39	60
65		1.23	2.37	60
66		1.27	2.42	60
67		1.26	2.47	60
68		1.21	2.37	60
69		1.25	2.51	60

Table 2 (Continued)

70		1.26	2.54	60
71		1.29	2.76	60
72		1.32	2.57	60

Recently, Gielen and coworkers have reported the synthesis of a large variety of tri- and diorganotin carboxylates and have tested their in vitro anti-tumor activity [7,70]. Representative examples of some triorganotin compounds are given in Table 4 [7,70]. Many of these compounds show excellent in vitro activity against a number of tumor lines. However, the insolubility of these compounds in aqueous medium has to be overcome before meaningful in vivo studies can be carried out.

3. Diorganotin derivatives

3.1. Diorganotin oxides $[R_2SnO]_n$ and related compounds

The complete hydrolysis of diorganotin dichlorides leads to the formation of the oxide $[R_2SnO]_n$. There is no report on the isolation of a molecular dihydroxide of

the type $R_2Sn(OH)_2$. This may be contrasted with the situation with silicon where several discrete silane diols have been synthesized and structurally characterized [71]. The structures of many diorganotin oxides $[R_2SnO]_n$ ($R = \text{Me, Et, } n\text{-Bu, Ph}$) are polymeric due to intermolecular *crosslinking* as a result of Sn-O interactions [72]. The polymeric nature of these oxides precludes their solubility in common organic solvents. However, well defined molecular diorganotin oxides containing four- or six-membered rings are accessible by introducing sterically hindered substituents on tin $[\{(Me_3Si)_2CH\}_2SnO]_2$ [73], $[\{(Me_3Si)_2CH\}(Me)Sn]\{Sn-(Me)C(SiMe_3)_3\}_2O_3$ [74], $(t\text{-Bu}_2SnO)_3$ [75,76], $[(t\text{-C}_5\text{H}_{11})_2SnO]_3$ [76], $[(2,6\text{-Et}_2\text{C}_6\text{H}_3)_2SnO]_3$ [77], $[(2,4,6\text{-Me}_3\text{C}_6\text{H}_2)_2SnO]_3$ [78] and $[(2,4,6\text{-(CF}_3)_3\text{C}_6\text{H}_2)_2SnO]_3$ [79] (Fig. 12). The synthesis of these oxides is accomplished in a variety of ways as outlined in Scheme 4. An interesting example of a *distannanol* $[\{CH(SiMe_3)_2\}_2Sn(OH)_2(\mu\text{-O})]$ is obtained by the hydrolysis of $[\{CH(SiMe_3)_2\}_2Sn(\mu\text{-O})_2]$ [73]. In organosilicon chemistry analogous disilanol $[\{R_2Si(OH)_2\}_2O]$ are very well known and in fact have been extensively used as synthons for the preparation of metallasiloxanes [80]. Cage type diorganotin oxides have been recently synthesized using alkyl bridged di tin derivatives $R(Cl)_2Sn-G-Sn(Cl)_2R$ ($R = (Me_3Si)_2CH$; $G = C(Me)_2, CH_2-CH_2, (CH_2)_3$) [81] (Fig. 13). The X-ray structures of a few molecular diorganotin oxides have been determined and the data is summarized in Table 5 [73,74,76–78,81]. The four-membered distannoxane $[\{CH(SiMe_3)_2\}_2Sn(\mu\text{-O})_2]$ is planar with the average Sn-O bond length being 1.94 Å. Nearly similar Sn-O bond distances are found for the six-membered and cage stannoxanes. Most of the six-membered stannoxanes are

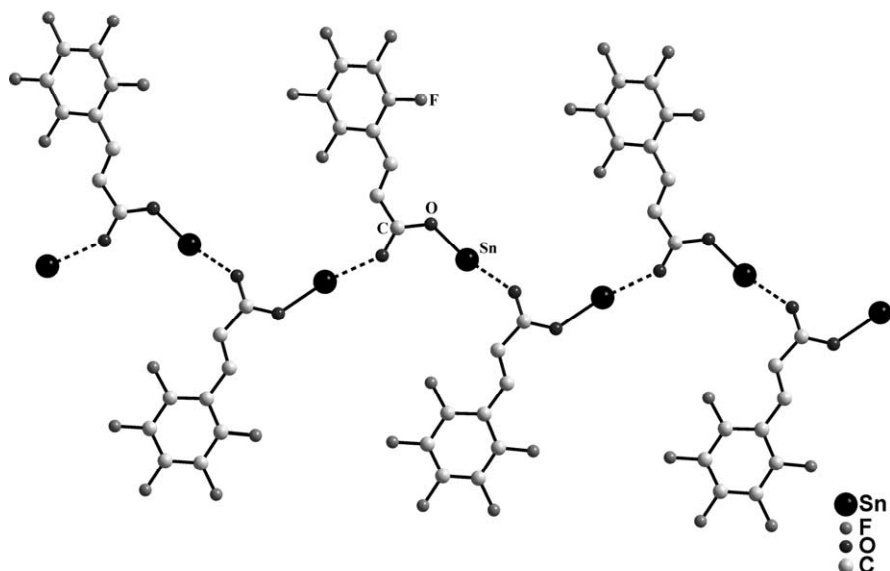


Fig. 10. The structure of $n\text{-Bu}_3\text{SnO}_2\text{CCH=CHC}_6\text{F}_5$ showing the polymeric form (the alkyl groups on tin have been omitted for clarity) [48].

Table 3

¹¹⁹Sn-NMR data for some triorganotin carboxylates

S.No.	Compound	δ^a	Ref
1		126.9	40
2		148.2	40
3		148.1 (24.7)	46
4		138.0 (-10.9)	47
5		138.7 (-6.6)	47
6		150.4	54
7		129.0	59
8		133.0	61
9		120.0 (17.0)	46
10		106.0	61
11		107.0	38
12		106.0	38
13		106.0	38
14		103	38

Table 3 (Continued)

15		118.2	43
16		125.1	43
17		125.2	43
18		132.6	43
19		125.6	43
20		130.4	43
21		124.1	43
22		130.7	43
23		122.7	43
24		123.0 (23.3)	46
25		148.0 (38.2, 36.1)	48
26		127.2 (-22.5, -25.2)	48
27		118.7 (-29.0)	48
28		110.3	49
29		110.7 (-48.0)	49
30		107.9 (-55.0)	49
31		108.2	56

Table 3 (Continued)

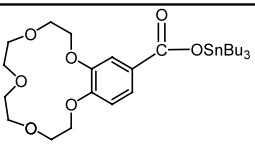
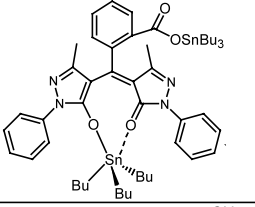
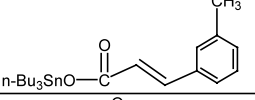
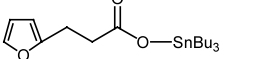
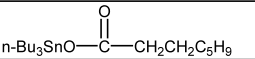
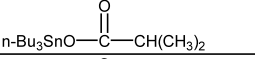
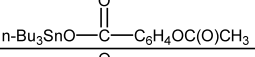
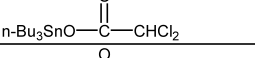
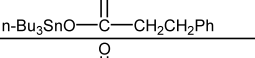
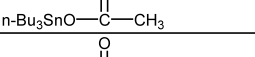
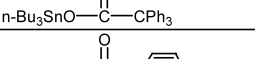
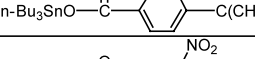
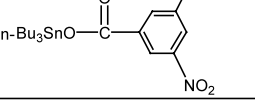
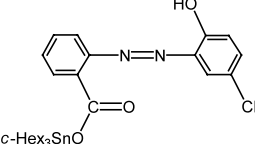
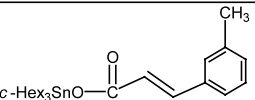
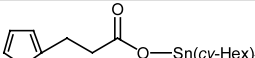
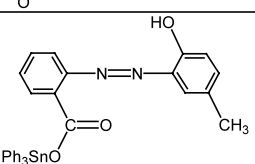
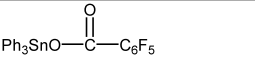
32		107.4	56
33		106.1	44
34		108.0	59
35		104.0	61
36		101.6	62
37		100.6	62
38		112.7	62
40		156.7 (39, 45) 151.2	62 63
41		108.9 (-47) 96.5	62 63
42		123.1 (-47, -53)	63
43		119.4	63
44		110.5	63
45		144.7	63
46		23.7 (-8.5)	46
47		12	59
48		12.0	56
49		-105.9 (-106.3)	46
50		-83.3 (-189.9, -216.1)	48

Table 3 (Continued)

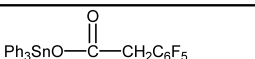
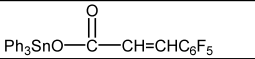
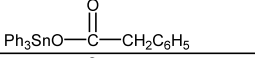
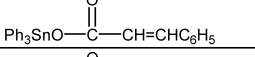
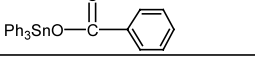
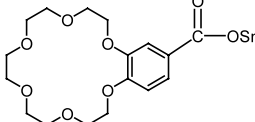
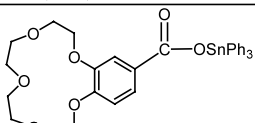
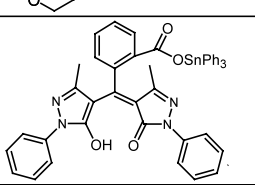
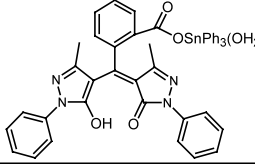
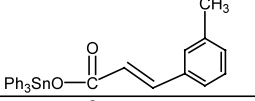
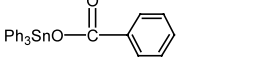
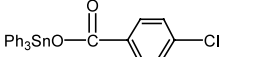
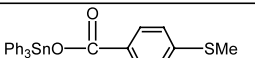
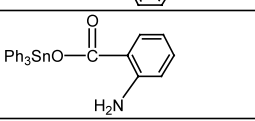
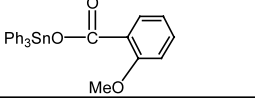
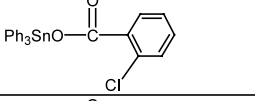
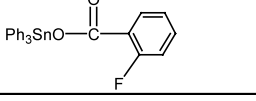
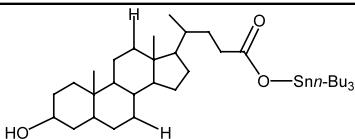
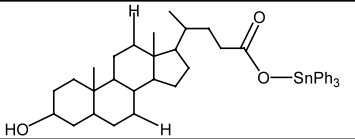
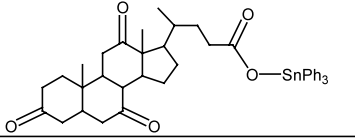
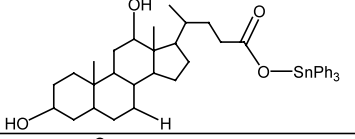
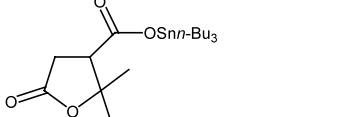
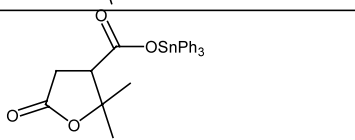
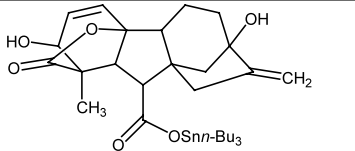
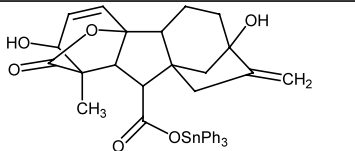
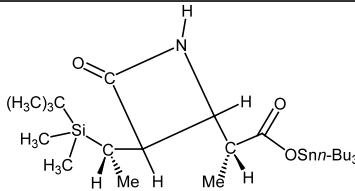
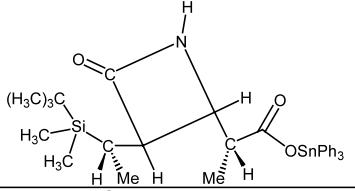
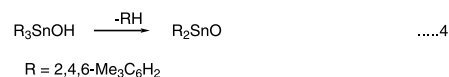
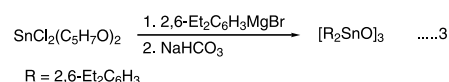
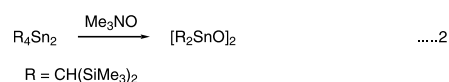
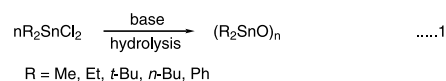
51		-96.0 (-275.0)	48
52		-104.3 (-274.6)	48
53		-109.0 (-288)	49
54		-114.5 (-261)	49
55		-117.7 (-117)	49
56		-115.7	56
57		-116.3	56
58		-84.0	52
59		-95.4	54
60		-114.3	59
61		-114.3	60
62		-108.2	60
63		-115.6	60
64		-119.5	60
65		-121.9	60
66		-106.3	60
67		-108.9	60

Table 4
Examples of some biologically important triorganotin carboxylates

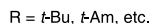
S.No.	Compound	Ref
1		70
2		70
3		70
4		70
5		70
6		70
7		70
8		70
9		70
10		70
11	$n\text{-Bu}_3\text{SnO}-\text{C}(=\text{O})-\text{CH}_2\text{OCH}_2\text{CH}_2\text{OCH}_3$	70
12	$n\text{-Bu}_3\text{SnO}-\text{C}(=\text{O})-\text{CH}_2(\text{OCH}_2\text{CH}_2)_2\text{OCH}_3$	70
13	$\text{Ph}_3\text{SnO}-\text{C}(=\text{O})-\text{CH}_2\text{OCH}_2\text{CH}_2\text{OCH}_3$	70
14	$\text{Ph}_3\text{SnO}-\text{C}(=\text{O})-\text{CH}_2(\text{OCH}_2\text{CH}_2)_2\text{OCH}_3$	70



Scheme 4.

and B). Two fluoro-bridged ladders have been recently reported (Fig. 18C and D) and these have been prepared by slightly different routes (Scheme 5) [81,85]. Thus the compound [*t*-Bu₂(F)SnOSn(F)*t*-Bu₂]₂ is prepared by the reaction of [*t*-Bu₂SnO]₃ with (*t*-BuF₂Si)₂ [85] while the other fluoro bridged ladder [*R*(F)Sn(CH₂)₃Sn(F)*R*]₂ (R = CH(SiMe₃)₂) is prepared by the reaction of treatment of KF and water with R(Cl)₂Sn(CH₂)₃Sn(Cl)₂R (R = CH(SiMe₃)₂) (Scheme 5) [81]. This latter compound contains two alkylene bridges that connect alternate tins in a *trans* geometry (Fig. 19). Recently, an example of a dihydroxy bridged ladder containing the alkylene bridges in a *cis* geometry has been reported by the reaction of the acetylene bridged di-tin derivative [Me₃SiCH₂(Cl)₂SnCH₂(Me₂Si)₂C₂ with [*t*-Bu₂SnO]₃ [86] (Fig. 20). The X-ray structure of this *cis* derivative is shown in Fig. 21. All of these ladders are dimers of the tetraorganodistannoxane motif; the distannoxane ring within the dimer is planar and the coordination at all the four tins may be considered as pentacoordinate. Representative X-ray data are summarized in Table 7 [81,85–88,92]. All of these ladder compounds seem to retain the dimeric structures in solution as well [82,89–91] although evidence has been accumulating in recent years for a complex dynamic behavior in solution [93–95]. The solution ¹¹⁹Sn-NMR of these compounds shows two types of tin resonances corresponding to the *exo* and *endo* tin environments. These are summarized in Table 8 [81,85,86,91,92].

In contrast to the symmetric dimers with ladder structures unsymmetrical dimers with similar structures [*t*-Bu₂(Cl)SnOSn(Cl)R₂]₂ (R = Me, Et, *i*-Pr, *n*-Bu) are accessible exclusively by the reaction of R₂SnCl₂ with [*t*-Bu₂SnO]₃ [92]. A hydroxy bridged ladder [*t*-Bu₂(Cl)SnOSn(OH)*t*-Bu₂]₂ is obtained by the reaction of [*t*-Bu₂Sn(OH)Cl]₂ with [*t*-Bu₂SnO]₃ (Scheme 5). In contrast to the symmetric dimers (Fig. 18A and B) in the unsymmetrical dimers the terminal chlorides are involved in further bridging to the *endo* tin atoms (Fig.



18E). This leads to a situation where the endo tins are hexa-coordinate with a skew-trapezoidal geometry while the exo tins are pentacoordinated with distorted trigonal-bipyramidal geometry. Representative X-ray structures of two unsymmetrical dimer ladders $[t\text{-Bu}_2(\text{Cl})\text{SnOSn}(\text{Cl})\text{Me}_2]_2$ and $[t\text{-Bu}_2(\text{Cl})\text{SnOSn}(\text{Cl})n\text{-Bu}]_2$ are shown in Figs. 22 and 23. Another point of

difference is that the unsymmetrical dimer ladders are more labile in solution and seem to dissociate [91,92]. This has been confirmed by detailed solution NMR studies. Interestingly addition of Me_2SnCl_2 to the unsymmetrical dimer ladder $[\text{-Bu}_2(\text{Cl})\text{SnOSn}(\text{Cl})\text{Me}_2]_2$ leads to the formation of the symmetric dimer ladder $[\text{Me}_2(\text{Cl})\text{SnOSn}(\text{Cl})\text{Me}_2]$. It is believed that the mechan-

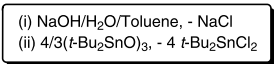
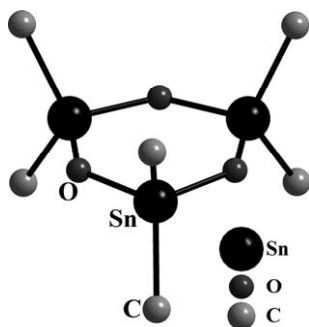
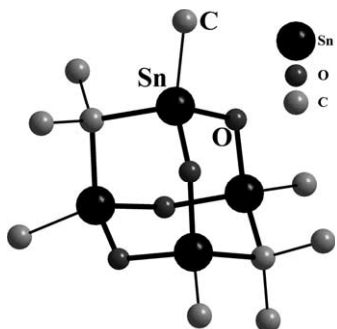


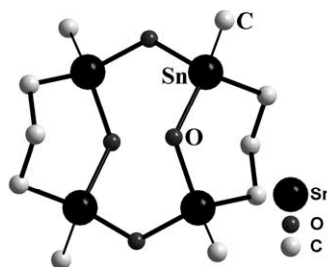
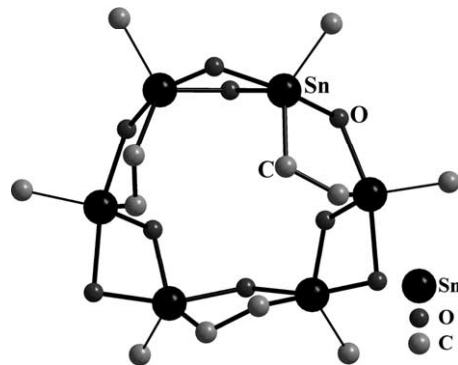
Fig. 13. Diorganotin oxides with cage type structures formed from hydrolysis reaction of $\text{RSn}(\text{Cl})_2\text{XSn}(\text{Cl})_2\text{R}$, $\{\text{X} = (\text{CH}_2)_3; (\text{CH}_2)_2, \text{C}(\text{CH}_3)_2\}$ [81].

Fig. 14. X-ray structure of $(t\text{-Bu}_2\text{SnO})_3$ [75,76].Fig. 15. X-ray structure of $[(\text{Me}_3\text{Si})_2\text{CHSn}(\text{O})\text{C}(\text{Me})_2\text{Sn}(\text{O})\text{CH}(\text{SiMe}_3)_2]$. (Me_3Si groups are not shown for clarity) [81].

ism as outlined in the Fig. 24 is operative in this transformation. The driving force for the transformation appears to be the ease of dissociation of the bulky $t\text{-Bu}_2\text{SnCl}_2$ from the dimeric tetraorganodistannoxane structure [92].

3.3. Alkyl bridged double and triple ladders

Novel alkyl bridged di-tin derivatives $[\text{R}(\text{Cl})_2\text{Sn}(\text{CH}_2)_3\text{Sn}(\text{Cl})_2\text{R}]$ which can be prepared as outlined in

Fig. 16. X-ray structure of $[(\text{Me}_3\text{Si})_2\text{CHSn}(\text{O})(\text{CH}_2)_3\text{Sn}(\text{O})\text{CH}(\text{SiMe}_3)_2]$. (Me_3Si groups not shown) [81].Fig. 17. X-ray structure of $[\text{O}\{(\text{RSn}(\text{CH}_2)_2\text{SnR})\text{OH}\}\text{OH}]_3 \cdot 2\text{H}_2\text{O}$, $\text{R} = [(\text{Me}_3\text{Si})_2\text{CH}]$ (Me_3Si groups are not shown) [81].

Scheme 6 [96] have been reacted with the oxide transfer reagent $[t\text{-Bu}_2\text{SnO}]_3$ to afford the tetrameric double ladder $[\{\text{R}(\text{Cl})\text{Sn}(\text{CH}_2)_3\text{Sn}(\text{Cl})\text{R}\}\text{O}]_4$ [97] (Fig. 25). Similarly base assisted hydrolysis of $[\text{R}(\text{Cl})_2\text{Sn}(\text{CH}_2)_3\text{Sn}(\text{Cl})_2\text{R}]$ affords the tetramer double ladder $[\{\text{R}(\text{Cl})\text{Sn}(\text{CH}_2)_3\text{Sn}(\text{OH})\text{R}\}\text{O}]_4$ (Fig. 25). The X-ray structure of $[\{\text{R}(\text{Cl})\text{Sn}(\text{CH}_2)_3\text{Sn}(\text{Cl})\text{R}\}\text{O}]_4$ ($\text{R} = \text{Me}_3\text{-SiCH}_2$) shows that the two dimer ladders are bridged by four alkylene chains (Fig. 26). The inter ladder spacing of about 7.0 Å is rather small to allow any host–

Table 5

X-Ray data for some diorganotin oxides

Sl. no.	Compound	Sn–O ^a (Å)	Structure	Reference
1	$[\{\text{SnR}_2(\mu\text{-O})\}_2]$, $\text{R} = \text{CH}(\text{SiMe}_3)_2$	1.960(2)	Four-membered planar ring	[73]
2	$[\{\text{SnR}_2(\text{OH})(\mu\text{-O})\}_2]$, $\text{R} = \text{CH}(\text{SiMe}_3)_2$	1.956(4), 2.032(7) ^b	Distannanol	[73]
3	$[\{\text{Sn}(\text{MeR})(\mu\text{-O})\}_2\{\text{Sn}(\text{MeR})(\mu\text{-O})\}]$, $\text{R}'' = \text{C}(\text{SiMe}_3)_3$, $\text{R} = \text{CH}(\text{SiMe}_3)_2$	1.960(1)	Planar six-membered ring	[74]
4	$(t\text{-Bu}_2\text{SnO})_3$	1.965(2)	Planar six-membered ring	[76]
5	$(t\text{-Am}_2\text{SnO})_3$	1.961(11)	Planar six-membered ring	[76]
6	$[(\text{C}_6\text{H}_3\text{Et}_2\text{-2,6})_2\text{SnO}]_3$	1.950(2)	Planar six-membered ring	[77]
7	$[(\text{C}_6\text{H}_2\text{Me}_3\text{-2,4,6})_2\text{SnO}]_3$	1.973(1)	Flattened boat shaped, six-membered ring	[78]
8	$[\{(\text{SiMe}_3)_2\text{CH}(\text{O})\text{Sn}\}_2\{\text{CMe}_2\}_2]$	1.9678(8)	Adamantane type	[81]
9	$[\{(\text{SiMe}_3)_2\text{CH}(\text{O})\text{Sn}\}_2\{(\text{CH}_2)_3\}_2]$	1.9645(2)	Eight-membered chair with <i>trans</i> propylene bridges	[81]
10	$[\text{O}\{(\text{SiMe}_3)_2\text{CHSn}(\text{CH}_2)_2\text{Sn}(\text{SiMe}_3)_2\text{CH}(\text{OH})\}\text{OH}]_3$	1.984(7), 2.203(9) ^b	Hexanuclear tin cluster containing oxide, hydroxyl, <i>cis</i> ethylene bridges	[81]

^a Average Sn–O distances.

^b Average Sn–OH distances.

Table 6

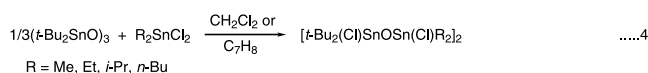
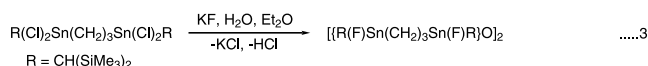
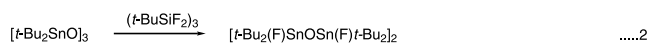
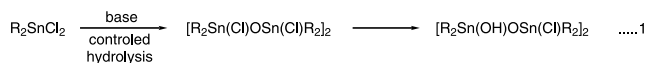
¹¹⁹Sn-NMR data for some diorganotin oxides

Sl. no.	Compound	δ^a	Reference
1	$[\{\text{Sn}(\text{CH}(\text{SiMe}_3)_2(\text{OH})\}_2(\mu\text{-O})]$	17.5	[73]
2	$[\text{Me}_2\text{SnO}]_n$	(−152.0)	[72]
3	$[n\text{-BuSnO}]_n$	(−177.0)	[72]
4	$(t\text{-Bu}_2\text{SnO})_3$	−84.3	[76]
5	$(t\text{-Am}_2\text{SnO})_3$	−72.9	[76]
6	$[(2,6\text{-Et}_2\text{-C}_6\text{H}_3)_2\text{SnO}]_3$	−125.0	[77]
7	$[(2,4,6\text{-Me}_3\text{-C}_6\text{H}_2)_2\text{SnO}]_3$	−104.0	[78]
8	$[\{(\text{SiMe}_3)_2\text{CH}(\text{O})\text{Sn}\}_2\{\text{CMe}_2\}]_2$	23.8 (24.4)	[81]
9	$[\{(\text{SiMe}_3)_2\text{CH}(\text{O})\text{Sn}\}_2\{(\text{CH}_2)_2\}]_2$	24.7	[81]
10	$[\{(\text{SiMe}_3)_2\text{CH}(\text{O})\text{Sn}\}_2\{(\text{CH}_2)_3\}]_2$	24.9 (34.3, 24.0)	[81]
11	$[\text{O}\{(\text{SiMe}_3)_2\text{CHSn}(\text{CH}_2)_2\text{Sn}(\text{SiMe}_3)_2\text{CH}(\text{OH})\}\text{OH}]_3$	(−163.3, −168.5)	[81]

^a ¹¹⁹Sn CP MAS spectral values are given in parenthesis.

guest chemistry to be carried out. This methodology has been extended to prepare several types of tetramer double ladders [96] including mixed tetramer double ladders [98]. Attempts to prepare the mixed tetramer double ladder by the reaction of the unsymmetrical di-tin derivative $\text{PhSn}(\text{Cl})_2(\text{CH}_2)_3\text{Sn}(\text{Cl})_2\text{CH}_2\text{SiMe}_3$ with $(t\text{-Bu}_2\text{SnO})_3$ affords a mixture of five isomers; the structure of one of these is shown in Fig. 27 [98]. However, the reaction between the symmetric di-tin derivative $\text{R}(\text{Cl})\text{Sn}(\text{CH}_2)_4\text{Sn}(\text{Cl})\text{R}$ and the symmetric di-tin oxides $[\text{R}'\text{Sn}(\text{O})(\text{CH}_2)_4\text{Sn}(\text{O})\text{R}']_n$ affords mixed tetramer double ladders (Fig. 28) [98]. From NMR studies it has also been shown that two symmetric tetramer double ladders with different substituents can undergo scrambling reaction to afford mixed double ladders [98]. The X-ray structure of one of the tetramer mixed double ladders is shown in Fig. 29.

The tetramer double ladders can also be chemically modified while retaining their overall structure. Thus, the reaction of $[\{\text{R}(\text{Cl})\text{Sn}(\text{CH}_2)_3\text{Sn}(\text{Cl})\text{R}\}\text{O}]_4$ with silver acetate affords the complete replacement of all the chlorides to afford $[\{\text{R}(\text{OAc})\text{Sn}(\text{CH}_2)_3\text{Sn}(\text{OAc})\text{R}\}\text{O}]_4$



Scheme 5.

[96] (Fig. 30). The acetate ligand is involved in two types of binding. While the exo tins are bound exclusively by a chelating acetate group generating a four-membered ring alternate tins within the dimeric ladder sub-unit are bridged by the second type of acetate forming a six-membered ring (Fig. 30). Most of these bridged derivatives seem to retain their structural

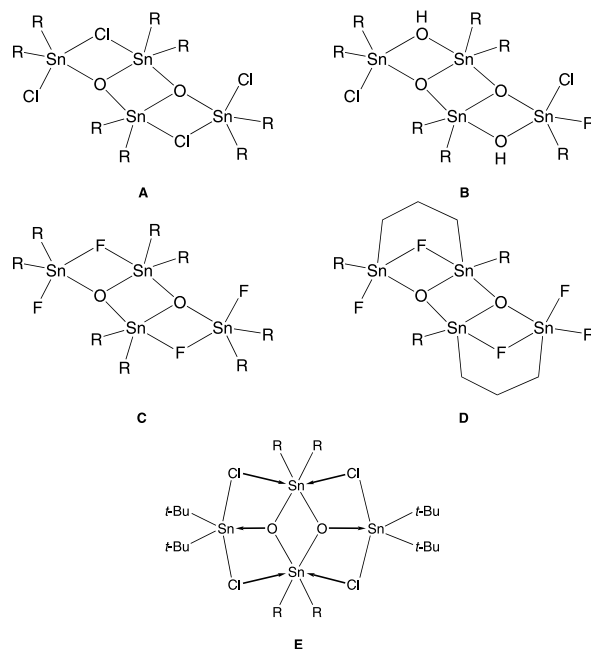
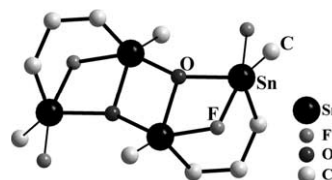


Fig. 18. Different types of dimeric structures of tetraorganodistannoxanes [81–92].

Fig. 19. X-ray structure of $[\{\text{R}(\text{F})\text{Sn}(\text{CH}_2)_3\text{Sn}(\text{F})\text{R}\}\text{O}]_2$, $\text{R} = [(\text{Me}_3\text{-Si})_2\text{CH}]$ (the SiMe_3 group is not shown) [81].

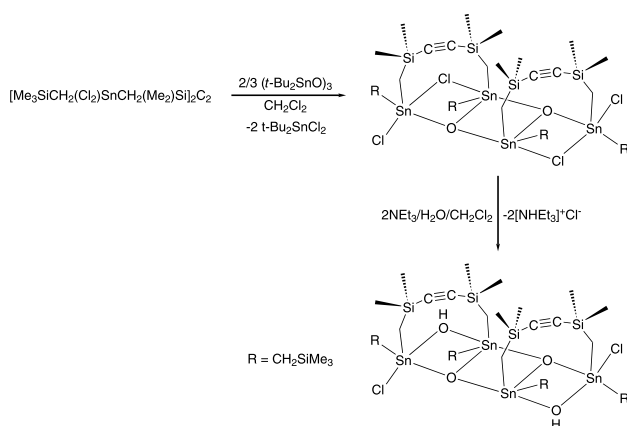


Fig. 20. Formation of *cis* bridged tetraorganodistannoxane with a ladder structure [86].

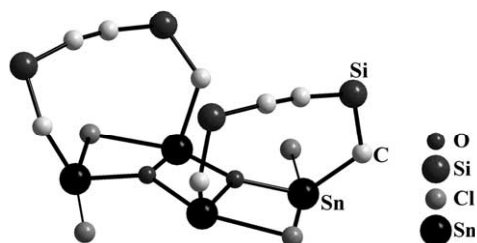


Fig. 21. X-ray structure of *cis*[(Me₂SiCH₂(Cl)SnCH₂(Me₂)SiC≡CSi(Me₂)CH₂Sn(Cl)CH₂SiMe₃)O]₂ [86].

integrity in solution. The tetramer double ladders also show two resonances in the tin NMR corresponding to the exo and endo tins of the two dimer sub-units (Table 9) [96–99].

Reaction of a tri-tin derivative [Me₃SiCH₂Sn(Cl)₂]₂SnCl₂, with [*t*-Bu₂SnO]₃ affords a hexamer triple ladder structure containing alkylene bridges (Fig. 31) [99]. The X-ray structure of the hexamer triple ladder is shown in Fig. 32. Attempts to prepare assemblies containing four ladders joined to each other by the use of RSn(Cl)₂(CH₂)₃Sn(Cl)₂CH₂Si(Me₃)₂CH₂Sn(Cl)₂-(CH₂)₃Sn(Cl)₂R however afforded tetramer double ladders containing *cis* and *trans* [–CH₂Si(Me₃)₂–CH₂] alkylene bridges [99] (Fig. 31). Fig. 33 shows the X-ray structure of the *trans* bridged tetramer double ladder [(Me₃SiCH₂(Cl)Sn(CH₂)₃Sn(Cl)CH₂)₂SiMe₂]O₂. Representative X-ray data for the various types of bridged ladders are summarized in Table 10 [96–99]. The solution dynamics of the bridged ladders is interesting. Most of the bridged ladders do retain their structures in solution. However, with certain doubly bridged compounds (R = Me₃SiCH₂, Me₃CCH₂, Me₂CHCH₂) and when the alkylene bridge is long (–CH₂)₄ an equilibrium exists between the tetramers (double ladders) and dimers (ladder) compounds (Fig. 34A and B). Also, when the R = Me₃SiCH₂ and when the alkylene bridge

Table 7

X-Ray data for some tetraorganodistannoxane derivatives^a

Sl. no.	Compound	X/Y	Sn–X _{ter} (Å)	Sn–Y _{bri} (Å)	X _{ter} –Sn _{endo} (Å)	Sn _{exo} –O (Å)	Sn _{endo} –O (Å)	Reference
1	[<i>t</i> -Bu ₂ (X)SnOSn(X) <i>t</i> -Bu ₂] ₂	F	1.981(7)	2.177(6)–2.196(7)	3.656(7)	2.077(8)	2.056(7)–2.118(7)	[85]
2	[{R(X)SnCH ₂ (Me ₂)SiC≡CSi(Me ₂)Sn(X)R}O] ₂ , R = Me ₃ SiCH ₂	Cl	2.507(2)–2.453(2)	2.503(2)–2.740(2)	3.490(2)–3.497(2)	2.024(3)–2.018(3)	2.049(3)–2.159(3)	[86]
3	[Pr ₂ (X)SnOSn(Y)Pr] ₂	Cl/OH	2.560(2)	2.140(2)–2.270(2)	–	2.020(1)	1.990(2)–2.170(2)	[87]
4	[R(X)SnOSn(Y)R] ₂ , R = CH ₂ SiMe ₃	Cl/OH	2.490(1)–2.520(1)	2.240(2)–2.400(2)	–	1.950(2)–1.990(2)	2.070(1)–2.170(1)	[87]
5	[R(X)SnOSn(X)Bu] ₂ , R = CH ₂ SiMe ₃	OH	2.016	2.151–2.299	–	–	2.014–2.164	[87]
6	[R(X)SnOSn(X)R] ₂ , R = CH ₂ SiMe ₃	Cl	2.460–2.477	2.595–2.934	–	–	2.056–2.204	[87]
7	[Pr ₂ (X)SnOSn(X)Pr] ₂	Cl	2.462	2.675–2.803	–	–	2.037–2.163	[87]
8	[Me ₂ (X)SnOSn(X)Me] ₂	Cl	2.438(4)	2.788(5)–2.710(5)	3.411(5)	2.029(9)	2.054(8)–2.115(9)	[88]
9	[Bu ₂ (X)SnOSn(X)Me] ₂	Cl	2.516(5)	2.675(1)–2.802(2)	3.126(6)	2.028(8)	2.074(8)–2.104(7)	[92]
10	[Bu ₂ (X)SnOSn(X)Bu] ₂	Cl	2.575(2)	2.598(3)–2.907(7)	3.014(2)	2.033(7)	2.075(6)–2.080(1)	[92]
11	[{R(X)Sn(CH ₂) ₃ Sn(X)R}O] ₂ , R = (Me ₃ Si) ₂ CH	F	1.995(6)	2.142(2)–2.235(2)	3.832(4)	2.038(7)	2.077(1)–2.127(2)	[81]

^a ter, terminal; bri, bridging.

Table 8
 ^{119}Sn -NMR data for some tetraorganodistannoxane derivatives

Sl. no.	Compound	δ^a	Reference
1	$[t\text{-Bu}_2(\text{Cl})\text{SnOSn}(\text{Cl})\text{Me}_2]_2$	–138.3, –145.6 ^b (–145.8, –172.0)	[92]
2	$[t\text{-Bu}_2(\text{Cl})\text{SnOSn}(\text{Cl})\text{Et}_2]_2$	–159.0, –163.9 ^b	[92]
3	$[t\text{-Bu}_2(\text{Cl})\text{SnOSn}(\text{Cl})i\text{-Pr}]_2$	–165.3, –180.2 ^b	[92]
4	$[t\text{-Bu}_2(\text{Cl})\text{SnOSn}(\text{Cl})n\text{-Bu}]_2$	–150.7, –157.6 ^b (–153.5, –169.0)	[92]
5	$[t\text{-Bu}_2(\text{OH})\text{SnOSn}(\text{Cl})n\text{-Bu}_2]_2$	–181.7, –220.9 (–178.0, –220.5)	[92]
6	$[t\text{-Bu}_2(\text{F})\text{SnOSn}(\text{F})t\text{-Bu}_2]_2$	–226.0, –290.0	[85]
7	$[\{\text{R}(\text{F})\text{Sn}(\text{CH}_2)_3\text{Sn}(\text{F})\text{R}\}\text{O}]_2$, R = $(\text{Me}_3\text{Si})_2\text{CH}$	–153.8, –115.1; –153.7, –108.4	[81]
8	$[\{\text{R}(\text{Cl})\text{SnCH}_2(\text{Me}_2)\text{SiC}\equiv\text{CSi}(\text{Me}_2)\text{Sn}(\text{Cl})\text{R}\}\text{O}]_2$, R = Me_3SiCH_2	–75.8, –132.4	[86]
9	$[\{\text{R}(\text{OH})\text{SnCH}_2(\text{Me}_2)\text{SiC}\equiv\text{CSi}(\text{Me}_2)\text{Sn}(\text{OH})\text{R}\}\text{O}]_2$, R = Me_3SiCH_2	–152.2, –153.1	[86]
10	$[\{n\text{-Bu}_2\text{Sn}(\text{Cl})\}_2\text{O}]_2$	–90.2, –143.1	[91]
11	$[\{n\text{-Bu}_2\text{Sn}(\text{OMe})\}_2\text{O}]_2$	–173.9, –185.9	[91]
12	$[\{n\text{-Bu}_2\text{Sn}(\text{OPh})\}_2\text{O}]_2$	–176.4, –177.8	[91]
13	$[n\text{-Bu}_2(\text{Cl})\text{SnOSn}(\text{O}_2\text{CMe})n\text{-Bu}_2]_2$	–158.0, –186.8	[91]
14	$[n\text{-Bu}_2(\text{Cl})\text{SnOSn}(\text{OPh})n\text{-Bu}_2]_2$	–134.3, –171.9	[91]
15	$[n\text{-Bu}_2(\text{Cl})\text{SnOSn}(\text{OMe})n\text{-Bu}_2]_2$	–152.8, –176.3	[91]
16	$[n\text{-Bu}_2(\text{MeCO}_2)\text{SnOSn}(\text{OPh})n\text{-Bu}_2]_2$	–195.6, –203.2	[91]
17	$[n\text{-Bu}_2(\text{MeCO}_2)\text{SnOSn}(\text{OMe})n\text{-Bu}_2]_2$	–180.6, –216.0	[91]
18	$[n\text{-Bu}_2(\text{CF}_3\text{CO}_2)\text{SnOSn}(\text{OPh})n\text{-Bu}_2]_2$	–170.9, –182.5	[91]
19	$[\{n\text{-Bu}_2\text{Sn}(\text{Cl})\}_2\text{O} \cdot n\text{-Bu}_2(\text{Cl})\text{SnOSn}(\text{O}_2\text{CMe})n\text{-Bu}_2]$	–93.7, –146.9, –155.7, –178.1	[91]
20	$[\{n\text{-Bu}_2\text{Sn}(\text{O}_2\text{CMe})\}_2\text{O} \cdot n\text{-Bu}_2(\text{Cl})\text{SnOSn}(\text{O}_2\text{CMe})n\text{-Bu}_2]$	–158.9, –181.5, –218.4, –223.8	[91]
21	$[\{n\text{-Bu}_2\text{Sn}(\text{Cl})\}_2\text{O} \cdot n\text{-Bu}_2(\text{Cl})\text{SnOSn}(\text{OPh})n\text{-Bu}_2]$	–87.1, –132.2, –132.7, –180.2	[91]
22	$[\{n\text{-Bu}_2\text{Sn}(\text{OPh})\}_2\text{O} \cdot n\text{-Bu}_2(\text{Cl})\text{SnOSn}(\text{OPh})n\text{-Bu}_2]$	–135.7, –171.2, –175.4, –179.2	[91]
23	$[\{n\text{-Bu}_2\text{Sn}(\text{Cl})\}_2\text{O} \cdot n\text{-Bu}_2(\text{Cl})\text{SnOSn}(\text{OMe})n\text{-Bu}_2]$	–88.4, –134.1, –147.2, –181.7	[91]
24	$[\{n\text{-Bu}_2\text{Sn}(\text{OMe})\}_2\text{O} \cdot n\text{-Bu}_2(\text{Cl})\text{SnOSn}(\text{OMe})n\text{-Bu}_2]$	–156.2, –172.3, –179.6, –185.6	[91]
25	$[\{n\text{-Bu}_2\text{Sn}(\text{O}_2\text{CMe})\}_2\text{O} \cdot n\text{-Bu}_2(\text{O}_2\text{CMe})\text{SnOSn}(\text{OPh})n\text{-Bu}_2]$	–200.8, –216.6, –219.8, –224.1	[91]
26	$[\{n\text{-Bu}_2\text{Sn}(\text{OPh})\}_2\text{O} \cdot n\text{-Bu}_2(\text{O}_2\text{CMe})\text{SnOSn}(\text{OPh})n\text{-Bu}_2]$	–179.8, –185.8, –193.4, –202.1	[91]
27	$[\{n\text{-Bu}_2\text{Sn}(\text{O}_2\text{CMe})\}_2\text{O} \cdot n\text{-Bu}_2(\text{O}_2\text{CMe})\text{SnOSn}(\text{OMe})n\text{-Bu}_2]$	–200.7, –208.8, –218.0, –232.2	[91]
28	$[\{n\text{-Bu}_2\text{Sn}(\text{OMe})\}_2\text{O} \cdot n\text{-Bu}_2(\text{O}_2\text{CMe})\text{SnOSn}(\text{OMe})n\text{-Bu}_2]$	–171.6, –172.3, –181.6, –216.3	[91]
29	$[\{n\text{-Bu}_2\text{Sn}(\text{OPh})\}_2\text{O} \cdot n\text{-Bu}_2(\text{OPh})\text{SnOSn}(\text{O}_2\text{CCF}_3)n\text{-Bu}_2]$	–168.8, –173.6, –175.8, –184.5	[91]

^a Values in paranthesis are for solid-state measurements.

^b Major peaks.

is $-\text{CH}_2-\text{Si}(\text{Me})_2-\text{CH}_2-$ only the dimer (Fig. 34B) seems to predominate [98].

3.4. Triflic acid mediated synthesis of four-membered $[\text{Sn}-\text{O}]_2$ rings and related systems

The reactions of triflic acid with diorganotin oxides have been recently investigated [100–106]. These reactions have brought about the importance of the variation of subtle synthetic factors in determining the type of organotin assembly formed. A 1:1 reaction of R_2SnO

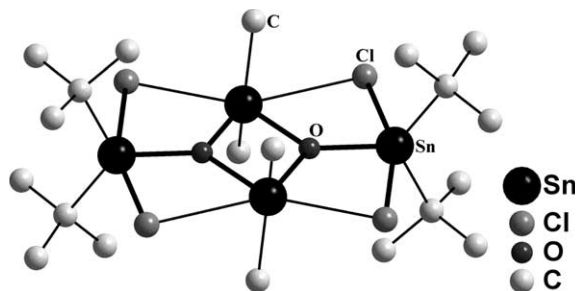


Fig. 22. X-ray structure of the mixed distannoxane dimer $[t\text{-Bu}_2(\text{Cl})\text{SnOSn}(\text{Cl})(\text{Me})_2]_2$ [92].

and $\text{CF}_3\text{SO}_3\text{H}$ in presence of small amounts of moisture afforded the compound $\text{R}_2\text{Sn}(\text{OTf})(\text{H}_2\text{O})(\text{OH})$ (R = *n*-Bu, *t*-Bu, 2-phenylbutyl) in nearly quantitative yields (Fig. 35) [100,101]. The compound with R = *n*-Bu can also be accessed from the reaction of the ladder $[\text{ClBu}_2\text{SnOBu}_2\text{Cl}]_2$ with the silver salt of triflic acid

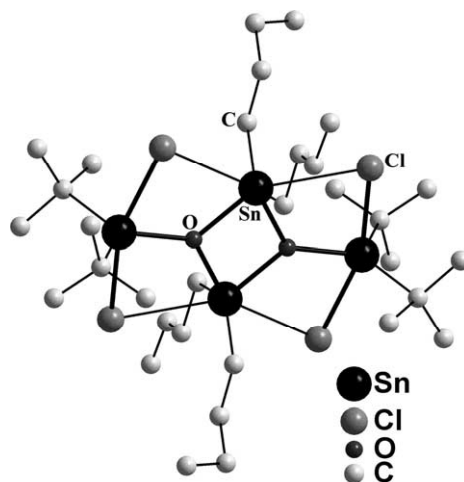
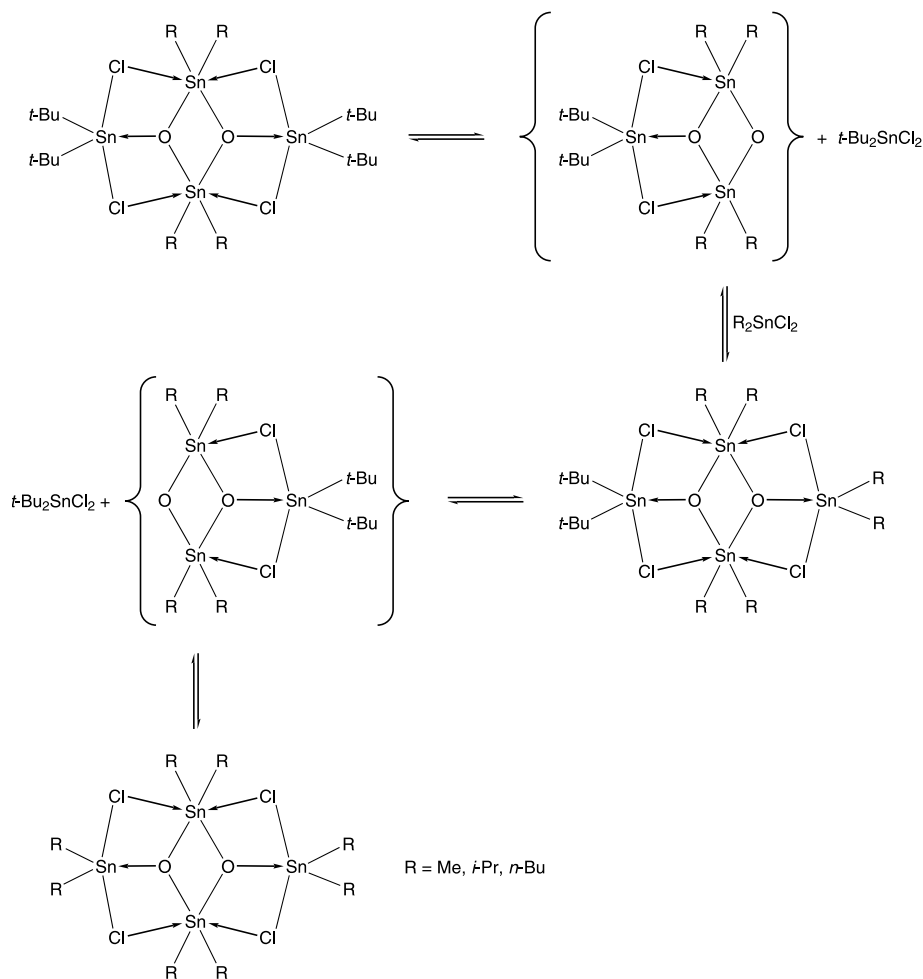
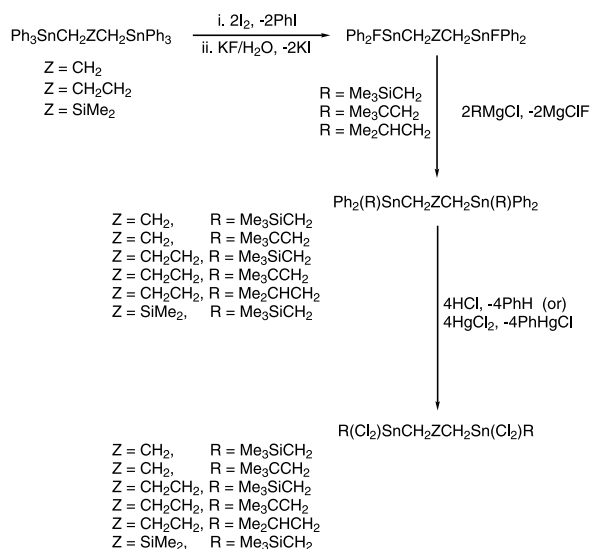


Fig. 23. X-ray structure of the mixed distannoxane dimer $[t\text{-Bu}_2(\text{Cl})\text{SnOSn}(\text{Cl})(n\text{-Bu})_2]_2$ [92].

Fig. 24. Conversion of $[t\text{-Bu}_2\text{Sn}(\text{Cl})\text{OSn}(\text{Cl})\text{R}_2]_2$ into $[\text{R}_2\text{Sn}(\text{Cl})\text{OSn}(\text{Cl})\text{R}_2]_2$ [92].

(Fig. 35). Other coordinating solvents can replace the water of solvation present in these compounds. Thus treatment of $[n\text{-Bu}_2\text{Sn}(\text{OTf})(\text{H}_2\text{O})(\text{OH})]$ with hexam-



Scheme 6.

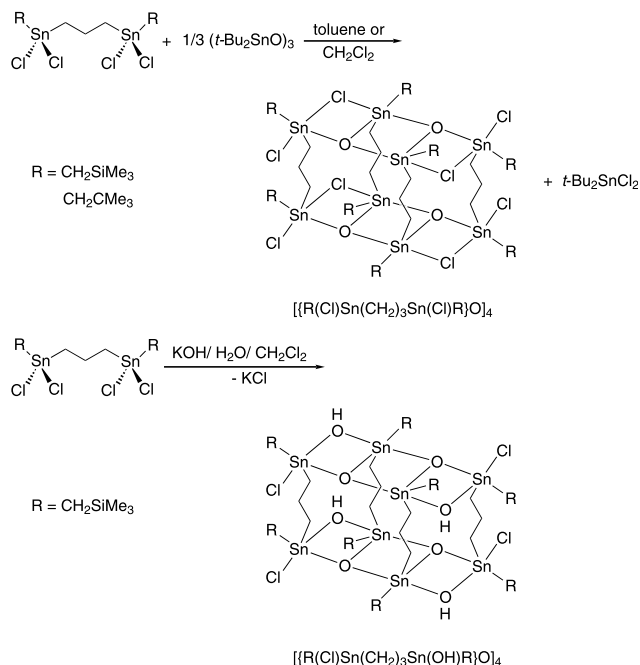


Fig. 25. Preparation of trimethylene-bridged double ladders [97].

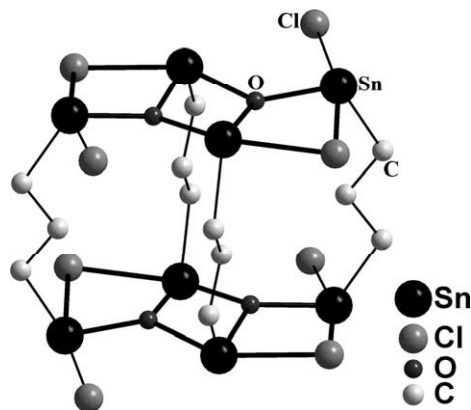


Fig. 26. X-ray structure of propylene-bridged double ladder $[\{R(Cl)Sn(CH_2)_3Sn(Cl)R\}_4]$, $R = Me_3SiCH_2$ (the R groups on Sn are not shown for clarity) [97].

ethyl phosphorus triamide (HMPA) results in the replacement of water with the more strongly coordinating HMPA [101]. The X-ray structures of these compounds reveal that they are dimeric and contain hydroxyl bridging groups. Thus the X-ray structure of $[n-Bu_2Sn(OTf)(H_2O)(OH)]_2$ is shown in Fig. 36. The X-ray structure of an analogous compound $[t-Bu_2Sn(OH)(NO_3)]_2$ [101] is shown in Fig. 37. Other diorganotin compounds having similar structures have also been found for $[t-Bu_2Sn(OH)Cl]_2$ [104], $[Me_2Sn(OH)(NO_3)]_2$ [105] and $[(C_4H_5N_3)_2(Ph_2SnOCl)_2]$ [106]. The latter is obtained in a reaction of Ph_2SnCl_2 with 2-aminopyridine in presence of water. The X-ray data for these compounds and some related derivatives are summarized in Table 11 [100–102,107,108]. The organotin triflate $[n-Bu_2Sn(OTf)(H_2O)(OH)]_2$ and related derivatives contain a Sn_2O_2 core and the geometry around tin is distorted octahedral. The Sn–O distances in the core are normal (Table 11). While the bond angle at oxygen in the core is nearly about 109° the corresponding angle at tin is considerably more acute (ca. 70°). An interesting feature of the solid-state structures of the organotin triflates is that the interaction between the oxygen of the triflate anion and tin is weak. Thus the Sn–O distance corresponding to this interaction in $[n-Bu_2Sn(OTf)(H_2O)(OH)]_2$ is 2.622 \AA [100]. Increasing the steric bulk of the alkyl substituents on tin leads to the formation of dimeric cations $[R_2Sn(OH)(H_2O)]_2[OTf]_2$

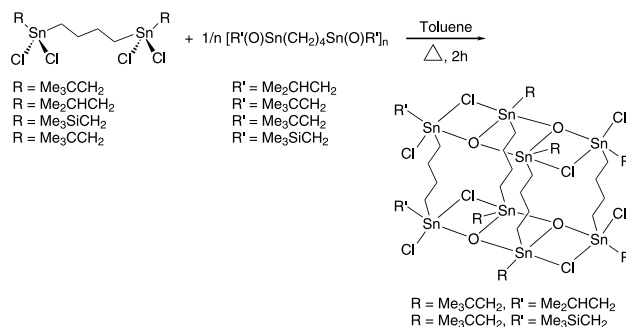


Fig. 28. Preparation of butylene-bridged mixed double ladders [98].

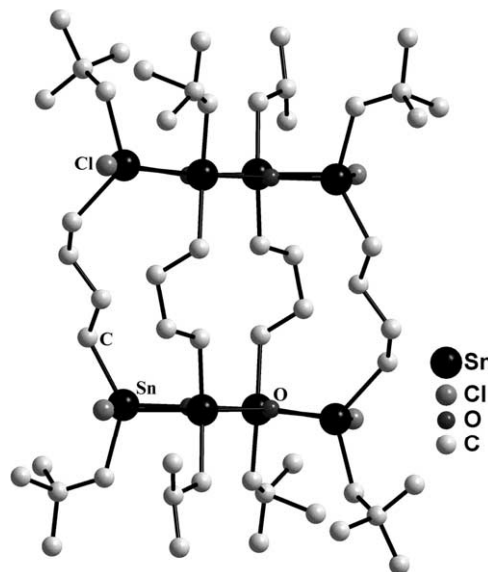


Fig. 29. X-ray structure of the butylene-bridged mixed double ladder $[\{R(Cl)Sn(CH_2)_4Sn(Cl)R\}\{R'(Cl)Sn(CH_2)_4Sn(Cl)R'\}_2]_2$, ($R = Me_3CCH_2$; $R' = Me_3SiCH_2$) [98].

($R = t\text{-Bu}$; 2-phenylbutyl) in the solid-state [101]. In these compounds the triflate anion is *not* bonded to the tin and the corresponding Sn–O distances are much larger ($4.148\text{--}4.821 \text{ \AA}$) than the sum of the *van der Waals* radii of Sn and O (3.70 \AA). In solution all the triflate derivatives (including $R = n\text{-Bu}$) behave as 1:2 electrolytes indicating the complete ionization of these compounds. In contrast the non-triflate dimers $[t-Bu_2Sn(OH)Cl]_2$ and $[t-Bu_2Sn(OH)(NO_3)]_2$ do not dissociate in solution and dimeric structures are retained.

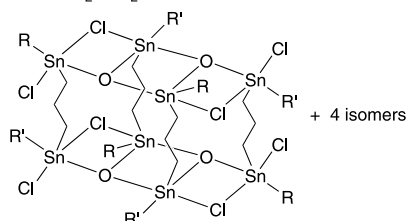
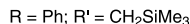
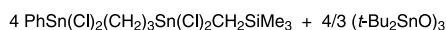


Fig. 27. Preparation of propylene-bridged mixed double ladders using $(t\text{-Bu}_2SnO)_3$ as an oxide transfer agent [98].

The variation in solution and solid-state ^{119}Sn -NMR data for $[n\text{-Bu}_2\text{Sn}(\text{OH})(\text{OTf})(\text{H}_2\text{O})]_2$ in contrast to the constant chemical shifts observed for $[t\text{-Bu}_2\text{Sn}(\text{OH})(\text{OTf})(\text{H}_2\text{O})]_2$ (Table 12) further supports the conductivity data.

The assembly of the triflate-assisted structures is dependent on the stoichiometry of the reactants and other subtle variations. Thus in a 2:1 reaction between Bu_2SnO and TfOH affords $[(\text{TfO})\text{Bu}_2\text{SnOSnBu}_2(\text{OH})]_n$. The basic structural unit of this compound is the ladder like dimeric distannoxane. Intermolecular coordination through the terminal SO_3 groups leads to a sheet-like structure made up of interconnected 24-membered macrocyclic rings (Fig. 38) [102,103].

The reaction of R_2SnO ($\text{R} = n\text{-Pr}$, $n\text{-Bu}$, $i\text{-Bu}$, $c\text{-Hex}$) with dimethyl sulfite $\text{MeOS}(\text{O})\text{OMe}$ proceeds in an Arbusov type rearrangement to afford the compound $\text{R}_2\text{Sn}(\text{OMe})\text{OS}(\text{O})_2\text{Me}$ [107]. While the structures of these compounds themselves could not be determined, reaction of these with β -diketones leads to the replacement of the OMe group to afford $[\text{R}_2\text{Sn}(\text{diket})\text{OS}(\text{O})_2\text{Me}]_2$ (diket = acetylacetonate, benzyl acetonate, dibenzoyl methanoyl). These compounds are dimeric in the solid-state; the MeSO_3 group functions as a bridging ligand to generate an over all central $\text{Sn}_2\text{O}_4\text{S}_2$ eight-membered ring (Fig. 39). The two tin centers are also part of a six-membered ring formed by the chelating β -diketonate moiety. The initially formed compound $\text{R}_2\text{Sn}(\text{OMe})\text{OS}(\text{O})_2\text{Me}$ can also undergo a facile hydrolysis to afford the hydroxy derivative, $\text{R}_2\text{Sn}(\text{OH})\text{OS}(\text{O})_2\text{Me}$. The X-ray structure of this compound ($\text{R} = n\text{-Bu}$) shows that it is made up of four-membered $[\text{Sn}\mu\text{-}(\text{OH})_2]$ units, which are linked in an intermolecular manner by the bridging sulfonate groups to afford sheet-like polymer structures. The presence of large 20-membered macrocyclic rings within the polymeric sheets is readily seen (Fig. 40) [107].

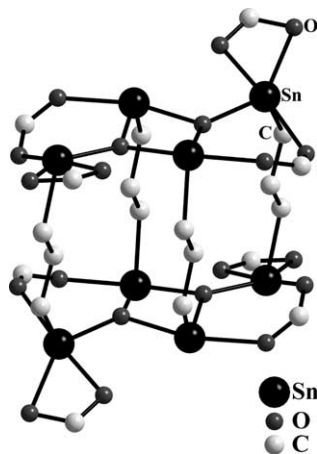


Fig. 30. X-ray structure of the acetate substituted di ladder $[\{\text{R}(\text{OAc})\text{Sn}(\text{CH}_2)_3\text{Sn}(\text{OAc})\text{R}\}]_4$, $\text{R} = \text{Me}_3\text{SiCH}_2$ (the R group on tin not shown) [96].

Table 9
X-Ray data for some spacer-bridged tetraorganodistannoxanes

Sl. no.	Compounds	R/R'	Sn–Cl _{ter} (Å)	Sn–Cl _{bri} (Å)	Sn _{endo} –O (Å)	Sn _{exo} –O (Å)	Reference
1	$[\{\text{R}(\text{Cl})\text{Sn}(\text{CH}_2)_3\text{Sn}(\text{Cl})\text{R}\}]_4$	Me_3SiCH_2	2.453(3)–2.457(3)	2.678(3)–2.728(3)	2.031(5)–2.039(5)	2.060(5)–2.135(5)	[97]
2	$[\{\text{R}(\text{Cl})\text{Sn}(\text{CH}_2)_3\text{Sn}(\text{Cl})(\text{CH}_2)_3\text{Sn}(\text{Cl})\text{R}\}]_4$	Me_3SiCH_2	2.428(5)–2.434(6)	2.616(5)–2.783(6)	2.003(11)–2.032(11)	2.127(11)–2.155(11)	[99]
3	$[\{\text{R}(\text{Cl})\text{Sn}(\text{CH}_2)_3\text{Sn}(\text{Cl})(\text{CH}_2)_3\text{Sn}(\text{Me}_2)\text{O}_2\}]_2$	Me_3SiCH_2	2.448(3)–2.463(3)	2.673(3)–2.781(3)	2.016(5)–2.055(5)	2.119(5)–2.145(5)	[99]
4	$[\{\text{R}(\text{Cl})\text{Sn}(\text{CH}_2)_3\text{Sn}(\text{Cl})\text{R}\}]_4$	Me_3CCH_2	2.437(2)–2.452(2)	2.577(2)–2.809(2)	2.020(3)–2.029(3)	2.046(3)–2.187(3)	[96]
5	$[\{\text{R}(\text{Cl})\text{Sn}(\text{CH}_2)_3\text{Sn}(\text{Cl})\text{R}\}]_4$	Me_3SiCH_2	2.497(4)–2.514(4)	2.677(3)–2.829(3)	2.010(6)–2.018(6)	2.063(7)–2.111(6)	[96]
6	$[\{\text{R}(\text{Cl})\text{Sn}(\text{CH}_2)_4\text{Sn}(\text{Cl})\text{R}\}]_2$	$\text{Me}_3\text{CCH}_2/\text{Me}_2\text{CHCH}_2$	2.435(3)–2.488(3)	2.687(3)–2.810(3)	2.017(5)–2.020(5)	2.051(5)–2.134(7)	[98]
7	$[\{\text{R}(\text{Cl})\text{Sn}(\text{CH}_2)_4\text{Sn}(\text{Cl})\text{R}\}]_2$	$\text{Me}_3\text{CCH}_2/\text{Me}_3\text{SiCH}_2$	2.474(2)–2.478(2)	2.724(2)–2.760(2)	2.009(3)–2.017(3)	2.052(3)–2.140(3)	[98]
8	$[\{\text{R}(\text{OAc})\text{Sn}(\text{CH}_2)_3\text{Sn}(\text{OAc})\text{R}\}]_4$	Me_3SiCH_2	2.208(6) ^a –2.634(7)	2.231(6) ^b –2.282(6)	2.054(5)–2.062(4)	2.027(4)–2.168(4)	[96]

ter, terminal; bri, bridging.

^a Sn–O(acetate)_{ter}.

^b Sn–O(acetate)_{bri}.

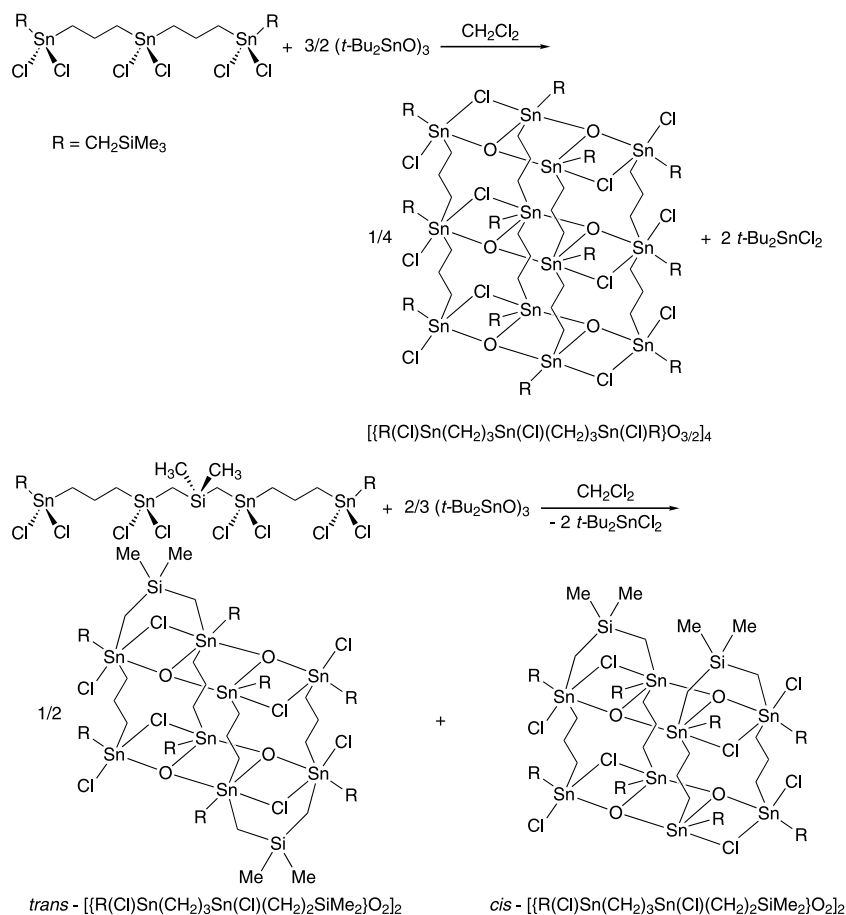


Fig. 31. Reactions of alkylene bridged tri- and di-tin precursors with the oxide transfer agent $[t\text{-Bu}_2\text{SnO}]_3$ [99].

The reaction of $n\text{-Bu}_2\text{SnO}$ with mesityl sulfonic acid in a 1:1 stoichiometry affords $[n\text{-Bu}_2\text{Sn}(\text{OSO}_2\text{C}_6\text{H}_2\text{-}2,4,6\text{-Me}_3)_2]_n$, which hydrolyzes to give $[n\text{-Bu}_2\text{Sn}(\text{OSO}_2\text{C}_6\text{H}_2\text{-}2,4,6\text{-Me}_3)(\text{OH})]_n$ [108]. Both these compounds are polymeric. The former contains an infinite array of polymeric sheets made up of $\text{Sn}_2\text{O}_4\text{S}_2$ eight-membered rings that share a common tin (Fig. 41).

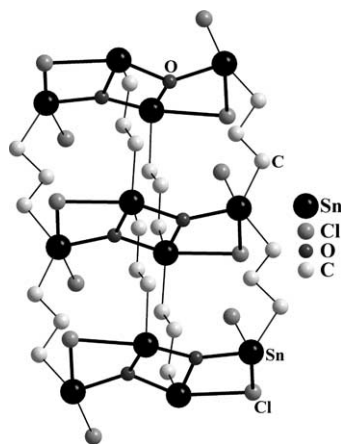


Fig. 32. X-ray structure of the propylene bridged triple ladder $[\{[\text{R}(\text{Cl})\text{Sn}(\text{CH}_2)_3\text{Sn}(\text{Cl})(\text{CH}_2)_3\text{Sn}(\text{Cl})\text{R}]_3\text{O}_{3/2}\}_4]$, $\text{R} = \text{CH}_2\text{SiMe}_3$ (the SiMe_3 substituent is not shown) [99].

In this structure the sulfonate group functions as an isobidentate bridging ligand. The immediate coordination environment around each tin contains four oxygens in a square plane and the alkyl groups are located above and below this plane in *trans* manner. The partially hydrolyzed compound $[n\text{-Bu}_2\text{Sn}(\text{OSO}_2\text{C}_6\text{H}_2\text{-}2,4,6\text{-Me}_3)(\text{OH})]_n$ is also polymeric; however, in this case the polymer consists of the four-membered $[n\text{-Bu}_2\text{Sn}(\text{OH})]_n$ units that are intermolecularly bridged by the mesityl sulfonate [108] (Fig. 42).

3.5. Reaction of R_2SnO with organoboronic acids

The reaction of $(t\text{-Bu}_2\text{SnO})_3$ with $\text{RB}(\text{OH})_2$ ($\text{R} = \text{Ph}$, $2,4,6\text{-Me}_3\text{C}_6\text{H}_2$) affords two cyclic products, a boron rich compound, $[(t\text{-Bu}_2\text{SnO})(\text{RBO})_2]$ and a tin rich compound $[\{t\text{-Bu}_2\text{Sn}(\text{OH})_2\}\{t\text{-Bu}_2\text{SnO}_2(\text{OBR})\}]$ (Fig. 43) [109]. The former resonates in the ^{119}Sn -NMR at -127.8 ($\text{R} = \text{Ph}$) or -131.6 ($\text{R} = 2,4,6\text{-Me}_3\text{C}_6\text{H}_2$) while the latter shows two distinct resonances at -260.3 and -278.5 ($\text{R} = 2,4,6\text{-Me}_3\text{C}_6\text{H}_2$). The boron rich compound exists alongside with the acyclic hydrolyzed product $t\text{-Bu}_2\text{Sn}[\text{OB}(\text{OH})\text{R}_2]$; the extent of the hydrolyzed product being as much as 84% when $\text{R} = 2,4,6\text{-Me}_3\text{C}_6\text{H}_2$. The X-ray structure of the tin rich

Table 10

¹¹⁹Sn-NMR data for some spacer-bridged tetraorganodistannoxanes

Sl. no.	Compound	R/R'	Structure	δ (¹¹⁹ Sn) ^a	Reference
1	[{R(Cl)Sn(CH ₂) ₃ Sn(Cl)R}O] ₄	Me ₃ SiCH ₂	Double ladder	−96.1, −132.9 (1:1)	[97]
2	[{R(Cl)Sn(CH ₂) ₃ Sn(OH)R}O] ₄	Me ₃ SiCH ₂	Double ladder	−96.1, −132.9 (1:1)	[97]
3	[{R(Cl)Sn(CH ₂) ₃ Sn(Cl)(CH ₂) ₃ Sn(Cl)R}O _{3/2}] ₄	Me ₃ SiCH ₂	Triple ladder	−94.0, −114.4, −134.0, −142.8 (2:1:2:1)	[99]
4	[{R(Cl)Sn(CH ₂) ₃ Sn(Cl)(CH ₂) ₂ SiMe ₂ }O ₂] ₂	Me ₃ SiCH ₂	Double ladder with <i>trans</i> CH ₂ SiMe ₂ CH ₂ bridge	−91.2, −106.7, −129.4, −141.7 (1:1:1:1)	[99]
5	[{R(Cl)Sn(CH ₂) ₃ Sn(Cl)(CH ₂) ₂ SiMe ₂ }O ₂] ₂	Me ₃ SiCH ₂	Double ladder with <i>cis</i> CH ₂ SiMe ₂ CH ₂ bridge	−99.4, −121.3, −133.7, −141.3 (1:1:1:1)	[99]
6	[{R(Cl)Sn(CH ₂) ₃ Sn(Cl)R}O] ₄	Me ₃ CCH ₂	Double ladder	−106.0, −155.1	[96]
7	[{R(Cl)Sn(CH ₂) ₄ Sn(Cl)R}O] ₄	Me ₃ SiCH ₂	Double ladder ^b	−68.1 (48%), −143.0 (48%) −68.9 (2%), −141.2 (2%)	[96]
8	[{R(Cl)Sn(CH ₂) ₄ Sn(Cl)R}O] ₄	Me ₃ CCH ₂	Double ladder ^b	−84.7 (25%), −152.5 (25%) −86.1 (25%), −153.0 (25%)	[96]
9	[{R(Cl)Sn(CH ₂) ₄ Sn(Cl)R}O] ₄	Me ₂ CHCH ₂	Double ladder ^b	−77.6 (10%), −147.2 (10%) −78.8 (10%), −149.8 (40%)	[96]
10	[{R(Cl)Sn(CH ₂) ₂ SiMe ₂ Sn(Cl)R}O] ₄	Me ₃ SiCH ₂	Spacer bridged ladder	−60.6, −116.6 (1:1)	[96]
11	[{R(OAc)Sn(CH ₂) ₃ Sn(OAc)R}O] ₄	Me ₃ SiCH ₂	Double ladder with acetate bridges ^b	−169.0 (45%), 202.0 (45%) −194.9 (5%), −224.4 (5%)	[96]
12	[{R(Cl)Sn(CH ₂) ₄ Sn(Cl)R} ₂ {R'(Cl)Sn(CH ₂) ₄ Sn(Cl)R'} ₂ O ₂] ₂	Me ₃ CCH ₂ /Me ₂ CHCH ₂	Mixed double ladder ^c	−83.0 (36%), −145.2 (35%) −78.2 (7%), −144.4 (14%) −84.2 (7%), −146.9 (1%)	[98] [98]
13	[{R(Cl)Sn(CH ₂) ₄ Sn(Cl)R} ₂ {R'(Cl)Sn(CH ₂) ₄ Sn(Cl)R'} ₂ O ₂] ₂	Me ₃ CCH ₂ /Me ₃ -SiCH ₂	Mixed double ladder ^c	−84.5 (27%), −140.7 (33%) −87.0 (11%), −139.5 (10%) −68.5 (5%), −144.9 (5%) −70.6 (1%), −143.2 (2%) −83.8 (5%), −85.6 (1%)	

^a Values in paranthesis indicate the intensity ratio of the signals.^b A mixture of a major and a minor compound.^c A mixture of one major and other minor products.

product shows that a μ_3 -O atom holds three tins together. The structure may be described as tricyclic and consists of a six-membered Sn₂BO₃ and two four-membered Sn₂O₂ rings (Fig. 44) [109].

3.6. Reactions of R₂SnO with carboxylic acids

The reactions of diorganotin oxides, R₂SnO with carboxylic acids, R'COOH have been studied in con-

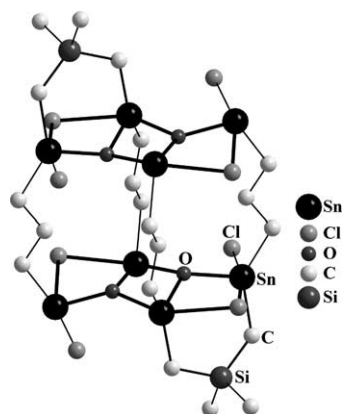
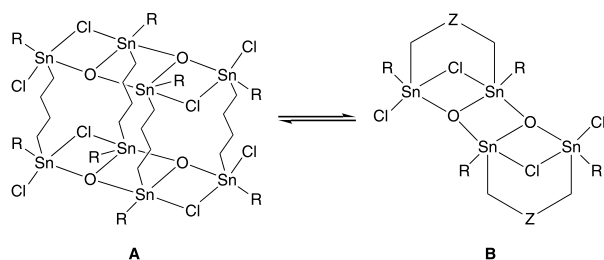


Fig. 33. X-ray structure of the *trans* double ladder $[\{R(Cl)Sn(CH_2)_3Sn(Cl)CH_2\}_2SiMe_2]O_2$, $R = CH_2SiMe_3$ (the $SiMe_3$ group is not shown) [99].



$R = Me_3SiCH_2, Me_3CCH_2, Me_2CHCH_2$; $Z = CH_2CH_2, SiMe_2$

Fig. 34. Double ladder—ladder equilibrium [98].

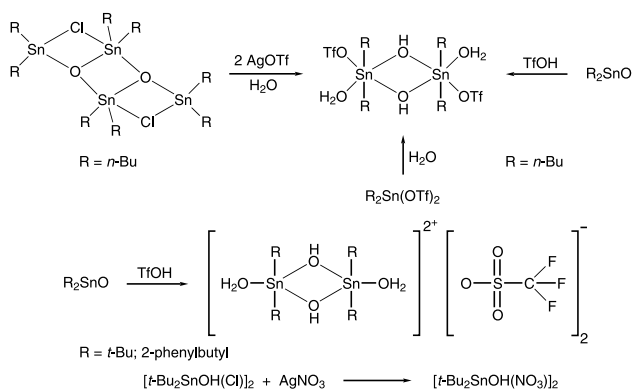


Fig. 35. Preparative routes for the assembly of dimeric diorganotin triflates and related derivatives [100,101].

siderable detail and depending on the carboxylic acid and the stoichiometry of the reaction several products are possible. The first step of the reaction is likely to generate $[R_2Sn(OH)(O_2CR')]$ which can self-condense by losing water to generate $[R_2(O_2CR')SnO-Sn(O_2CR')R_2]$ or react with another molecule of carboxylic acid to afford the dicarboxylate $R_2Sn(O_2CR')_2$. The 1:1 reaction product $[R_2(O_2CR')SnOSn(O_2CR')R_2]$ is usually dimeric. These reactions are summarized in Scheme 7. This account deals with only these two types

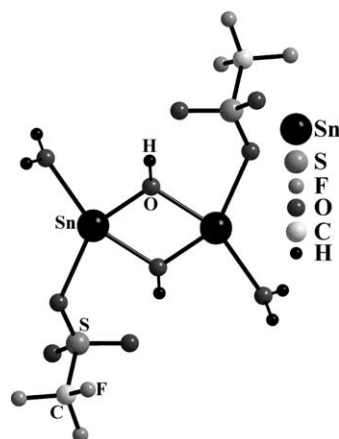


Fig. 36. X-ray structure of $[n-Bu_2Sn(OH)(OSO_2CF_3)(H_2O)]_2$ [100].

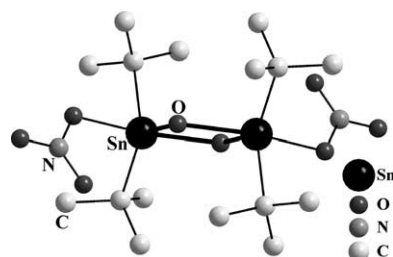


Fig. 37. X-ray structure of $[t-Bu_2Sn(OH)(NO_3)]_2$ [101].

of carboxylates. Other types diorganotin carboxylates that are not discussed in this account include $[R_2Sn(O_2CR')]_n$ and $[R_2Sn(O_2CR')X]$. Also, diorganotin carboxylates formed from the reactions of dicarboxylic acids are also not dealt here. Two comprehensive and critical reviews on the structural aspects of organotin carboxylates have appeared earlier [20,21].

The dicarboxylates $R_2Sn(O_2CR')_2$ are monomeric and the tin is hexa-coordinate in a skewed trapezoidal bipyramid geometry resulting from a chelating anisobidentate coordination mode of the two dicarboxylate ligands (Table 13) [110–113]. The shorter Sn–O bond distance corresponds to the normal covalent Sn–O bond distance while the longer bond distance varies from 2.48 to 2.71 Å. A representative X-ray structure of $n-Bu_2Sn[O_2CC_6H_3-2-NH_2-5-Cl]_2$ [112] is given in Fig. 45. The ^{119}Sn -NMR of the dicarboxylates shows a single resonance (Table 14) [56,110,113–115]. Recently a mixed chelate diorganotin compound has been prepared in reaction with di-*n*-butyltin oxide with 2,6-pyridinedicarboxylic acid followed by reaction with bis(dicyclohexylammonium)oxalate. In this compound the tin is seven-coordinate and is pentagonal bipyramid. The equatorial plane is made of chelating oxalate (O_2) and pyridine-2,6-dicarboxylate (O_2N). The two *trans* axial sites are occupied by the alkyl groups [116].

Table 11
X-Ray data for some diorganotin sulfonates

Sl. no.	Compound	Sn–O _{Hydroxy} (Å)	Sn–O _{Water} (Å)	Sn–O _{Sulfur} (Å)	Reference
1	[<i>n</i> -Bu ₂ Sn(OH)(Otf)(H ₂ O)] ₂	2.085(3)–2.147(3)	2.409(3)	2.622(4)	[100]
2	[<i>t</i> -Bu ₂ Sn(OH)(Otf)(H ₂ O)] ₂	2.044(4)–2.181(4)	2.294(5)	4.148–4.821	[101]
3	[{(2-Ph) <i>n</i> -Bu} ₂ Sn(OH)(Otf)(H ₂ O)] ₂	2.035(7)–2.193(6)	2.255(8)–2.278(8)	3.859–4.294	[101]
4	[<i>n</i> -Bu ₂ Sn(OH)(Otf)(HMPA)] ₂	2.070(1)–2.170(1)	2.290(1)–2.100(1) ^a	2.820(1)–2.880(2)	[101]
5	[<i>t</i> -Bu ₂ Sn(OH)(NO ₃) ₂]	2.048(3)–2.187(2)	2.224(2)–3.060(2) ^b	–	[101]
6	[(Otf)(<i>n</i> -Bu) ₂ SnOSn(<i>n</i> -Bu) ₂ (OH)] ₂ ^c	2.063(3)–2.263(4)	–	2.691(5)–2.685(5)	[102]
7	<i>n</i> -Bu ₂ Sn(acac)OS(O) ₂ Me	–	2.117(4)–2.157(5) ^d	2.379(5)–2.431(4)	[107]
8	<i>n</i> -Bu ₂ Sn(OH)OS(O) ₂ Me	2.085(4)–2.122(4)	–	2.410(4)–2.492(4)	[107]
9	[(<i>n</i> -Bu) ₂ Sn{μ-OSO ₂ C ₆ H ₂ (Me) ₃ } ₂] _n	–	–	2.199(3)–2.313(3)	[108]
10	[(<i>n</i> -Bu) ₂ Sn{(μ-OH)μ-OSO ₂ C ₆ H ₂ (Me) ₃ } ₂] _n	2.066(8)–2.107(6)	–	2.399(2)–2.783(3)	[108]

^a Sn–O_{HMPA}.

^b Sn–O_{Nitrate}.

^c It has the ladder type structure. The Sn_{exo}–O distance is 2.040(3)–2.059(3) Å and the Sn_{endo}–O distance is 2.049(3)–2.133(3) Å.

^d Sn–O_{acac}.

Other types of dicarboxylates have also been described such as, Me₂Sn(O₂CH)₂ (polymeric sheet like structure because of *bridging* carboxylate) [117], Ph₂Sn(O₂CC₅H₄N-2)₂ (discrete structure involving chelating binding to tin through the pyridyl nitrogen and the oxygen atom of COO) [118], [Me₂Sn(O₂C₅H₄N-2)]_n

(polymeric chain type structure) [119], [*n*-Bu₂Sn(O₂CCH₂C₆H₅)₂(OH)₂] (discrete hepta-coordinate structure) [120] and [(CH₂=CH)₂Sn(O₂CCF₃)₂(bipy)] (discrete structure; six-coordinate tin; monodentate carboxylate ligands and chelating bipyridyl ligand) [121]. The Mössbauer spectra of the diorganotin dicar-

Table 12
¹¹⁹Sn-NMR data for diorganotin triflates and related compounds

Sl. no.	Compound	δ ^a	Reference
1	[<i>n</i> -Bu ₂ Sn(OH)(Otf)(H ₂ O)] ₂ ^b	–210 (–241.6)	[101]
2	[<i>t</i> -Bu ₂ Sn(OH)(Otf)(H ₂ O)] ₂ ^b	–250 (–253.0, –254.1)	[101]
3	[{(2-Ph) <i>n</i> -Bu} ₂ Sn(OH)(Otf)(H ₂ O)] ₂ ^b	–188.4	[101]
4	[<i>n</i> -Bu ₂ Sn(OH)(Otf)(HMPA)] ₂	–224.4	[101]
5	[<i>t</i> -Bu ₂ Sn(OH)(NO ₃) ₂]	–293.6	[101]
6	[(Otf)Et ₂ SnOSnEt ₂ (OH)] ₂	–152, –156	[102]
7	[(Otf)(<i>n</i> -Bu) ₂ SnOSn(<i>n</i> -Bu) ₂ (OH)] ₂	–146, –150	[102]
8	[(Otf)(C ₈ H ₁₇) ₂ SnOSn(C ₈ H ₁₇) ₂ (OH)] ₂	–149, –152	[102]
9	[Et ₂ Sn(OH)(Otf)(H ₂ O)] ₂	–214	[102]
10	[(C ₈ H ₁₇) ₂ Sn(OH)(Otf)(H ₂ O)] ₂	–205	[102]
11	[<i>n</i> -Bu ₂ Sn{(Otf) <i>n</i> -Bu ₂ Sn(OH) ₂ } ₂]	–137, –170	[102]
12	Et ₂ Sn(Otf) ₂	–367	[102]
13	<i>n</i> -Bu ₂ Sn(Otf) ₂	–342/–342	[102]
14	(C ₈ H ₁₇) ₂ Sn(Otf) ₂	–343/–343	[102]
15	[(<i>n</i> -Bu) ₂ Sn{μ-OSO ₂ C ₆ H ₂ (Me) ₃ } ₂] _n	–342.9	[108]
16	[(<i>n</i> -Bu) ₂ Sn{(μ-OH)μ-OSO ₂ C ₆ H ₂ (Me) ₃ } ₂] _n	–324.1	[108]
17	[<i>n</i> -Pr ₂ Sn(OMe)OS(O) ₂ Me]	–181.7	[107]
18	[<i>n</i> -Bu ₂ Sn(OMe)OS(O) ₂ Me]	–181.4	[107]
19	[<i>i</i> -Bu ₂ Sn(OMe)OS(O) ₂ Me]	–178.9	[107]
20	[(C ₆ H ₁₁) ₂ Sn(OMe)OS(O) ₂ Me]	–262.7	[107]
21	[<i>n</i> -Pr ₂ Sn(acac)OS(O) ₂ Me]	–242.1	[107]
22	[<i>n</i> -Bu ₂ Sn(acac)OS(O) ₂ Me]	–239.3	[107]
23	[<i>n</i> -Pr ₂ Sn(bzac)OS(O) ₂ Me]	–239.9	[107]
24	[<i>n</i> -Bu ₂ Sn(bzac)OS(O) ₂ Me]	–246.3	[107]
25	[<i>n</i> -Pr ₂ Sn(bzac)OS(O) ₂ Me]	–270.6	[107]
26	[<i>n</i> -Bu ₂ Sn(bzbz)OS(O) ₂ Me]	–274.0	[107]
27	[<i>i</i> -Bu ₂ Sn(bzbz)OS(O) ₂ Me]	–231.7	[107]
28	[<i>n</i> -Pr ₂ Sn(OH)OS(O) ₂ Me]	–188.2, –182.9, –176.4, –175.6, –169.9, –163.1	[107]
29	[<i>n</i> -Bu ₂ Sn(OH)OS(O) ₂ Me]	–189.3, –182.9, –175.3, –172.8, –168.3, –162.7	[107]
30	[<i>i</i> -Bu ₂ Sn(OH)OS(O) ₂ Me]	–176.9, –171.6, –148.0	[107]

^a The values in parentheses are solid-state values.

^b These compounds behave as 1:2 electrolytes in solution.

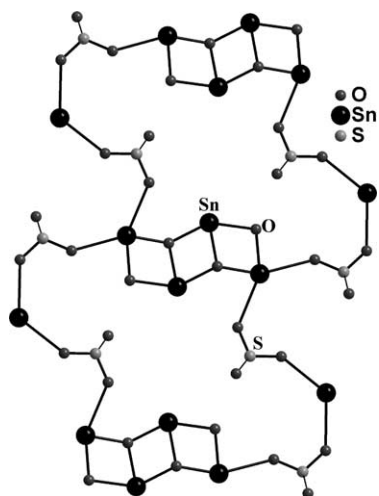


Fig. 38. The X-ray structure of $[\{n\text{-Bu}_2\text{Sn}(\text{OSO}_2\text{CF}_3)\text{Sn}(\text{OH})n\text{-Bu}_2\}_2]_n$ showing a sheet like polymeric structure (the alkyl groups are omitted from tin and sulfur) [102,103].

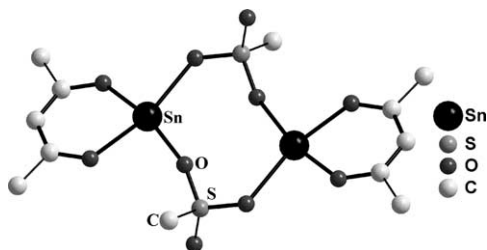


Fig. 39. X-ray structure of $[\text{R}_2\text{Sn}(\text{acac})\text{OSO}_2\text{Me}]_2$, $\text{R} = n\text{-Bu}$, acac = acetyl acetonate (the alkyl groups on tin have been omitted) [107].

boxylates are characterized by high quadrupole splitting parameters indicative of the higher coordination number in these types of compounds. Data on selected diorganotin dicarboxylates is presented in Table 15 [56,110,122,123].

Several X-ray structures of the diorganotin carboxylates $[\text{R}_2(\text{O}_2\text{CR}')\text{SnOSn}(\text{O}_2\text{CR}')\text{R}_2]_2$ obtained from the 1:1 reaction have been determined. Tiekink has classified these structures into four major types [20]. Following this classification some representative X-ray data of compounds belonging to Type I, II and IV are summarized in Tables 16–18 [68,110,113,115,123–132]. The common feature of all the structures is presence of the central distannoxane motif. The differences in the structural types arise from the mode of binding of the carboxylate ligand. The various modes of the carboxylate binding are shown in Tables 16–18. Other structural types also are formed because of the presence of heteroatoms on the carboxylate moiety [20,21]. Representative X-ray structures of compounds belonging to Type I, II and IV are shown in Figs. 46–48. $[\{\text{Me}_2\text{Sn}(\text{O}_2\text{CCH}_3)\}_2\text{O}]_2$ belongs to a different structural type (Type III) [133]. In this compound the mode of binding of each carboxylate ligand is different (Fig. 49). It appears that the energy differences between these

various structural types are very small and the preference for a particular carboxylate to adopt a type of structure seems to stem from a combination of very subtle factors.

In solution also the integrity of the compounds $[\text{R}_2(\text{O}_2\text{CR}')\text{SnOSn}(\text{O}_2\text{CR}')\text{R}_2]_2$ seem to be retained; two chemical shifts corresponding to the exo and the endo tins are seen. The exact assignment of these chemical shifts has to be done with care by using 2D NMR experiments; 2D gradient assisted ^1H – ^{119}Sn HMQC experiments have to be carried out in each case to clearly assign the chemical shifts. Thus, such an experiment for $[\{\text{Me}_2\text{Sn}(\text{O}_2\text{C}-t\text{-Bu})\}_2\text{O}]_2$ suggests that a peak at -194.8 corresponds to the exo tins while the peak at -187.8 corresponds to the endo tins. However, based on a similar experiment the assignment for $[\{\text{Me}_2\text{Sn}(\text{O}_2\text{C}-\text{Me})\}_2\text{O}]_2$ is reversed: the low frequency signal at -190.2 ppm is assigned to the endo tins while the high frequency signal at -173.8 ppm is assigned to the exo tins [128]. Solution ^{119}Sn -NMR data for

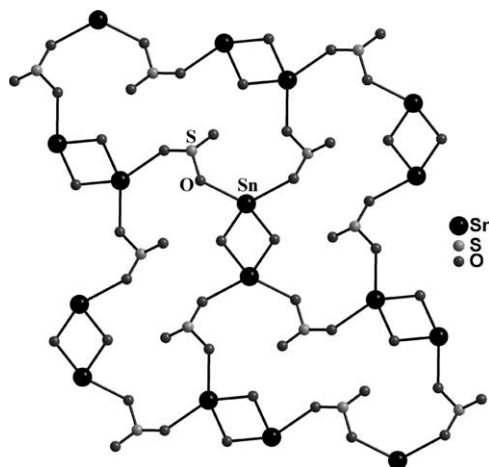


Fig. 40. The X-ray structure of $[\{\text{R}_2\text{Sn}(\mu\text{-OH})\text{OSO}_2\text{Me}\}_2]_n$, $\text{R} = n\text{-Bu}$ showing the distannoxane units linked intermolecularly by the methyl sulfonate (the alkyl groups on tin and sulfur have been omitted) [107].

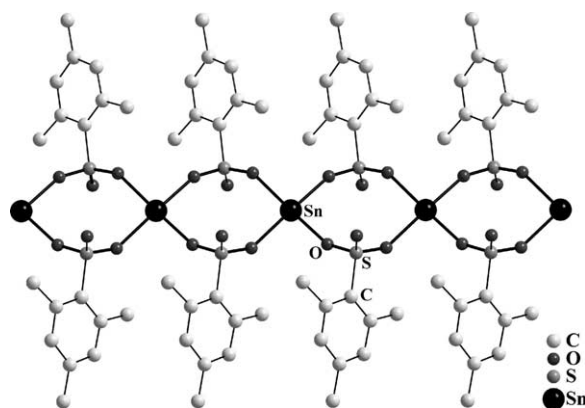


Fig. 41. The X-ray structure of $[(n\text{-Bu}_2\text{Sn}(\mu\text{-OSO}_2\text{C}_6\text{H}_2\text{-2,4,6-Me}_3)_2)]_n$ (the alkyl groups on tin have been omitted) [108].

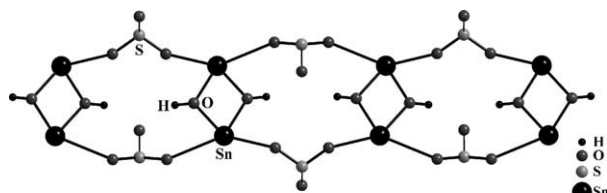


Fig. 42. The X-ray structure of $[n\text{-Bu}_2\text{Sn}(\mu\text{-OH})(\mu\text{-OSO}_2\text{C}_6\text{H}_2\text{-2,4,6-Me}_3)]_n$ (the alkyl groups on tin and the aromatic substituent on sulfur have been omitted) [108].

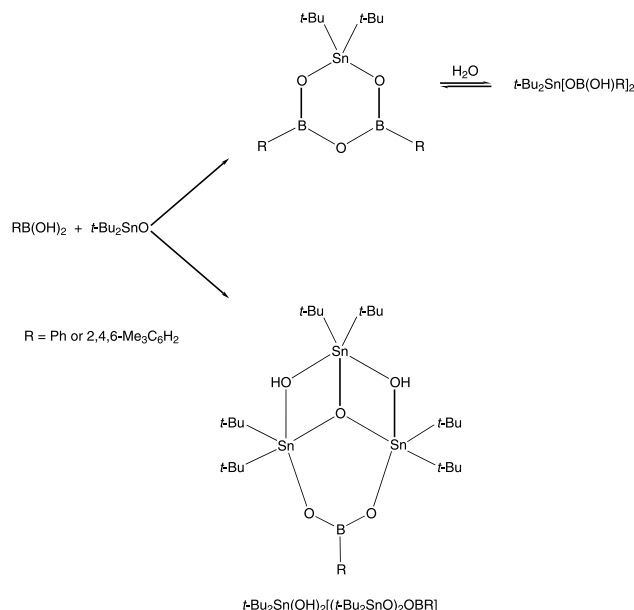


Fig. 43. The formation of Sn–O–B heterocyclic ring in the reaction between $\text{RB}(\text{OH})_2$ and $(t\text{-Bu}_2\text{SnO})_3$ [109].

representative examples of $[\text{R}_2(\text{O}_2\text{CR}')\text{SnOSn}(\text{O}_2\text{>CR}')\text{R}_2]_2$ are summarized in Table 19 [57,110,113,114,124,125,127,128,131]. The Mössbauer data for these compounds are summarized in Table 20 [56,110,115,122,123,125,129,126]. While most of the compounds show two distinct quadrupole splitting parameters corresponding to the exo and endo tins others show only one quadrupole splitting parameter. The latter is suggestive of the near similar coordination environments in these compounds for the two types of tins.

3.6.1. $(n\text{-Bu}_2\text{SnO}_2\text{CCCl}_3)_2(\mu_2\text{-OH})(\text{O}_2\text{CCCl}_3)$

Recently an interesting 2:3 (tin–carboxylate) product has been isolated in a 1:2 reaction reaction between $n\text{-Bu}_2\text{SnO}$ and CCl_3COOH (Fig. 50). The X-ray structure of this product shows that the two tin units are bridged by a hydroxyl group and a isobidentate carboxylate group. This arrangement generates a six-membered heterocyclic $\text{Sn}_2\text{O}_3\text{C}$ ring. Each tin also has a unidentate carboxylate (Fig. 51) [134].

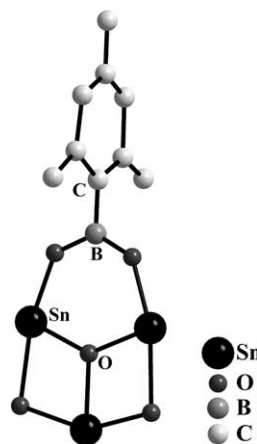
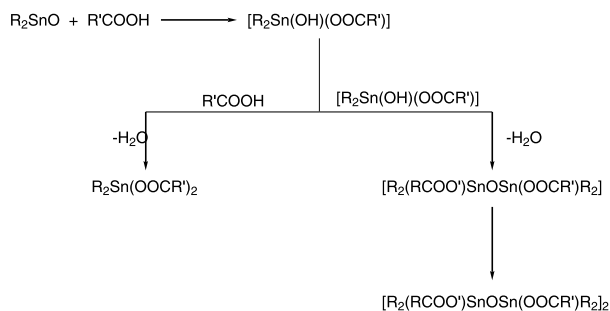


Fig. 44. The X-ray structure of $[\{t\text{-Bu}_2\text{SnOH}\}\{(t\text{-Bu}_2\text{SnO})_2(\text{OBR})\}]$, $\text{R} = 2,4,6\text{-Me}_3\text{C}_6\text{H}_2$ (the alkyl groups on tin have been omitted) [109].



Scheme 7.

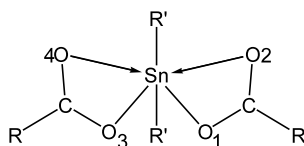
3.6.2. $[n\text{-Bu}_2\text{Sn}(\text{pyridine-2-phosphonate-6-carboxylate})]_2$

The reaction of tetra- n -butyldi- n -propoxydistannoxane, $n\text{-Bu}_2\text{Sn}(\text{O-Pr-}n)\text{OSn}(\text{OPr-}n)n\text{-Bu}_2$ (generated in situ by the reaction $n\text{-Bu}_2\text{SnO}$ with *iso*-propanol [135,136]) with dihydrogenpyridine-2-phosphonate-6-carboxylate in a 1:1 ratio affords $[n\text{-Bu}_2\text{Sn}(\text{pyridine-2-phosphonate-6-carboxylate})]_2$ in a very high yield (Fig. 52) [136]. The X-ray structure of this compound is shown in Fig. 53. The structure is a centrosymmetric dimer built around an Sn_2O_2 core. Each tin is bound by the dianionic ligand in a tridentate manner. However, each carboxyl oxygen of the ligand functions in a μ_2 -bridging manner to generate the central distannoxane core. Thus, the over all geometry around tin is based on a pentagonal bipyramid; the two alkyl groups attached to the tin are *trans* to each other and occupy the axial position.

3.6.3. $[(\text{PhCH}_2)_2\text{Sn}\{\text{O}_2\text{P}(c\text{-Hex})_2\}_2\{(c\text{-Hex})_2\text{PO}_2\text{H}\}_2]$

The reactions of dibenzyltin dichloride, $(\text{C}_6\text{H}_5\text{CH}_2)_2\text{SnCl}_2$ with silver salts of phosphinic acids and carboxylic acids have been studied [137]. Some of these lead to products resulting from an Sn–C bond

Table 13

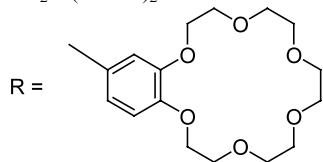
X-Ray data for some selected diorganotin dicarboxylates, $R_2Sn(O_2CR')_2$ 

Sl. no.	Compound	Sn–O1 (Å)	Sn–O2 (Å)	Reference
1	$n\text{-Bu}_2\text{Sn}[O_2CC_5H_3N(SMe-2)]_2$	2.103(5); 2.123(5)	2.711(5); 2.579(5)	[110]
2	$n\text{-Bu}_2\text{Sn}[O_2CC_6H_3(OH)_2-2,4]_2$	2.110(4); 2.124(4)	2.559(4); 2.508(4)	[111]
3	$n\text{-Bu}_2\text{Sn}[O_2CC_6H_3(NH_2-2, Cl-5)]_2$	2.123(4); 2.123(4)	2.484(5); 2.484(5)	[112]
4	$[Me_2Sn(O_2CC_6H_4NH_2-p)]_2$	2.077(3); 2.097(3)	2.556(3); 2.543(3)	[113]

Table 14

 ^{119}Sn -NMR data for some diorganotin dicarboxylates, $R_2Sn(O_2CR')_2$

Sl. no.	Compound	δ	Reference
1	$Me_2Sn(O_2CCHCHC_4H_3O)_2$	–123.0	[114]
2	$Me_2Sn[O_2CC_6H_4NH_2-p]_2$	–226.0	[113]
3	$Et_2Sn[O_2CC_5H_3N(SMe-2)]_2$	–138.9	[110]
4	$n\text{-Bu}_2Sn[O_2CC_5H_3N(SMe-2)]_2$	–133.7	[110]
5	$n\text{-Bu}_2Sn(O_2CCHCHC_4H_3O)_2$	–152.0	[114]
6	$n\text{-Bu}_2Sn[O_2CC_6H_3(OH)_2-2,4]_2$	–128.0	[115]
7	$n\text{-Bu}_2Sn(OCOR)_2$	–156.2	[56]



8	$n\text{-Bu}_2Sn(OCOR)_2$	–156.8	[56]
---	---------------------------	--------	------

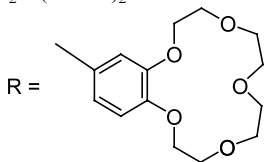
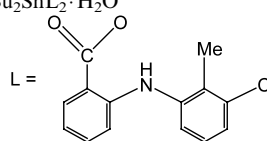


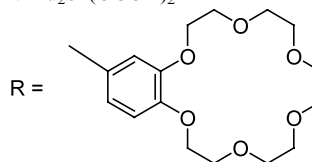
Table 15

Mössbauer data for some diorganotin dicarboxylates

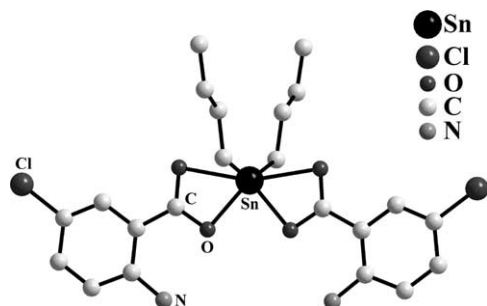
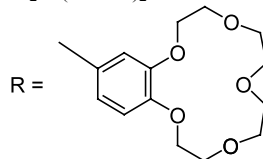
Sl. no.	Compound	δ (mm s $^{-1}$)	ΔE_Q (mm s $^{-1}$)	Reference
1	$Me_2Sn(O_2CCH_2S_2CNMe_2)_2$	1.31	3.80	[122]
2	$Et_2Sn[O_2CC_5H_3N(2-SMe)]_2$	1.51	3.71	[110]
3	$n\text{-Bu}_2Sn(O_2CCH_2S_2CNMe_2)_2$	1.47	3.92	[122]
4	$n\text{-Bu}_2Sn[O_2CC_5H_3N(2-SMe)]_2$	1.48	3.61	[110]
5	$Bu_2SnL_2 \cdot H_2O$	1.34	3.32	[123]



6	$n\text{-Bu}_2Sn(OCOR)_2$	1.39	3.40	[56]
---	---------------------------	------	------	------



7	$n\text{-Bu}_2Sn(OCOR)_2$	1.41	3.28	[56]
---	---------------------------	------	------	------

Fig. 45. The X-ray structure of $[n\text{-Bu}_2Sn(O_2CR)_2]$, $R = 2,5\text{-Cl}_2\text{-C}_6\text{H}_3$ [112].

scission. One of the products obtained in this reaction is $[(\text{PhCH}_2)_2\text{Sn}\{O_2P(c\text{-Hex})_2\}_2\{(c\text{-Hex})_2\text{PO}_2\text{H}\}_2]$ where the Sn–C bonds cleavage does not occur (Fig. 54). In this mononuclear diorganotin phosphinate, two molecules of phosphinic acid are found to co-crystallize. These are held in place as a result of intramolecular hydrogen bonding to the phosphoryl group of the covalently bound phosphinate unit. In addition the P=

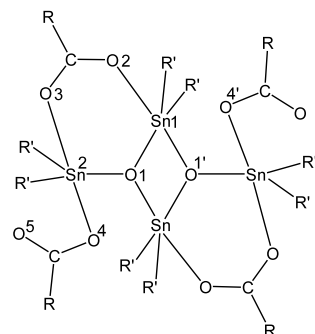
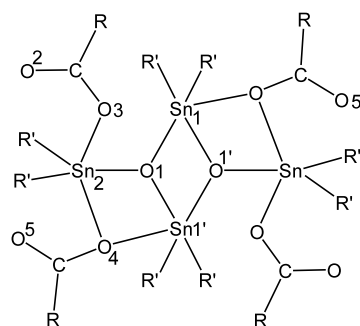
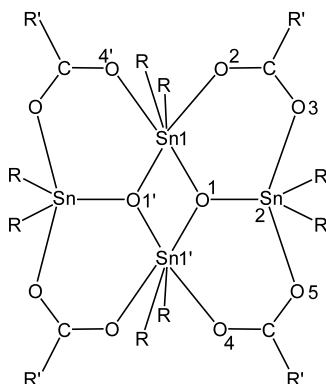
X-Ray data for some Type I diorganotin carboxylates, $[\{R'_2SnO_2CR\}_2O]_n$ [illegible]

Table 17

X-Ray data for some Type II diorganotin carboxylates, $[\{R'_2SnO_2CR\}_2O]_2$ 

Sl. no.	Compound	Sn ₁ –O ₁ (Å)	Sn ₁ –O ₁ ¹ (Å)	Sn ₁ –O ₅ ¹ (Å)	Sn ₂ –O ₃ (Å)	Sn ₂ –O ₁ (Å)	Sn ₂ –O ₄ (Å)	Sn ₁ ¹ –O ₄ (Å)	Sn ₂ –O ₂ (Å)	Reference
1	$[\{n\text{-Bu}_2\text{SnO}_2\text{CCH}_2\text{C}_6\text{H}_4\text{F}-(p)\}_2\text{O}]_2$	2.021(4)	2.148(4)	3.301(6)	2.093(5)	2.003(4)	2.498(5)	2.206(4)	2.746(6)	[125]
2	$[\{n\text{-Bu}_2\text{SnO}_2\text{CCH}_2\text{CH}_2\text{COC}_6\text{H}_5\}_2\text{O}]_2$	2.047(6)	2.171(6)	–	2.121(6)	1.993(6)	2.517(7)	2.191(6)	2.746(7)	[130]
3	$[\{n\text{-Bu}_2\text{Sn}(\text{OC}_6\text{H}_4\text{OMe}-2)\}_2\text{O}]_2$	2.038(5)	2.150(5)	–	2.061(5)	2.011(5)	2.470(5)	2.198(5)	–	[131]
4	$[\{\text{Me}_2\text{SnO}_2\text{C}_6\text{H}_4\text{NH}_2-p\}_2\text{O}]_2$	2.036(5)	2.166(5)	3.315(6)	2.104(6)	2.009(5)	2.688(5)	2.202(6)	2.573(6)	[113]

Table 18

X-Ray data for some of Type IV diorganotin carboxylates, $[\{R'_2SnO_2CR\}_2O]_2$ 

Sl. no.	Compound	Sn ₁ –O ₁ (Å)	Sn ₁ –O ₁ ¹ (Å)	Sn ₁ –O ₂ (Å)	Sn ₂ –O ₃ (Å)	Sn ₂ –O ₁ (Å)	Sn ₂ –O ₅ (Å)	Sn ₁ ¹ –O ₅ (Å)	Reference
1	$[\{Me_2Sn(O_2C^iBu)\}_2O]_2$	2.110(5)	2.088(5)	2.353(7)	2.228(8)	2.005(5)	2.243(6)	2.330(7)	[124]
2	$[Me_2LSnOSnLMe_2]_2$	2.105(2)	2.093(2)	2.422(2)	2.191(2)	2.005(2)	2.165(2)	2.491(2)	[129]
3	$[\{Ph_2SnO_2CCCl_3\}_2O]_2$	2.138		2.432	2.207	2.015	2.199	2.400	[68]

O group of the free phosphinic acid also coordinates to the tin. Thus, the tin is six-coordinate in an approximate octahedral environment with the two alkyl groups being trans with respect to each other (Fig. 55) [137].

3.6.4. $[\{n-Bu_2Sn(O_2P(OH)R)\}_2(O_3PMe)]$

The reaction of the $[\{n-Bu_2Sn(OPr-n)\}_2O]$ (generated in situ by the reaction of $n-Bu_2SnO$ with n -propanol [135]) with methyl phosphonic acid, $MeP(O)(OH)_2$ affords the Sn–O ring system $[\{n-Bu_2Sn(O_2P(OH)R)\}_2(O_3PMe)]$ (Fig. 56) [138]. The X-ray structure of this compound reveals the presence of an eight-

membered ring where two RPO_3 groups are involved in an anisobidentate bridging coordination mode with the two $n-Bu_2Sn$ units. Each tin also is bound to a terminal uni-dentate phosphonate (Fig. 57). The coordination geometry around each tin is distorted trigonal-bipyramidal.

3.7. Reactions of R_2SnO with salicylaldoxime

The reactions of R_2SnO ($R = Me$ or $n-Bu$) with salicylaldoxime $o-HON=CH-C_6H_4OH$ proceeds in a 2:3 manner to afford a trinuclear tin assembly $[(R_2Sn)(R_2SnO)(R_2SnOH)(OHN=C_6H_4O)(ON=$

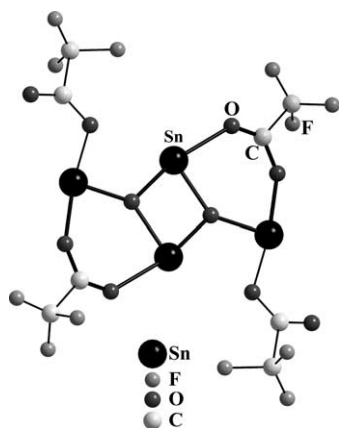


Fig. 46. The X-ray structure of $[\{n-Bu_2Sn(O_2CCF_3)\}_2O]_2$, Type I (the alkyl groups on tin have been omitted) [115].

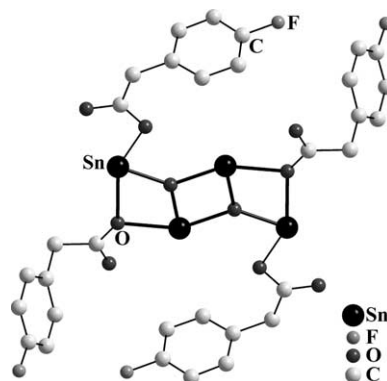


Fig. 47. The X-ray structure of $[\{n-Bu_2Sn(O_2CCH_2C_6H_4-p-F)\}_2O]_2$, Type II (the alkyl groups on tin have been omitted for clarity) [125].

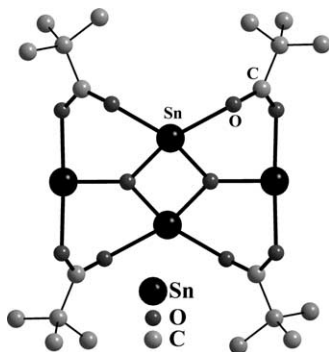


Fig. 48. The X-ray structure of $[\{n\text{-Bu}_2\text{SnO}_2\text{C}(\text{CH}_3)_3\}_2\text{O}]_2$, Type IV (the alkyl groups on tin have been omitted) [124].

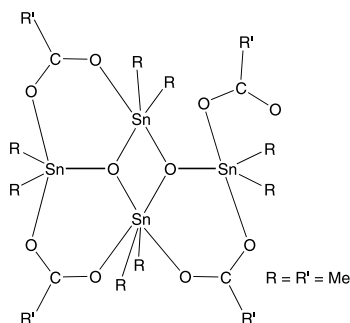


Fig. 49. The structure of $[\{\text{Me}_2\text{Sn}(\text{O}_2\text{CMe})\}_2\text{O}]_2$, Type III [133].

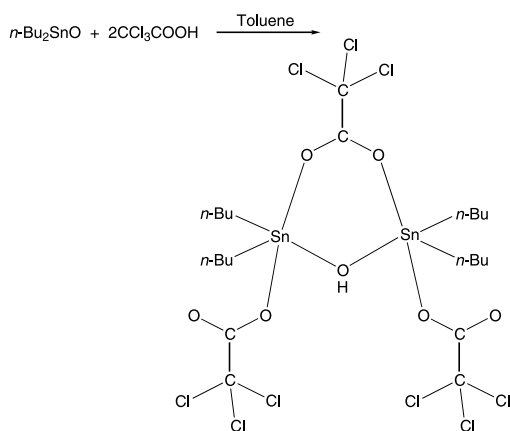


Fig. 50. The reaction of di *n*-butyl tin oxide with trichloroacetic acid to afford a μ -hydroxo bridged di tin derivative [134].

$\text{C}_6\text{H}_4\text{O}]$ (Scheme 8). Other variations of this formulation are $[(\text{R}_2\text{Sn})(\text{R}_2\text{SnO})(\text{R}_2\text{SnZ})(\text{LH})(\text{L})]$ ($\text{Z} = \text{OR}'$ or F ; $\text{LH} = -\text{OH}-\text{N}=\text{CH}-2\text{-C}_6\text{H}_4-\text{O}$) (Fig. 58) [139–143]. These trinuclear complexes consist of three R_2Sn units linked by two inequivalently bonded salicylaldoximate ligands (as depicted by rings A and B in Fig. 58). While one of the oximate ligands is uninegative the other is dinegative being deprotonated both at the $\text{N}-\text{OH}$ and $\text{C}-\text{OH}$ ends. Both the oximate ligands function as tridentate ligands. Of the three R_2Sn units the central tin (Sn1) is seven-coordinate and adopts a distorted

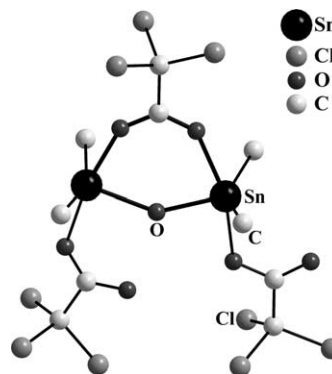


Fig. 51. The X-ray structure of $(n\text{-Bu}_2\text{SnO}_2\text{CCCl}_3)_2(\text{OH})(\text{O}_2\text{CCCl}_3)$ (the alkyl groups on tin are shown as single atoms) [134].

pentagonal bipyramidal geometry; the apical positions being occupied by the alkyl groups and the equatorial plane comprised of a N_2O_3 environment. The other two tins (Sn2 and Sn3) are five-coordinate and are present in a distorted trigonal-bipyramidal geometry; two alkyl groups and a common oxygen atom (O1) occupy the equatorial positions while the axial positions are taken up by either two oxygens (O3 and O4 or O2 and O4) or one oxygen and a fluoride (O3 and F or O2 and F). The X-ray structural data for representative examples of these classes of compounds are summarized in Table 21 [140,141]. The X-ray structures of $[(\text{R}_2\text{Sn})(\text{R}_2\text{SnO})(\text{R}_2\text{SnZ})(\text{OHN}=\text{C}_6\text{H}_4\text{O})(\text{ON}=\text{C}_6\text{H}_4\text{O})]$ ($\text{Z} = \text{OH}$, $\text{OPr-}i$, F , and $2\text{-HO}-\text{C}_6\text{H}_4-\text{CH}=\text{N}-$) are shown in Figs. 59–62. The two tins Sn2 and Sn3 are linked by O1 which also is involved in binding to Sn1 . Further connection between Sn2 and Sn3 is provided by a fluoride or by the oxygen atom O4 belonging to hydroxy, alkoxy, aryloxy or even an salicylaldoximate moiety. The ^{119}Sn -NMR data for a series of these tri tin compounds is shown in Table 22 [140,141]. The seven-coordinate tin (Sn1) resonates considerably upfield at -450.0 to -460.6 ppm while the other two five-coordinate tins (Sn2 and Sn3) show chemical shifts that are more downfield shifted. Detailed studies on the fate of the tri tin derivatives in solution revealed that several transient species are present. Recently, it has been shown that a similar structural type as the above tri tin derivatives can also be obtained in the reaction of Me_2SnCl_2 with a tetradentate schiff base *N*-2-[3'-(methoxysalicylideneimino)benzyl]-3''methoxysalicylideneimine [144].

In a related system it has been observed that the reaction of bis(2-hydroxy-3,5-di-*t*-butyl-phenylamido)oxalic acid with R_2SnCl_2 ($\text{R} = \text{Me}$, *n*-Bu, Ph) affords a di-tin derivative (Figs. 63 and 64). Each tin is five-coordinate and the coordination around the R_2Sn is completed by a nitrogen and two oxygen atoms [145].

Table 19

¹¹⁹Sn-NMR data for diorganotin carboxylates, $[\{R'_2\text{SnO}_2\text{CR}\}_2\text{O}]_2$

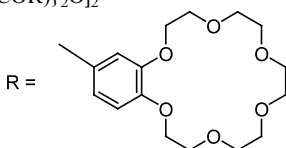
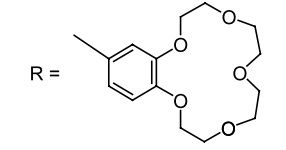
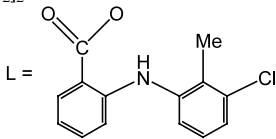
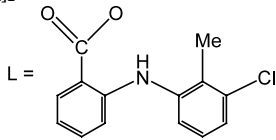
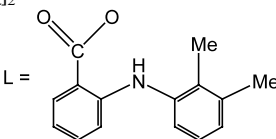
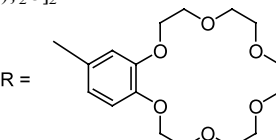
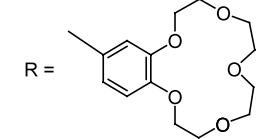
Sl. no.	Compound	δ values	Reference
1	$[\{\text{Me}_2\text{Sn}(\text{O}_2\text{C}^i\text{Bu})\}_2\text{O}]_2$	–188.0, –194.0	[124]
2	$[\{\text{Me}_2\text{Sn}(\text{OC}_6\text{H}_5)\}_2\text{O}]_2$	–138.0, –140.0	[131]
3	$[\{\text{Me}_2\text{Sn}(\text{OC}_6\text{H}_4\text{OEt}-2)\}_2\text{O}]_2$	–152.0, –171.0	[114]
4	$[\{\text{Me}_2\text{Sn}(\text{O}_2\text{CCHCHC}_4\text{H}_3\text{O})_2\}_2\text{O}]_2$	–175.0, –189.0	[113]
5	$[\{\text{Me}_2\text{SnO}_2\text{CC}_6\text{H}_4\text{NH}_2\text{-}o\}_2\text{O}]_2$	–172.9, –190.5	[113]
6	$[\{\text{Me}_2\text{SnO}_2\text{CC}_6\text{H}_4\text{NH}_2\text{-}p\}_2\text{O}]_2 \cdot 4\text{CH}_3\text{CN}$	–208.4, –217.0	[113]
7	$[\{\text{Me}_2\text{SnO}_2\text{CC}_6\text{H}_{11}\}_2\text{O}]_2$	–183.6, –189.7	[113]
8	$[\{\text{Me}_2\text{SnO}_2\text{CCH}_3\}_2\text{O}]_2$	–190.2, –173.8	[128]
9	$[\{\text{Me}_2\text{SnO}_2\text{CC}_6\text{H}_4\text{CH}_3\text{-}p\}_2\text{O}]_2$	–190.1, –179.4	[128]
10	$[\{\text{Et}_2\text{Sn}(\text{O}_2\text{C}^i\text{Bu})\}_2\text{O}]_2$	–211.0, –229.0	[124]
11	$[\{\text{Et}_2\text{Sn}(\text{OC}_6\text{H}_4\text{OMe}-2)\}_2\text{O}]_2$	–201.0	[131]
12	$[\{\text{Et}_2\text{SnO}_2\text{CC}_5\text{H}_3\text{N}(\text{SMe}-2)\}_2\text{O}]_2$	–209.2, –211.2	[110]
13	$[\{n\text{-Pr}_2\text{Sn}(\text{O}_2\text{C}^i\text{Bu})\}_2\text{O}]_2$	–216.0, –231.0	[124]
14	$[\{n\text{-Pr}_2\text{Sn}(\text{OC}_6\text{H}_4\text{Cl}-2)\}_2\text{O}]_2$	–169.0 (broad)	[131]
15	$[\{n\text{-Pr}_2\text{Sn}(\text{OC}_6\text{H}_4\text{OMe}-2)\}_2\text{O}]_2$	–205.0, –207.0	[131]
16	$[\{n\text{-Pr}_2\text{Sn}(\text{OC}_6\text{H}_4\text{OEt}-2)\}_2\text{O}]_2$	–194.0, –205.0	[131]
17	$[\{n\text{-Bu}_2\text{Sn}(\text{O}_2\text{C}^i\text{Bu})\}_2\text{O}]_2$	–194.0, –210.0	[131]
18	$[\{n\text{-Bu}_2\text{Sn}(\text{OC}_6\text{H}_5)\}_2\text{O}]_2$	–176.8, –177.4	[131]
19	$[\{n\text{-Bu}_2\text{Sn}(\text{OC}_6\text{H}_4\text{Cl}-2)\}_2\text{O}]_2$	–165.0 (broad)	[131]
20	$[\{n\text{-Bu}_2\text{Sn}(\text{OC}_6\text{H}_4\text{Me}-2)\}_2\text{O}]_2$	–162.0, –177.0	[131]
21	$[\{n\text{-Bu}_2\text{Sn}(\text{OC}_6\text{H}_4\text{OMe}-2)\}_2\text{O}]_2$	–199.0, –203.0	[131]
22	$[\{n\text{-Bu}_2\text{Sn}(\text{OC}_6\text{H}_4\text{OEt}-2)\}_2\text{O}]_2$	–188.0, –204.0	[131]
23	$[\{n\text{-Bu}_2\text{Sn}(\text{O}_2\text{CC}(\text{Ph})_3)\}_2\text{O}]_2$	–185.1, –238.6	[134]
24	$[\{n\text{-Bu}_2\text{Sn}(\text{O}_2\text{CC}_6\text{H}_4\text{C}(\text{CH}_3)_3\text{-}p\}_2\text{O}]_2$	–215.5	[134]
25	$[\{n\text{-Bu}_2\text{Sn}(\text{O}_2\text{CC}_6\text{H}_3(\text{NO}_2)_2(3,5))\}_2\text{O}]_2$	–195.6, –204.2	[134]
26	$[\{n\text{-Bu}_2\text{Sn}(\text{O}_2\text{CCHCl}_2)\}_2\text{O}]_2$	–191.5, –192.6	[134]
27	$[\{n\text{-Bu}_2\text{SnO}_2\text{CCH}(\text{CH}_3)_2\}_2\text{O}]_2$	–212.2, –218.0	[134]
28	$[\{n\text{-Bu}_2\text{SnO}_2\text{CCH}_2\text{CH}_2\text{Ph}\}_2\text{O}]_2$	–189.3, –190.9	[134]
29	$[\{n\text{-Bu}_2\text{SnO}_2\text{CCH}_2\text{CH}_2(\text{cyclopentyl})\}_2\text{O}]_2$	–206.0, –208.3	[134]
30	$[\{n\text{-Bu}_2\text{SnO}_2\text{C}_5\text{H}_3\text{N}(\text{SMe}-2)\}_2\text{O}]_2$	–210.0, –210.2	[110]
31	$[\{n\text{-Bu}_2\text{Sn}(\text{O}_2\text{CCHCHC}_4\text{H}_3\text{O})_2\}_2\text{O}]_2$	–205.0, –214.0	[114]
32	$[\{n\text{-Bu}_2\text{Sn}(\text{O}_2\text{CCH}_2\text{C}_6\text{F}_5)\}_2\text{O}]_2$	–204.6, –209.3	[125]
33	$[\{n\text{-Bu}_2\text{SnO}_2\text{CCH}_2\text{C}_6\text{H}_4\text{F}(-p)\}_2\text{O}]_2$	–207.9, –215.8	[125]
34	$[\{n\text{-Bu}_2\text{Sn}(\text{O}_2\text{CC}_6\text{H}_4\text{CH}_3\text{-}o\})\}_2\text{O}]_2$	–212.9, –213.4	[127]
35	$[\{n\text{-Bu}_2\text{Sn}(\text{O}_2\text{CC}_6\text{H}_4\text{Cl}-o\})\}_2\text{O}]_2$	–203.6, –201.2	[127]
36	$[\{n\text{-Bu}_2\text{Sn}(\text{O}_2\text{CC}_6\text{H}_4\text{OH}-o\})\}_2\text{O}]_2$	–205.1, –199.7, –188.9, –172.4, –157.5	[127]
37	$[\{n\text{-Bu}_2\text{Sn}(\text{O}_2\text{CCF}_3)_2\}_2\text{O}]_2$	–169.0, –175.2	[115]
38	$[\{n\text{-Bu}_2\text{Sn}(\text{O}_2\text{CCF}_2\text{CF}_3)_2\}_2\text{O}]_2$	–175.0, –175.9	[115]
39	$[\{n\text{-Bu}_2\text{Sn}(\text{O}_2\text{CCF}_2\text{CF}_2\text{CF}_3)_2\}_2\text{O}]_2$	–174.3, –175.0	[115]
40	$[\{n\text{-Bu}_2\text{SnO}_2\text{CC}(\text{Ph})_3\}_2\text{O}]_2$	–185.1, –238.6	[62]
41	$[\{n\text{-Bu}_2\text{SnO}_2\text{CC}_6\text{H}_4\text{C}(\text{CH}_3)_3\text{-}p\}_2\text{O}]_2$	–215.5	[62]
42	$[\{n\text{-Bu}_2\text{SnO}_2\text{CC}_6\text{H}_3(\text{NO}_2)_2(3,5)\}_2\text{O}]_2$	–195.7, –204.2	[62]
43	$[\{n\text{-Bu}_2\text{SnO}_2\text{CCHCl}_2\}_2\text{O}]_2$	–191.5, –192.6	[62]
44	$[\{n\text{-Bu}_2\text{SnO}_2\text{CCH}(\text{CH}_3)_2\}_2\text{O}]_2$	–212.2, –218.0	[62]
45	$[\{n\text{-Bu}_2\text{SnO}_2\text{CCH}_2\text{CH}_2\text{Ph}\}_2\text{O}]_2$	–189.3, –190.9	[62]
46	$[\{n\text{-Bu}_2\text{SnO}_2\text{CCH}_2\text{CH}_2(\text{cyclopentyl})\}_2\text{O}]_2$	–205.9, –218.3	[62]
47	$[n\text{-Bu}_2\text{Sn}\{1,7\text{-C}_{10}\text{H}_{11}\text{-}1\text{-COO}\}_2\text{O}]_2$	–207.0, –205.4	[126]
48	$[\{n\text{-Bu}_2\text{Sn}(\text{OCOR})\}_2\text{O}]_2$	–213.0, –217.3	[56]
			
49	$[\{n\text{-Bu}_2\text{Sn}(\text{OCOR})\}_2\text{O}]_2$	–212.5, –216.9	[56]
			

Table 20

Mössbauer data for some diorganotin carboxylates, $[\{R'_2SnO_2CR\}_2O]_2$

Sl. no.	Compound	IS (mm s ⁻¹)	QS (mm s ⁻¹)	Reference
1	$[Me_2LSnOSnLMe_2]_2$ 	1.37; 1.00	3.58; 3.21	[123]
2	$[\{Et_2SnO_2CC_5H_3N(2-SMe)\}_2O]_2$	1.33	3.42	[110]
3	$[\{n-Bu_2Sn(O_2CCH_2S_2CNMe_2)\}_2O]_2$	1.30	3.57	[122]
4	$[\{n-Bu_2SnO_2CC_5H_3N(2-SMe)\}_2O]_2$	1.32	3.44	[110]
5	$[\{n-Bu_2Sn(O_2CCH_2C_6F_5)\}_2O]_2$	1.29	3.39	[125]
6	$[(n-Bu_2SnO_2CCF_3)_2O]_2$	1.43; 1.45	4.14; 3.37	[115]
7	$[(n-Bu_2SnO_2CCF_2CF_3)_2O]_2$	1.45; 1.42	4.20; 3.29	[115]
8	$[(n-Bu_2SnO_2CCF_2CF_2CF_3)_2O]_2$	1.45	3.72	[115]
9	$[Bu_2LSnOSnLBu_2]_2$ 	1.33	3.34	[123]
10	$[Bu_2LSnOSnLBu_2]_2$ 	1.47	3.27	[129]
11	$[\{n-Bu_2Sn(1,7-C_2B_{10}H_{11}-1-COO)\}_2O]_2$	1.38	3.59	[126]
12	$[\{n-Bu_2Sn(OCOR)\}_2O]_2$ 	1.27	3.36	[56]
13	$[\{n-Bu_2Sn(OCOR)\}_2O]_2$ 	1.33	3.38	[56]
14	$[(n-BuPhSnO_2CCH_2S_2CNMe_2)_2O]_2$	1.23	3.32	[122]
15	$[(Ph_2SnO_2CCH_2S_2CNMe_2)_2O]_2$	1.14	3.23	[122]

4. Monoorganotin derivatives

4.1. Hydrolysis of $RSnCl_3$

The complete hydrolysis of $RSnCl_3$ leads to the formation of the stannonic acid $[RSn(O)OH]_n$, which is polymeric in nature. However, the structures of these

compounds are as yet unknown. The most commonly used stannonic acid is $[n-BuSn(O)OH]_n$ and in its ^{119}Sn -NMR shows peaks at -282.0 and -465.0 ppm [146]. The similarity of these resonance positions with those observed for the Sn_{12} oxo cage (vide infra) suggests that $[n-BuSn(O)OH]$ belongs to a similar structural type as that of the former. There are no reports on any example

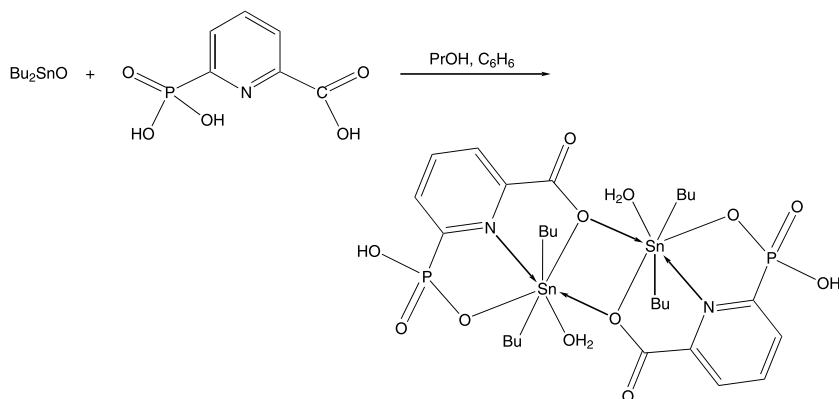


Fig. 52. The reaction of *n*-Bu₂SnO with pyridine-2-phosphonate-6-carboxylic acid to afford a di tin compound [135,136].

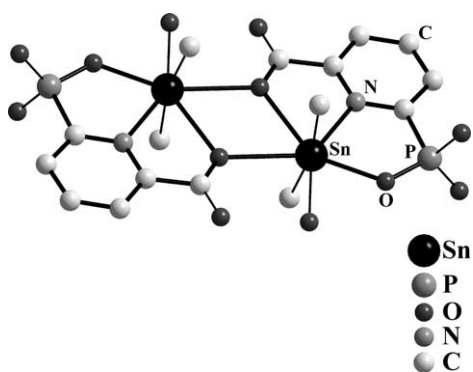


Fig. 53. The X-ray structure of dimeric din-butyltin pyridine-2-phosphonate-6-carboxylate. Each tin has a water molecule in its coordination sphere (the alkyl groups on tin are shown as single atoms) [136].

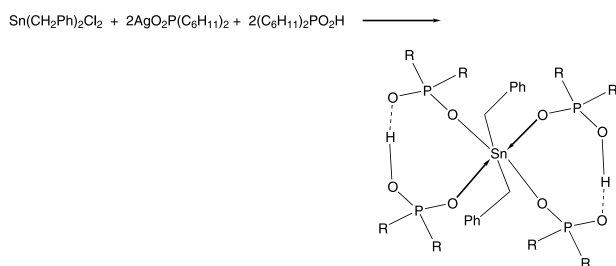


Fig. 54. The reaction of dibenzyltin dichloride with the silver salt of dicyclohexyl phosphinic acid and free dicyclohexyl phosphinic acid [137].

of an organotin trihydroxide $\text{RSn}(\text{OH})_3$. This may be contrasted with the situation in silicon where a number of organosilanetriols $\text{RSi}(\text{OH})_3$ are known [147,148]. Recently, there has been a report on the synthesis and characterization of a stable organo(bis-silanetriol) [149].

Partial hydrolysis of RSnCl_3 leads to stable products $[\text{RSnCl}_2(\text{OH}) \cdot \text{H}_2\text{O}]_2$ ($\text{R} = \text{Me}, \text{Et}, i\text{-Pr}, n\text{-Bu}, i\text{-Bu}$) [150–153]. The X-ray structures of these compounds show them to be dimeric, bridged by the OH groups. The Sn–O bond distances within the distannoxane units

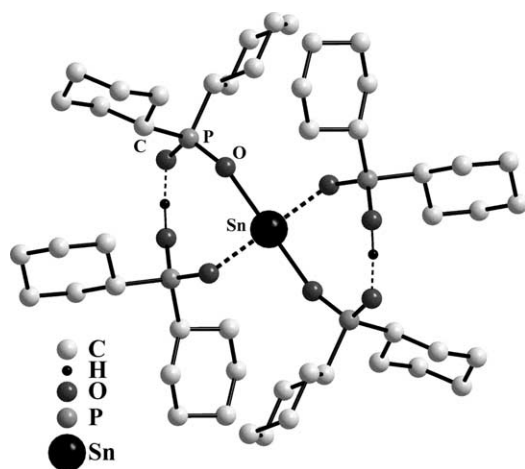


Fig. 55. The X-ray structure of $[\text{R}_2\text{Sn}\{\text{O}_2\text{P}(c\text{-Hex})_2\}_2]\{ (c\text{-Hex})_2\text{PO}_2\text{H} \}_2$ the benzyl substituents on tin have been omitted [137].

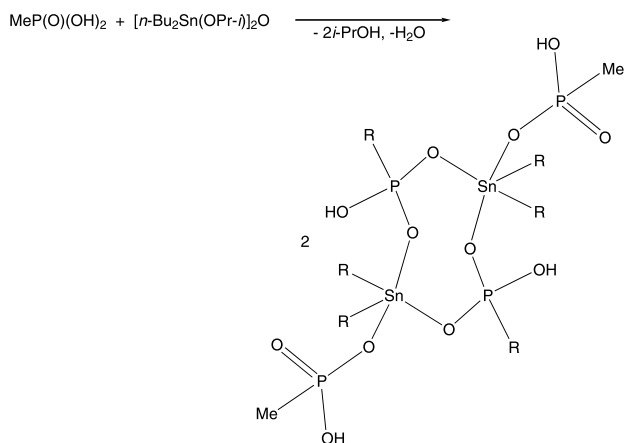


Fig. 56. The reaction of methylphosphonic acid with $[\{n\text{-Bu}_2\text{Sn}(i\text{-OPr})_2\}_2\text{O}]$ to afford an eight-membered Sn–O–P heterocyclic ring [138].

are normal (Table 23). Recently the hydrolysis of the bridged di-tin derivative $\text{Cl}_3\text{Sn}(\text{CH}_2)_3\text{SnCl}_3$ was studied [154]. It was observed that step-wise hydration of the di-tin derivative occurs followed by the hydrolysis of one

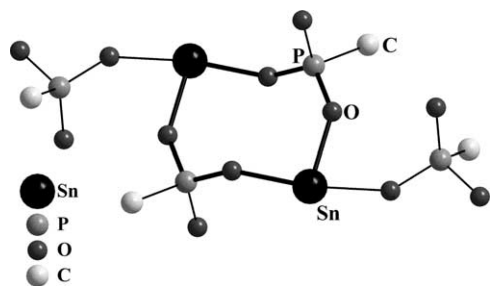
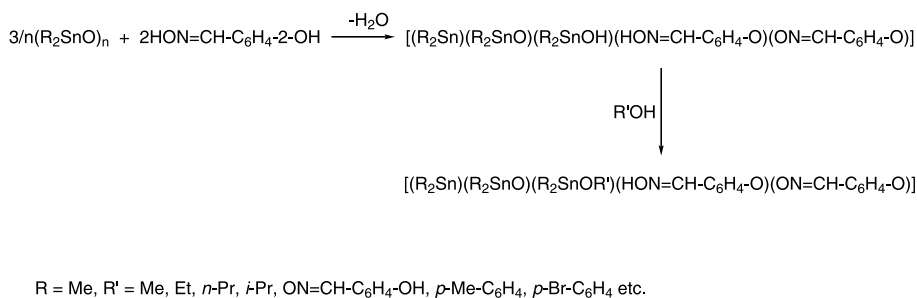


Fig. 57. The X-ray structure of $[n\text{-Bu}_2\text{Sn}(\mu\text{-O}_2\text{P}(\text{O})\text{Me})\text{MePO}_3]_2$ (the alkyl groups on tin have been omitted) [138].

chlorine on each tin to afford $[\text{Cl}_2(\text{OH})\text{Sn}(\text{CH}_2)_3\text{Sn}(\text{OH})\text{Cl}_2 \cdot 2\text{H}_2\text{O}]_n$ (Fig. 65). The structure of the latter compound shows that it is polymeric with the hydroxy bridged distannoxane units being linked by the alkylene bridges (Fig. 66).

4.2. $(R\text{Sn})_{12}$ oxo hydroxo cages and related systems

Puff and Reuter have observed that hydrolysis of *i*-PrSnCl₃ leads to the formation of a pyramidal cage $[(i\text{-PrSn})_9\text{O}_8(\text{OH})_6\text{Cl}_5]$ [155]. By using the dihydroxy chloride *i*-PrSnCl(OH)₂ instead of the trichloride they



Scheme 8.

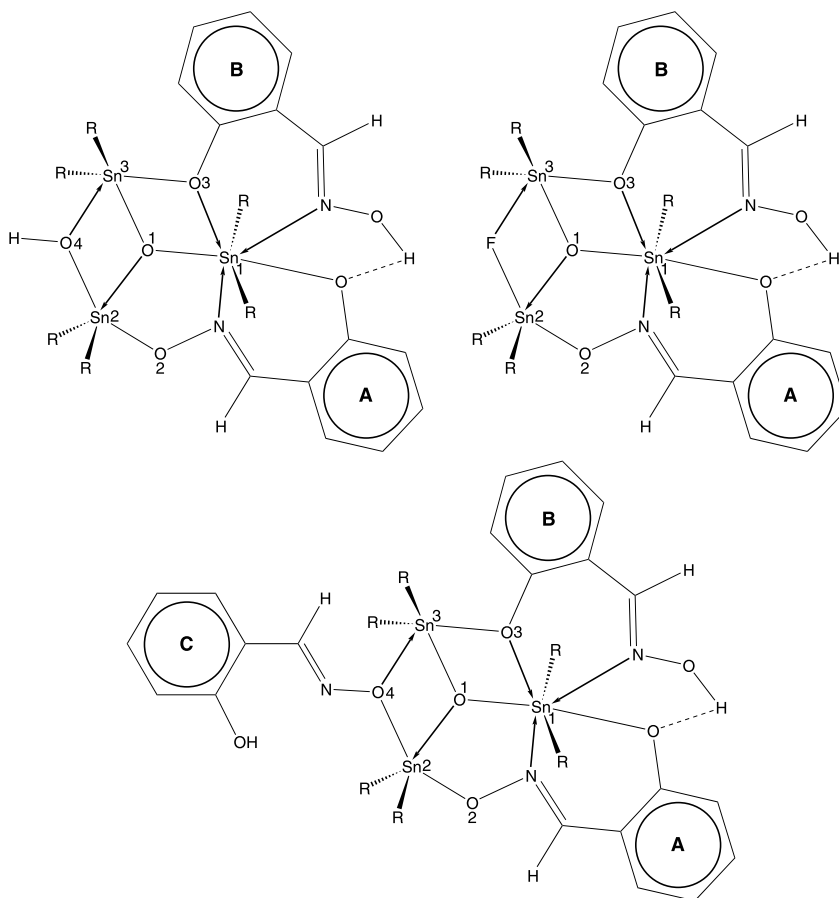


Fig. 58. The structures of the 2:3 condensation products between salicylaldehyde and diorganotin oxides [139–143].

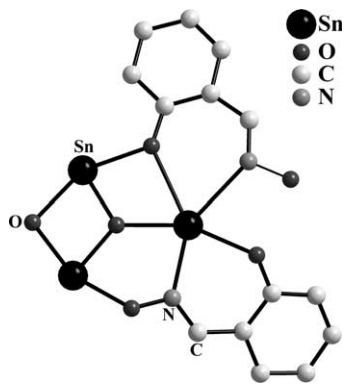


Fig. 59. The X-ray structure of $[(n\text{-Bu}_2\text{Sn})(n\text{-Bu}_2\text{SnO})(n\text{-Bu}_2\text{SnOH})(\text{LH})(\text{L})]$, $\text{LH} = \text{HO}-\text{N}=\text{CH}-2\text{-C}_6\text{H}_4-\text{O}$ (the alkyl groups on tin have been omitted) [139].

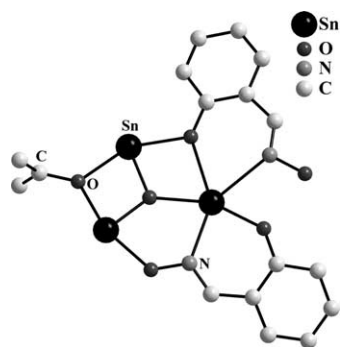


Fig. 60. The X-ray structure of $[(\text{Me}_2\text{Sn})(\text{Me}_2\text{SnO})(\text{Me}_2\text{SnOPr-}i)(\text{LH})(\text{L})]$, $\text{LH} = \text{HO}-\text{N}=\text{CH}-2\text{-C}_6\text{H}_4-\text{O}$ (the alkyl groups on tin have been omitted) [140].

obtained a dodecanuclear organotin cluster $[(i\text{-PrSn})_{12}\text{O}_{14}(\text{OH})_6][\text{Cl}]_2 \cdot \text{L}$ ($\text{L} = 3\text{H}_2\text{O}$; 2DMF ; $4\text{H}_2\text{O}$; 4DMPU) [156]. Several workers have since been able to synthesize the $(\text{RSn})_{12}$ cage by using a large variety of synthetic methodologies (Scheme 9) [157–161]. The most convenient method appears to be the reaction of $n\text{-BuSn}(\text{O})(\text{OH})$ with p -toluene sulfonic acid [160,161].

The X-ray structure of the $(\text{RSn})_{12}$ cage shows that it is a macro dication whose charge is compensated by two monoanionic counteranions; $[(\text{RSn})_{12}(\mu_3\text{-O}_{14})-(\mu_2\text{-OH})_6]^{2+}[\text{X}]_2^-$ (Table 23) [157,158,161]. The structure of the macro cation is like a *football* and consists of two trimeric sub-units $[(n\text{-BuSn})_3(\mu_3\text{-O})(\mu_2\text{-OH})_3]$ situated at the poles of the cage (Fig. 67). Within these sub-units the tins are hexa-coordinate and possess bridging oxide and hydroxide groups. The equator of the cage is spanned by a hexameric cycle $[(n\text{-BuSn})_6(\mu_2\text{-O})_{12}]$. In this sub-unit the tins are five-coordinate and nearly square pyramidal. Thus, it is possible to envisage the construction of the cage by capping each side of the hexameric cycle by the two trimeric units. The $\mu_2\text{-OH}$'s situated at the poles are involved in interaction with the anion generating a sheet like polymer structure. Weak interactions with donor solvents leads to several such polymer sheets being held

together. An example of this type of structure as observed for $[(n\text{-BuSn})_{12}(\mu_3\text{-O}_{14})(\mu_2\text{-OH})_6]^{2+}[p\text{-CH}_3\text{-C}_6\text{H}_4\text{-SO}_3]_2^- \cdot \text{dioxan}$ [161] is shown in Fig. 68. The anion–cation interactions are retained in solutions of low dielectric constant solvents such as CH_2Cl_2 . This is confirmed by the variation of the chemical shift of the six-coordinated tins situated at poles (-447.4 to -468.1 ppm) in contrast to the near constancy of the five-coordinated tins located at the equator (Table 23) [157–162]. Since the hydroxyl groups, which interact with the anion, bridge the tins at the poles an indirect influence is experienced by these tins leading to the observed chemical shift changes upon change of cation.

An interesting aspect of the cage $[(n\text{-BuSn})_{12}-(\mu_3\text{-O}_{14})(\mu_2\text{-OH})_6]^{2+}[\text{OH}]_2^-$ is that the hydroxyl anion can be replaced by other anions such as $[\text{Ph}_2\text{PO}_2]^-$ or $[\text{CH}_3\text{CO}_2]^-$ by the reaction of the cage with the appropriate acid [159,162]. This allows the use of the hydroxide anion containing cage for the generation of nanomaterials by reaction with dicarboxylic acids or diols [162].

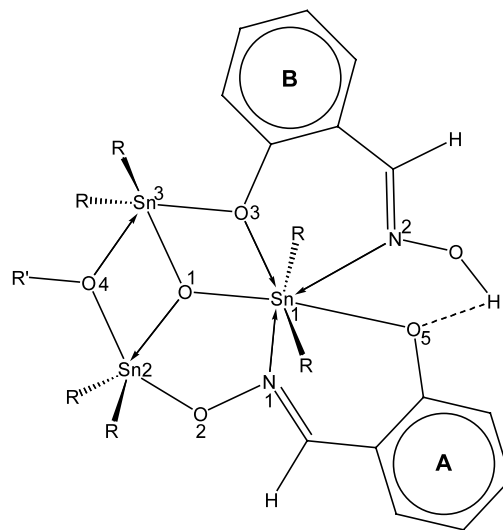
Recently an interesting example of a mixed tin/vanadium cage has been synthesized. Thus the reaction of $i\text{-PrSn}(\text{OH})_2\text{Cl}$ and $\text{VOSO}_4 \cdot 5\text{H}_2\text{O}$ in presence of a diamine leads to the formation of a cage $[(i\text{-PrSn})_{11}(\text{V}(\text{I-V})\text{O})(\mu_3\text{-O}_{14})(\mu_2\text{-OH})_6]^+[\text{Cl}]\cdot 2\text{DMF} \cdot \text{H}_2\text{O}$. The $\text{V}=\text{O}$ group occupies one of the square pyramidal tin positions at the cage [163].

Recently a new structural variation for the $(\text{RSn})_{12}$ oxo-cluster was discovered. Thus the compound $[\{\text{Sn}(\text{CH}_2)_3\text{Sn}\}_6(\text{CO}_2\text{ClCH}_2)_{14}(\text{OH})_2\text{O}_{10}]$ is obtained from the controlled hydrolysis of $[(\text{ClCH}_2\text{CO}_2)_3\text{Sn}(\text{CH}_2)_3\text{Sn}(\text{O}_2\text{CCH}_2\text{Cl})_3]_n$ (Scheme 10). This compound contains a coplanar Sn_{12} motif in contrast to the cage structures found above. The $\text{Sn}-\text{O}$ framework of this compound is shown in Fig. 69 [164]. The presence of the alkylene bridges between neighboring tins appears to preclude the cage formation in this system.

4.3. Reactions of $\text{RSn}(\text{O})\text{OH}$ with carboxylic or phosphorus based acids

The reactions of organostannonic acids with carboxylic acids RCOOH or phosphorus based acids such as $\text{R}_2\text{P}(\text{O})\text{OH}$, $(\text{OR})_2\text{P}(\text{O})\text{OH}$, $\text{RP}(\text{O})(\text{OH})_2$ lead to the formation of a large number of structural types (Schemes 11 and 12) (Figs. 70–78) [16,18–21,23,137,146,165–176]. In some cases the tin precursor used has been $n\text{-BuSn}(\text{OH})_2\text{Cl}$. Most of the multi-tin assemblies contain the distannoxane motif. The X-ray and ^{119}Sn -NMR parameters are summarized in Table 23. The reaction of $\text{RSn}(\text{O})\text{OH}$ with an excess of carboxylic acid leads to the formation of the hydrolytically sensitive tricarboxylate $\text{RSn}(\text{O}_2\text{CR}')_3$ which undergoes hydrolysis to afford the *ladder* $[(\text{RSn}(\text{O})\text{-O}_2\text{CR}')_2(\text{RSn}(\text{O}_2\text{CR}')_3)_2]$ (Scheme 11) [166,168]. In con-

Table 21
X-Ray data for some salicylaldehyde derivatives



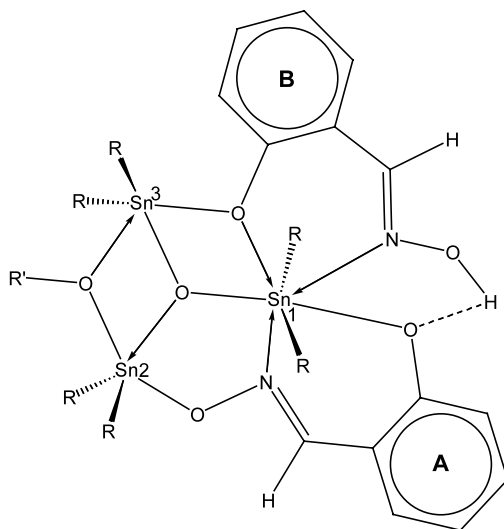
Sl. no.	R'	R	Sn1–O1 (Å)	Sn1–O3 (Å)	Sn1–O5 (Å)	Sn1–N1 (Å)	Sn1–N2 (Å)	Sn2–O1 (Å)	Sn2–O2 (Å)	Sn2–O4 (Å)	Sn3–O1 (Å)	Sn3–O3 (Å)	Sn3–O4 (Å)	Reference
1	Me	Me	2.170(5)	2.661(5)	2.189(5)	2.313(6)	2.588(7)	2.023(5)	2.108(5)	2.169(5)	1.933(5)	2.158(5)	2.178(5)	[140]
2	Et	Me	2.175(4)	2.678(5)	2.198(5)	2.307(6)	2.603(6)	2.033(4)	2.089(5)	2.150(5)	2.018(4)	2.151(5)	2.156(5)	[140]
3	<i>n</i> -Pr	Me	2.173(5)	2.681(5)	2.174(6)	2.286(7)	2.593(7))	2.025(5)	2.107(6)	2.151(5)	2.014(5)	2.150(5)	2.150(5)	[140]
4	<i>i</i> -Pr	Me	2.170(7)	2.647(8)	2.192(8)	2.330(1)	2.602(1)	2.039(7)	2.111(9)	2.195(8)	1.996(7)	2.146(7)	2.141(8)	[140]
5	L'H ^a	Me	2.177(4)	2.715(4)	–	–	–	2.020(4)	2.083(5)	2.248(5)	2.002(4)	2.153(4)	2.227(4)	[141]
6	<i>p</i> -Me–C ₆ H ₄ –	Me	2.178(3)	2.695(4)	–	–	–	2.010(4)	2.093(5)	2.255(4)	2.016(4)	2.145(4)	2.104(4)	[141]
7	<i>p</i> -Br–C ₆ H ₄ –	Me	2.181(4)	2.688(4)	–	–	–	2.008(4)	2.090(5)	2.274(4)	2.006(4)	2.140(4)	2.210(4)	[141]
8	LH ^b	Me	2.191(4)	2.729(4)	2.186(4)	2.282(5)	2.614(5)	2.019(4)	2.089(4)	2.239(4)	2.001(4)	2.127(4)	2.282(5)	[143]
9	F ^c	Me	2.207(9)	2.706(8)	2.169(9)	2.310(1)	2.570(1)	1.986(8)	2.070(1)	2.185(7)	1.998(8)	2.126(9)	2.231(8)	[143]
10	H	<i>n</i> -Bu	2.140(1)	2.680(1)	2.260(1)	2.290(1)	2.670(1)	2.040(1)	2.130(1)	2.170(1)	2.000(1)	2.170(1)	2.170(1)	[139]

^a –N=CH–C₆H₅.

^b –N=CH–C₆H₄–2-OH.

^c F occupies the position of OR'.

Table 22

¹¹⁹Sn-NMR data for some salicylaldehyde derivatives

Sl. no.	R'	R	Sn(1)	Sn(2)	Sn(3)	Reference
1	Me	Me	−455.5	−142.7	−130.6	[140]
2	Et	Me	−457.2	−144.3	−132.8	[140]
3	<i>n</i> -Pr	Me	−457.9	−143.8	−132.5	[140]
4	<i>i</i> -Pr	Me	−460.6	−147.8	−137.7	[140]
5	2-OH-C ₆ H ₄ -CH=N-	Me	−451.4	−122.9	−109.1	[140]
6	C ₆ H ₅ -CH=N-	Me	−452.7	−128.0	−114.4	[141]
7	<i>p</i> -Br-C ₆ H ₄ -	Me	−451.9	−133.1	−119.5	[141]
8	<i>m</i> -NO ₂ -C ₆ H ₄ -	Me	−450.0	−127.6	−113.9	[141]

trast a 6:6 reaction of $\text{R}^n\text{Sn}(\text{O})\text{OH}$ and a carboxylic acid $\text{R}'\text{COOH}$ affords the hexameric *drum* $[\text{R}^n\text{Sn}(\text{O})\text{O}_2\text{CR}']_6$ (Scheme 11) [137,166,167,169]. Utilizing this synthetic methodology recently a hexaferrocene assembly supported on a stannoxane framework has been prepared in near quantitative yields [167]. The X-ray structure of the hexaferrocene compound shows that the arrangement of the six ferrocene units around the stannoxane frame-

work is reminiscent of a giant wheel arrangement (Fig. 79). This compound is electrochemically and thermally robust. It shows a single reversible oxidation underscoring the equivalence of all the six ferrocene units. In contrast to the hexameric ferrocene assembly obtained as described above a tri ferrocene derivative has been prepared in the reaction of $n\text{-BuSn}(\text{OH})_2\text{Cl}$ with ferrocene carboxylic acid [146]. In this compound the three tins are bridged by a $\mu_3\text{-O}$ and a $\mu_2(\text{OH})$ (Fig. 80). Each ferrocene carboxylate binds two tins in a bidentate

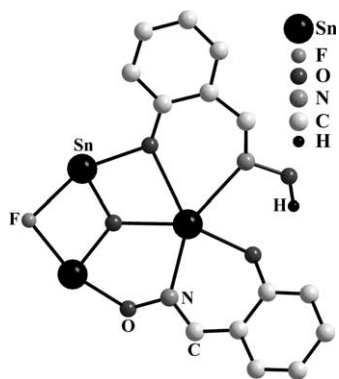


Fig. 61. The X-ray structure of $[(\text{Me}_2\text{Sn})(\text{Me}_2\text{SnO})(\text{Me}_2\text{SnF})(\text{LH})(\text{L})]$, $\text{LH} = \text{HO}-\text{N}=\text{CH}-2\text{-C}_6\text{H}_4-\text{O}$ (the alkyl groups on tin have been omitted) [142].

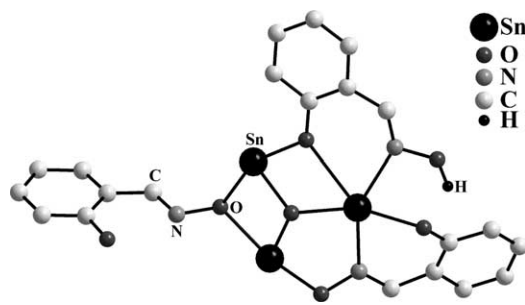


Fig. 62. The X-ray structure of $[(\text{Me}_2\text{Sn})(\text{Me}_2\text{SnO})(\text{Me}_2\text{SnL}'\text{H})(\text{LH})(\text{L})]$, $\text{LH} = \text{HO}-\text{N}=\text{CH}-2\text{-C}_6\text{H}_4-\text{O}$; $\text{L}'\text{H} = -\text{O}-\text{N}=\text{CH}-2\text{-C}_6\text{H}_4-\text{OH}$ (the alkyl groups on tin have been omitted) [143].

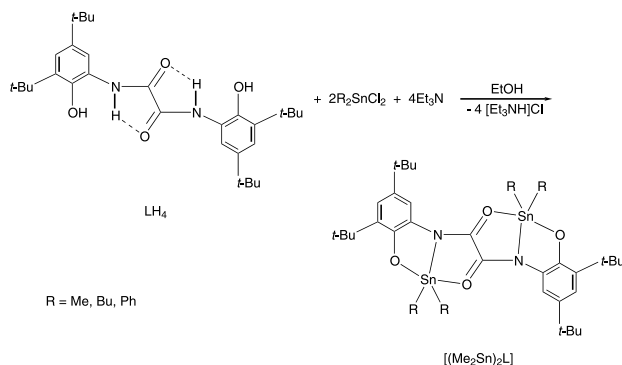


Fig. 63. Reaction of an oxalic acid diamide with diorganotin dichloride to afford a dinuclear tin compound [145].

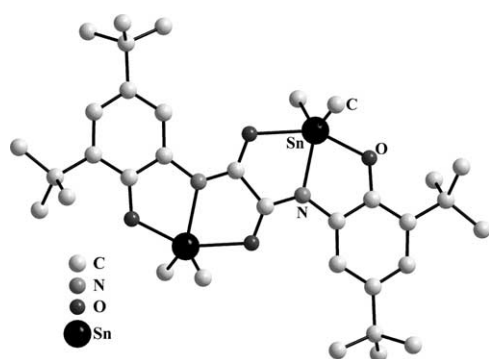


Fig. 64. The X-ray structure of $[(\text{Me}_2\text{Sn})_2(\text{L})]$, L = Oxalic acid diamido ligand [145].

manner [146]. The *drums* and *ladders* are also obtained in reactions with diorganotin and triorganotin precursors with carboxylic acids or silver salts of carboxylic acids by Sn–C scission reactions [68,137,165].

Recently the reaction between $\text{Sn}(\text{O}i\text{Bu}-t)_4$ and $\text{Sn}(\text{OAc})_4$ has been reported to proceed with the loss of $t\text{-BuOAc}$ to afford a hexameric drum $[(\text{O}i\text{Bu}-t)\text{Sn}(\text{O})(\text{O}_2\text{CMe})]_6$. This compound is structurally similar to the organostannoxane *drums* discussed above [177]. The presence of six oxygen atoms however, leads

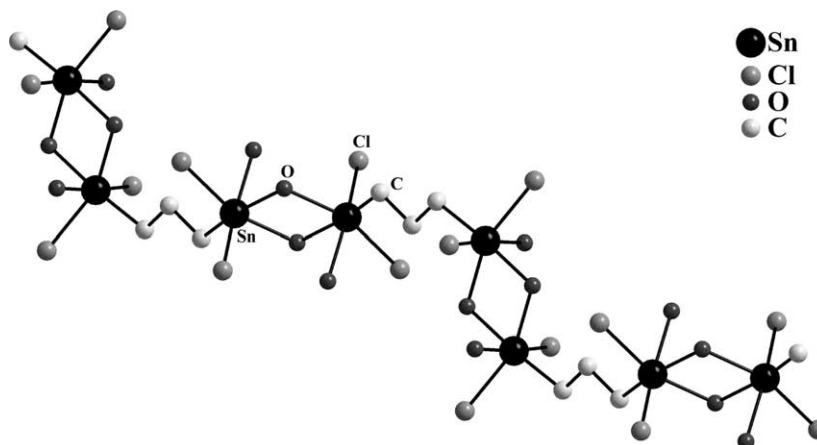


Fig. 66. The X-ray structure of $[\text{Cl}_2(\text{OH})\text{Sn}(\text{CH}_2)_3\text{Sn}(\text{OH})\text{Cl}_2 \cdot 2\text{H}_2\text{O}]_n$ [154].

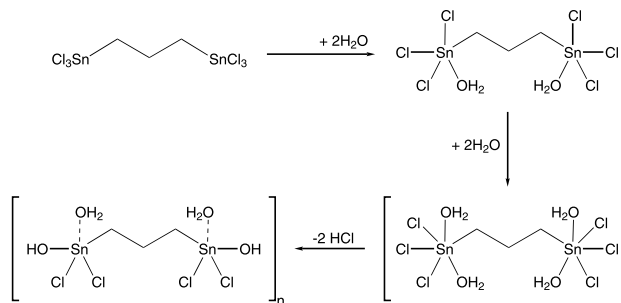
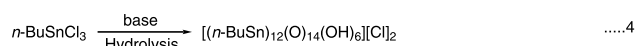
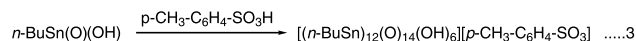
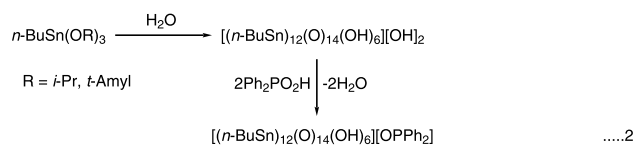
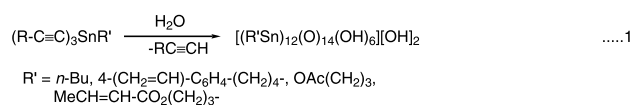


Fig. 65. Hydrolysis of $\text{Cl}_3\text{Sn}(\text{CH}_2)_3\text{SnCl}_3$ [154].



Scheme 9.

to an upfield shift in the ^{119}Sn -NMR value (-663.0). This may be contrasted with the value of around -480.0 observed for many drum molecules $[\text{RSn}(\text{O})(\text{O}_2\text{CR})]_6$ (Table 23).

The reactions of $\text{RSn}(\text{O})(\text{OH})$ with phosphorus based acids leads to a large variety of structure types [16,18,19,23,137,169–176]. These include *drum*, *cube*,

Table 23

X-ray and ^{119}Sn -NMR data for selected mono organotin cluster based on distannoxane units

Sl. no.	Compound	Structure	δ	Sn–O (Å)	Reference
1	$[n\text{-BuSn}(\text{OH})\text{Cl}_2(\text{H}_2\text{O})]_2$	Distannoxane	–408.6	2.108	[150]
2	$[(\text{Cl})_2(\text{OH})\text{Sn}(\text{CH}_2)_3\text{Sn}(\text{OH})(\text{Cl})_2 \cdot \text{H}_2\text{O}]_2$	Polymeric distannoxane	–472.0	2.097	[154]
3	$\{[n\text{-BuSn}(\text{SCH}_2\text{CH}_2\text{O})_2]_2\{n\text{-BuSnCl}\}\}$	Spiro stannoxane	–447.0, –42.6, –39.0	2.128	[179]
4	$[n\text{-BuSn}(\text{SCH}_2\text{CH}_2\text{O})(\text{SCH}_2\text{CH}_2\text{OH})]_2$	Distannoxane	28.7	2.204	[179]
5	$[(n\text{-BuSn})_{12}(\text{O})_{14}(\text{OH})_6][\text{X}]_2$, $\text{X} = \text{OH}^-$	Foot ball cage	–280.1 ^a , –447.4 ^b	2.054 ^c , 2.116 ^d , 2.096 ^e	[158]
6	$[(n\text{-BuSn})_{12}(\text{O})_{14}(\text{OH})_6][\text{X}]_2$, $\text{X} = \text{CH}_3\text{COO}^-$	Foot ball cage	–281.0 ^a , –457.0 ^b	–	[162]
7	$[(n\text{-BuSn})_{12}(\text{O})_{14}(\text{OH})_6][\text{X}]_2$, $\text{X} = 4\text{-CH}_3\text{-C}_6\text{H}_4\text{-SO}_3^-$	Foot ball cage	–282.8 ^a , –461.8 ^b	2.057 ^c , 2.098 ^d , 2.120 ^e	[160,161]
8	$[(n\text{-BuSn})_{12}(\text{O})_{14}(\text{OH})_6][\text{X}]_2$, $\text{X} = \text{Cl}^-$	Foot ball cage	–283.1 ^a , –468.1 ^b	–	[157]
9	$[(n\text{-BuSn})_{12}(\text{O})_{14}(\text{OH})_6][\text{X}]_2$, $\text{X} = [\text{Ph}_2\text{PO}_2]^-$	Foot ball cage	–283.3 ^a , –457.7 ^b	–	[159]
10	$[n\text{-BuSn}(\text{O})\text{OCOC}_5\text{H}_9]_6$	Drum	–485.8	2.086	[166]
11	$[\text{PhSn}(\text{O})\text{OCOC}_6\text{H}_{11}]_6$	Drum	Insoluble	2.079	[165]
12	$[n\text{-BuSn}(\text{O})\text{OCOC}_5\text{H}_4\text{FeC}_5\text{H}_5]_6$	Drum	–486.6	2.095	[167]
13	$[(\text{PhCH}_2)_2\text{Sn}(\text{O})\text{O}_2\text{CBu}^t]_6$	Drum	–523.1 ^f	–	[137]
14	$[(\text{PhCH}_2)_2\text{Sn}(\text{O})\text{O}_2\text{CC}_5\text{H}_4\text{N}]_6$	Drum	–519.8 ^f	–	[137]
15	$[(\text{PhCH}_2)_2\text{Sn}(\text{O})\text{O}_2\text{CCH}=\text{CMe}_2]_6$	Drum	–522.9 ^f	–	[137]
16	$[(\text{PhCH}_2)_2\text{Sn}(\text{O})\text{O}_2\text{CCHPh}]_6$	Drum	–525.0 ^f	–	[137]
17	$[n\text{-BuSn}(\text{O})\text{O}_2\text{P}(\text{OPh})_2]_6$	Drum	–492.7 (162.5 Hz) ^g	2.100	[169]
18	$\{[n\text{-BuSn}(\text{O})\text{OCOPh}]_2\{n\text{-BuSn}(\text{OCOPh})_3\}\}_2$	Ladder	–520.0, –536.0, –548.0, –608.0	2.067	[168]
19	$\{[n\text{-BuSn}(\text{O})\text{OCOMe}]_2\{n\text{-BuSn}(\text{OCOMe})_3\}\}_2$	Ladder	–522.0, –533.0, –549.0	2.060	[168]
20	$\{[(\text{PhCH}_2)_2\text{Sn}(\text{O})\text{O}_2\text{CMe}]_2(\text{PhCH}_2)_2\text{Sn}(\text{O}_2\text{CMe})_3\}_2 \cdot 2\text{CH}_2\text{Cl}_2$	Ladder	–530.0–580.0; –630.0–640.0	–	[137]
21	$\{[n\text{-BuSnCl}(\text{OCOC}_5\text{H}_4\text{FeC}_5\text{H}_5)]_3(\text{O})(\text{OH})\}$	$\mu_3\text{-Osnn}_3$	–	2.116	[146]
22	$[n\text{-BuSn}(\text{O})\text{O}_2\text{P}(t\text{-Bu})_2]_4$	Cube	–473.0 (125.0 Hz) ^g	2.116	[172]
23	$[n\text{-BuSn}(\text{O})\text{O}_2\text{P}(\text{CH}_2\text{C}_6\text{H}_5)_2]_4$	Cube	–464.4 (109.0 Hz) ^g	2.121	[172]
24	$[n\text{-BuSn}(\text{O})\text{O}_2\text{P}(\text{C}_6\text{H}_{11})_2]_4$	Cube	–462.8 (116.0 Hz)	2.108	[171]
25	$\{[n\text{-BuSnS}(\text{O}_2\text{PPh}_2)_3\text{O}]_2\text{Sn}\}$	Double cube	–467.7	–	[175]
26	$\{[n\text{-BuSn}(\text{OH})\text{O}_2\text{PPh}_2]_3\text{O}\}[\text{Ph}_2\text{PO}_2]$	O-capped	–498.5 (132.0 Hz) ^g	2.128, 2.070	[170]
27	$\{[n\text{-BuSn}(\text{OH})\text{O}_2\text{P}(\text{OPh})_2]_3\text{O}\}[\text{O}_2\text{P}(\text{OPh})_2]$	O-capped	–508.8 (189.2 Hz) ^g	–	[169]
28	$\{[n\text{-BuSn}(\text{OH})\text{O}_2\text{P}(\text{C}_6\text{H}_{11})_2]_3\text{O}\}[(\text{C}_6\text{H}_{11})_2\text{PO}_2]$	O-capped	–499.5 (128.0 Hz) ^g	–	[172]
29	$\{[\text{Sn}(\text{CH}_2\text{Ph})(\text{OH})\text{O}_2\text{P}(\text{C}_6\text{H}_{11})_2]_3\text{O}\}[\text{O}_2\text{P}(\text{C}_6\text{H}_{11})_2]$	O-capped	–535.7	–	[137]
30	$\{[n\text{-BuSn}(\text{OH})\text{O}_2\text{P}(\text{C}_6\text{H}_{11})_2]_3\text{O}\}[\{n\text{-BuSnCl}_2\text{O}_2\text{P}(\text{C}_6\text{H}_{11})_2\}_2\text{OH}]$	O-capped	–517.3, –525.8	–	[176]
31	$\{[n\text{-BuSn}(\text{OH})\text{O}_2\text{PMes}_2]_3\text{O}\}\text{Cl}$	O-capped	–509.99	–	[176]
32	$\{[n\text{-BuSn}(\text{OH})\text{O}_2\text{P}(\text{C}_6\text{H}_{11})_2]_2\}_2$	Butterfly	–547.4 (128.0 Hz) ^h ; 182.0 Hz) ⁱ	2.088	[172]
33	$[(n\text{-Bu})_2\text{Sn}_2\text{O}\{(t\text{-Bu})\text{P}(\text{OH})(\text{O})_2\}_4]_2$	Tetrameric cage	–630.4 (239.2, 286.5 Hz) ⁱ	2.094	[173]
34	$[(n\text{-Bu})_2\text{Sn}_2\text{Cl}_2(\text{OH})(\text{O}_2\text{PPh}_2)_3]_2 \cdot 2\text{CH}_2\text{Cl}_2$	Extended tetra nuclear cluster	–507.39; –615.36	2.112	[176]
35	$\{[n\text{-BuSn}(\text{O})\text{O}_2\text{P}(t\text{-Bu})_2]\{n\text{-BuSn}(\text{OH})_2\text{O}_2\text{P}(t\text{-Bu})_2\}_2[\text{H}][\text{O}_2\text{P}(t\text{-Bu})_2]\}$	Crown cluster	–535.3 ^j ; (181.0, 145.0 Hz)	2.086	[174]
36	$[(n\text{-Bu})_2\text{Sn}_2\text{OH}(\text{O}_2\text{PPh}_2)_3(\text{OSPPH}_2)_2]_2 \cdot 8\text{C}_6\text{H}_6$	Extended cluster	–575.0, –614.0	2.080	[174]
37	$\{[n\text{-BuSn}(\text{OH})\text{O}_2\text{P}(t\text{-Bu})_2]_4\text{O}_2\}[\text{H}][\text{Cl}][n\text{-BuSn}(\text{Cl})(\text{OH})\text{O}_2\text{P}(t\text{-Bu})_2]_2$	Crown-butterfly cluster	–499, –533.2	2.103	[176]

^a Chemical shift of five-coordinate tin.^b Chemical shift of six-coordinate tin.^c Average value of $\text{Sn}_{\text{penta coordinate}}\text{-O}$.^d Average value of $\text{Sn}_{\text{hexacoordinate}}\text{-O}$.^e Average value of $\text{Sn}_{\text{hexacoordinate}}\text{-OH}$.^f The chemical shifts of these drum structures are upfield shifted in comparison with $[n\text{-BuSn}(\text{O})\text{O}_2\text{CR}]_6$.^g Doublet; $^2J(^{119}\text{Sn}\text{-O-}^{31}\text{P})$.^h Doublet of triplets; $^2J(^{119}\text{Sn}\text{-O-}^{31}\text{P})$.ⁱ Triplet of triplets; $^2J(^{119}\text{Sn}\text{-O-}^{31}\text{P})$.^j Doublet of doublets; $^2J(^{119}\text{Sn}\text{-O-}^{31}\text{P})$.

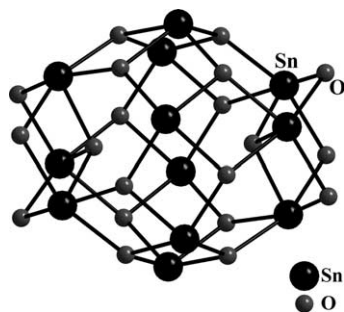


Fig. 67. The X-ray structure of $[(n\text{-BuSn})_{12}(\mu_2\text{-OH})_6(\mu_3\text{-O})_{14}[4\text{-CH}_3\text{-C}_6\text{H}_4\text{-SO}_3]_2\cdot\text{dioxan}]$ showing the Sn–O core (only the dodeca-nuclear unit is shown. All the alkyl groups have been omitted) [161].

butterfly, *O*-capped cluster, crown cluster, extended cluster, double cube and tetrameric cage (Schemes 11 and 12) (Figs. 70, 72–78). The ladder form has not been isolated in any of these reactions. The formation of these cluster compounds seems to be regulated by an extremely subtle balance of factors such as stoichiometry of reactants, nature of R group on phosphorus and other reaction conditions (Schemes 11 and 12). Thus, while the 1:1 reaction of $\text{RSn}(\text{O})\text{OH}$ with diphenyl phosphate $(\text{OPh})_2\text{P}(\text{O})(\text{OH})$ leads to a drum $[n\text{-BuSn}(\text{O})\text{O}_2\text{-P}(\text{OPh})_2]_6$ [169] the corresponding reaction with *t*- $\text{Bu}_2\text{P}(\text{O})\text{OH}$ or $(c\text{-Hex})_2\text{P}(\text{O})(\text{OH})$ leads to the formation of the tetrameric cube $[n\text{-BuSn}(\text{O})\text{O}_2\text{PR}_2]_4$ [171,172]. Similarly while a 3:4 reaction between the $\text{RSn}(\text{O})\text{OH}$ and $\text{Ph}_2\text{P}(\text{O})\text{OH}$ leads to the *O*-capped cluster $[\{n\text{-BuSn}(\text{OH})\text{O}_2\text{PPh}_2\}\text{O}][\text{Ph}_2\text{PO}_2]$ [170]. On the other hand a 1:2 reaction between $\text{RSn}(\text{O})\text{OH}$ and

$(c\text{-Hex})_2\text{P}(\text{O})\text{OH}$ leads to the dimeric butterfly $[n\text{-BuSn}(\text{OH})\text{O}_2\text{P}(c\text{-Hex})_2]_2$ [172]. Sn–C bond scission reactions can also be taken advantage in the assembly of some of these compounds. Thus, an *O*-capped cluster $[\{C_6H_5CH_2Sn(\text{OH})\text{O}_2\text{P}(c\text{-Hex})_2\}\text{O}][c\text{-Hex}_2\text{PO}_2]$ has been prepared in the reaction of dibenzyltin dichloride with the silver salt of dicyclohexylphosphinic acid in presence of moisture [137]. More recently it has been reported that the reaction of thiamine diphosphate hydrochloride reacts with methylphenyltin dichloride to afford an *O*-capped cluster by the scission of the Sn–Ph bond (Fig. 81) [178].

Many of these clusters can be rearranged into each other. Some of the prominent interconversions are summarized in Schemes 13 and 14.

4.4. Other stannoxanes

The reaction of $n\text{-BuSnCl}_3$ with the sodium salt of 2-mercaptoethanol affords a new type of trinuclear spirostannoxane (Fig. 82) [179]. The X-ray structure of the spirostannoxane reveals that two five-coordinated stannolanes are fused to a central $n\text{-BuSnCl}$ moiety. In the resulting compound the central tin is six-coordinate while the outer tins are five-coordinate (Fig. 83). This structure is retained in solution; ^{119}Sn -NMR shows signals at -39.04 and -42.6 ppm for the outer tins while a signal at -447.00 ppm is observed for the central tin. On the other hand reaction of *n*-butyl stannonic acid with mercaptoethanol affords a stanno-

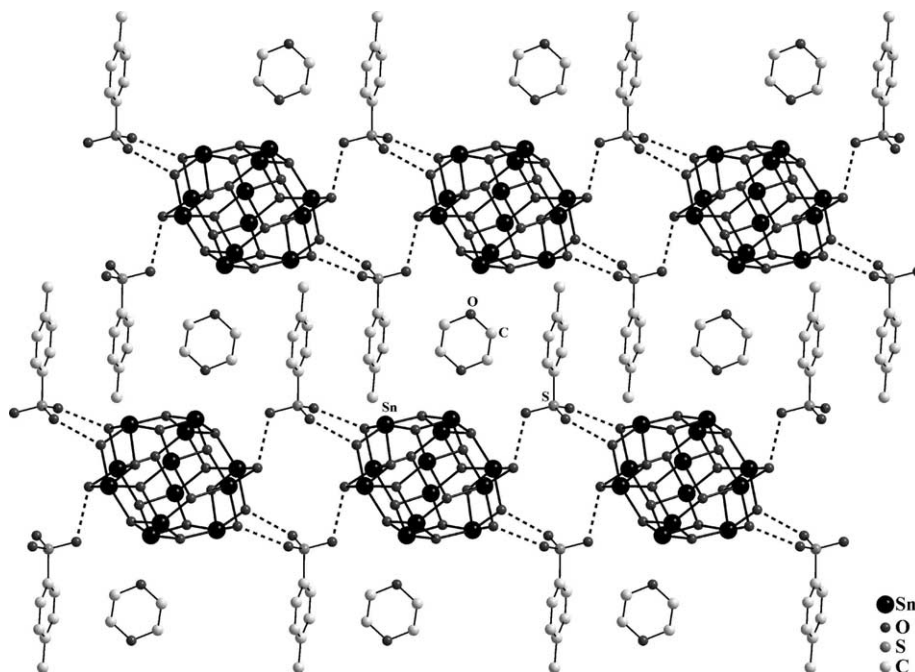
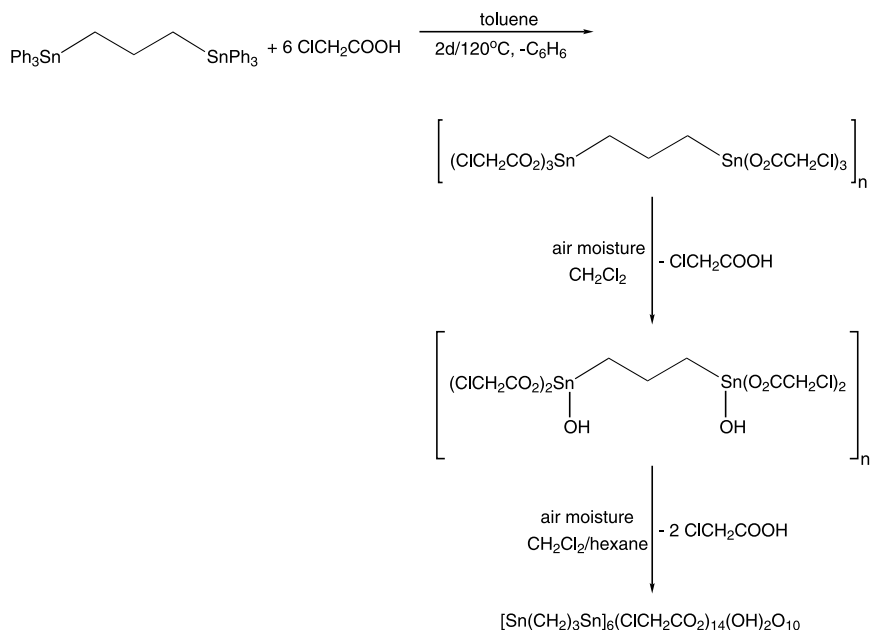


Fig. 68. Polymeric sheet formation as a result of $[p\text{-CH}_3\text{-C}_6\text{H}_4\text{-SO}_3]^-$ interaction with bridging hydroxyl groups in $[(n\text{-BuSn})_{12}(\mu_2\text{-OH})_6(\mu_3\text{-O})_{14}[4\text{-CH}_3\text{-C}_6\text{H}_4\text{-SO}_3]_2\cdot\text{dioxan}]$ [161].



Scheme 10.

lane $[n\text{-BuSn}(\text{SCH}_2\text{CH}_2\text{O})(\text{SCH}_2\text{CH}_2\text{OH})]$, which is dimeric in the solid-state as a result of intermolecular interactions (Fig. 84). The structural principles involved in the above stannolanes are analogous to ones established by Holmes and coworkers in their earlier work on five and six-coordinated tin compounds [180,181].

5. Conclusions

In conclusion it may be stated that the amazing structural diversity of the multi-tin assemblies derived from various organotin precursors will continue to

dominate this area of research. The distannoxane motif is ubiquitous in many of these structural types. However, in spite of the impressive cluster types known even simple compounds such as $\text{R}_2\text{Sn}(\text{OH})_2$ and $\text{RSn}(\text{OH})_3$ are non-existent. Kinetic stabilization of these compounds is clearly an attractive synthetic challenge. Further, in spite of the number of clusters that are known the understanding behind their formation in terms of reaction mechanisms is at a rudimentary level. Unless this is addressed discovery of new cluster types will be a matter of chance rather than on sound chemical principles. Hopefully this aspect will receive the attention it deserves in the coming years.

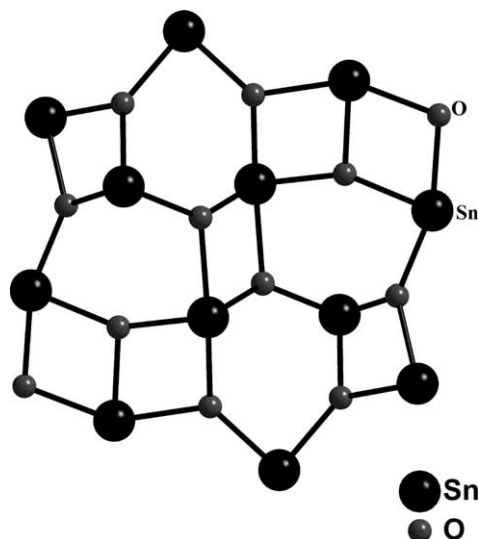
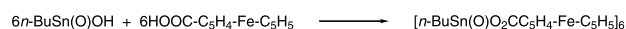
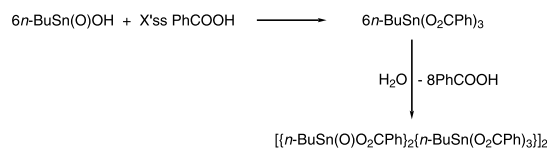


Fig. 69. X-ray structure showing the Sn–O core of $[\{\text{Sn}(\text{CH}_2)_3\text{Sn}\}_6(\text{ClCH}_2\text{CO}_2)_{14}(\text{OH})_2\text{O}_{10}]$ [164].

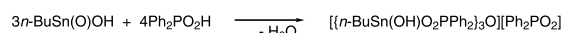
1. Drum



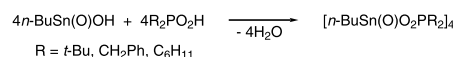
2. Ladder



3. O - Capped Cluster

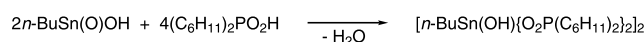


4. Cube

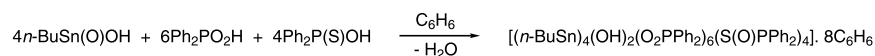


Scheme 11.

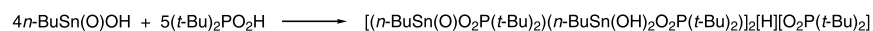
5. Butterfly



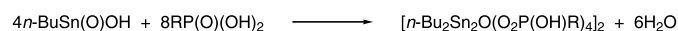
6. Extended Cluster



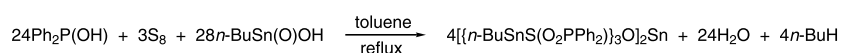
7. Crown Cluster



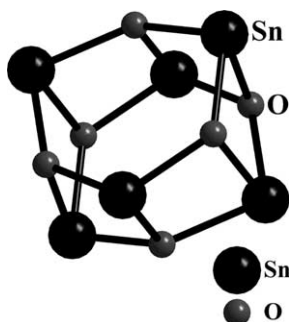
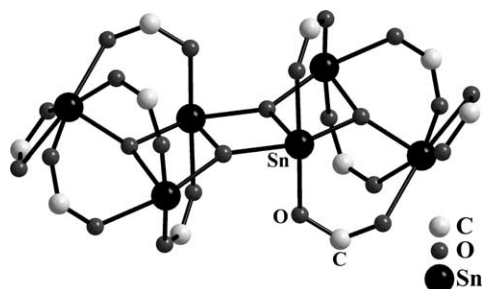
8. Tetrameric Cage



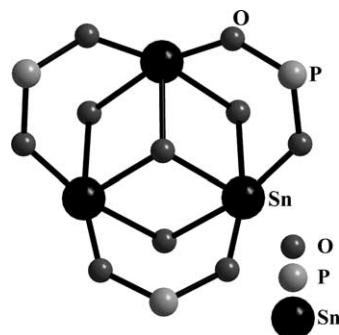
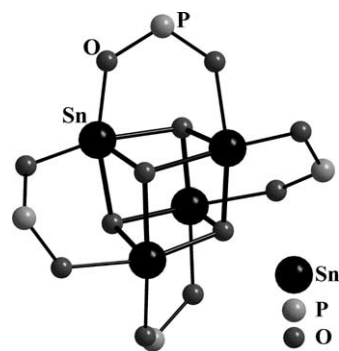
9. Double Cube



Scheme 12.

Fig. 70. The *drum* type Sn–O core found in $[n\text{-BuSn(O)O}_2\text{CC}_5\text{H}_4\text{-FeC}_5\text{H}_5]_6$ [167].Fig. 71. The X-ray structure of $[\{(\text{PhCH}_2)\text{Sn(O)O}_2\text{CMe}\}_2\{(\text{PhCH}_2)\text{Sn(O}_2\text{CMe)}_3\}]_2$ showing the *ladder* type of structure (the alkyl groups on tin and on the carboxylate carbon have been omitted) [137].

The possibility of preparing nanomaterials starting from molecular organotin precursors is likely to attract considerable interest in the years to come. Another area that is very nascent at the moment, but likely to blossom, is the utilization of the stannoxane cores as scaffolds for varied applications such as the construction of multi-site coordination ligands or as supports for redox-active substituents.

Fig. 72. The X-ray structure of $[\{(\text{PhCH}_2)\text{Sn(OH)}(\text{O}_2\text{P-C}_6\text{H}_{11})_3\text{O}\}[\text{O}_2\text{P}(\text{C}_6\text{H}_{11})_2]]$. The trinuclear cation with the *O-capped* structural form is shown (all the alkyl substituents on tin and phosphorus have been omitted) [137].Fig. 73. The X-ray structure of $[n\text{-BuSn(O)O}_2\text{P}(\text{CH}_2\text{Ph})_2]_4$ showing the *cube* form (the alkyl substituents on tin and phosphorus have been omitted) [172].

The application of organotin compounds containing Sn–O bonds in the catalysis of organic reactions such as trans-esterification is receiving wide spread attention. However, only a small fraction of organotin compounds

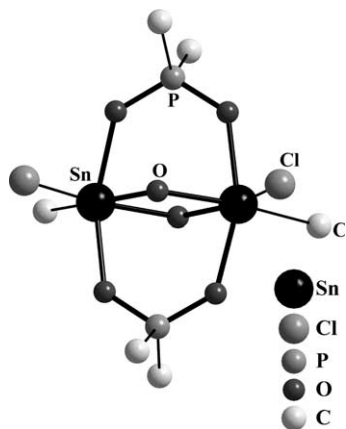


Fig. 74. The X-ray structure of the *butterfly cluster*, $[\{n\text{-BuSn}(\text{O}-\text{H})\text{O}_2\text{P}(t\text{-Bu})_2\}_4][\text{H}^+][\text{Cl}^-][n\text{-BuSn}(\text{OH})(\text{Cl})\text{O}_2\text{P}(t\text{-Bu})_2]_2$. The dinuclear core is shown (the alkyl substituents on tin and phosphorus are shown as single atom) [176].

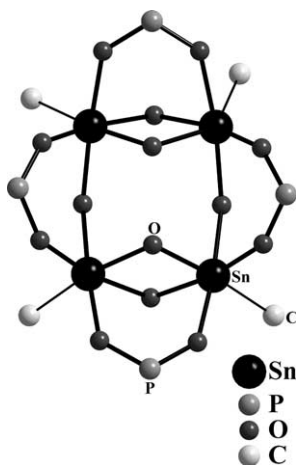


Fig. 75. The X-ray structure of a *crown-cluster* $[\{n\text{-BuSn}(\text{OH})\text{O}_2\text{P}(t\text{-Bu})_2\}_4\text{O}_2][\text{H}^+][\text{Cl}^-][n\text{-BuSn}(\text{OH})(\text{Cl})\text{O}_2\text{P}(t\text{-Bu})_2]_2$. The tetra-nuclear *crown core* is shown (the alkyl groups on tin have been shown as single atoms. The alkyl groups on phosphorus have been omitted) [176].

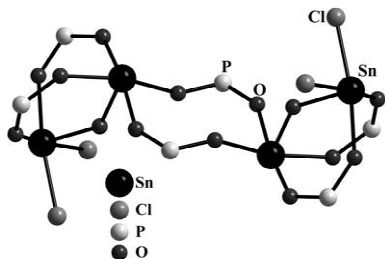


Fig. 76. The X-ray structure of $[n\text{-Bu}_2\text{Sn}_2\text{Cl}_2(\text{OH})\text{O}_2\text{PPh}_2]_3$ showing the extended cluster form (the alkyl groups on tin and phosphorus have been omitted) [176].

have been tested for their utility. Clearly there is considerable scope in this area in terms of utilizing many other types of organotin compounds as well as

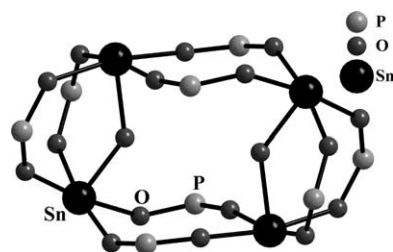


Fig. 77. The X-ray structure of $[n\text{-Bu}_2\text{Sn}_2\text{O}\{\text{O}_2\text{P}(\text{OH})-t\text{-Bu}\}_4]_2$ showing the tetrameric cage cluster (all the alkyl groups on tin and phosphorus have been omitted for clarity) [173].

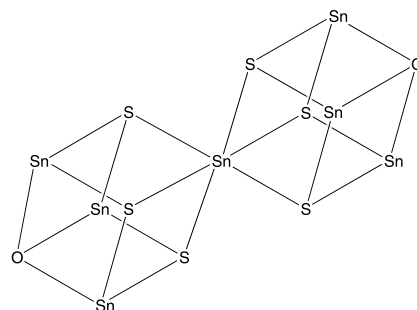


Fig. 78. Frame work of the double-cube $(\text{Sn}_3\text{S}_3\text{O})_2\text{Sn}$ as found in $[\{n\text{-BuSnS}(\text{O}_2\text{PPh}_2)_3\text{O}\}_2]_2$ [175].

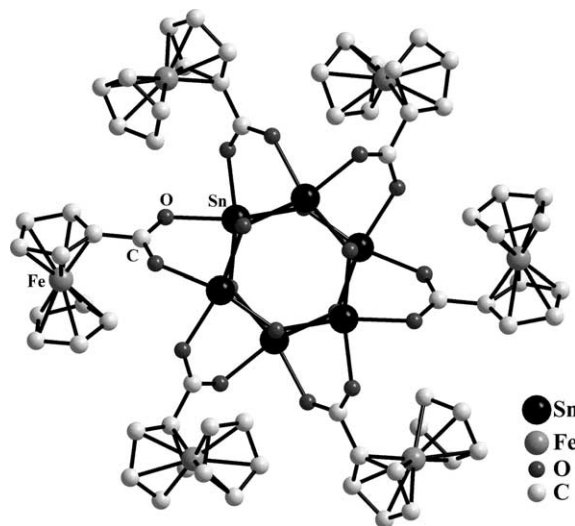


Fig. 79. The X-ray structure of $[n\text{-BuSn}(\text{O})\text{O}_2\text{CC}_5\text{H}_4\text{-Fe-C}_5\text{H}_5]_6$ showing the ferrocenes arranged in a wheel-like manner around the Sn–O framework (the alkyl groups on tin have been omitted) [167].

discovery of new reactions that can be mediated by organotin catalysts.

The biological applications of organotin compounds are receiving a good deal of attention. Most of the focus in recent years appears to be on the possible use of tri- and diorganotin compounds as anti-tumor drugs. One

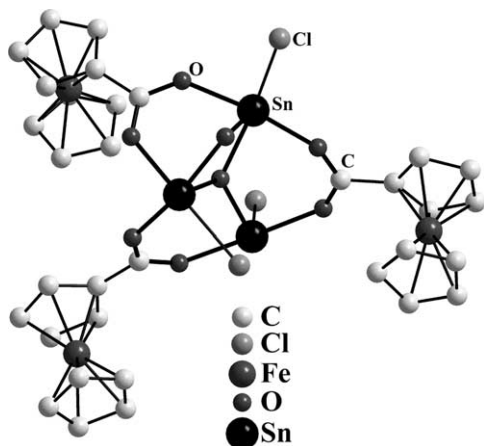


Fig. 80. The X-ray structure of $[\{ n\text{-BuSn}(\text{Cl})(\text{O}_2\text{CC}_5\text{H}_4\text{-Fe-C}_5\text{H}_5) \}_3(\text{O})(\text{OH})]$ (the alkyl groups on tin have been omitted) [146].

of the stumbling blocks in this endeavor appears to be the lack of solubility of many potential drug-candidates in aqueous medium. There is considerable scope for good synthetic designs for the assembly of such water-soluble organotin compounds. This would allow thorough in vivo studies to be made so that new drug discovery based on organotin compounds is possible.

Acknowledgements

We are thankful to the Department of Science and Technology, New Delhi for financial support. We are also thankful to the Council of Scientific and Industrial Research, New Delhi for a Senior Research Fellowship to one of us (SN).

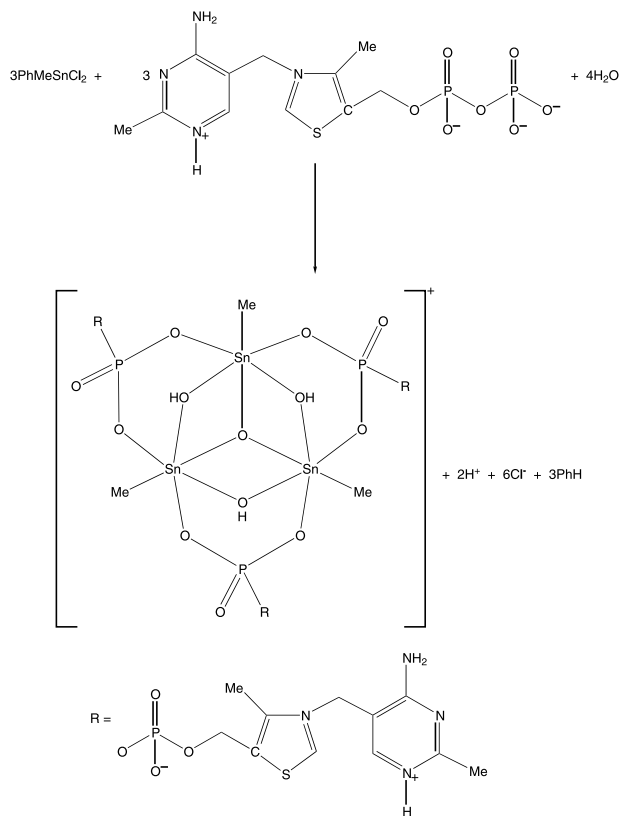
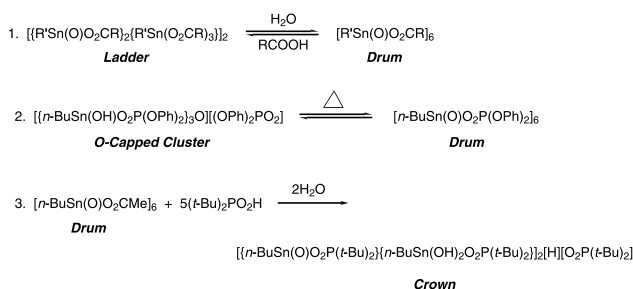
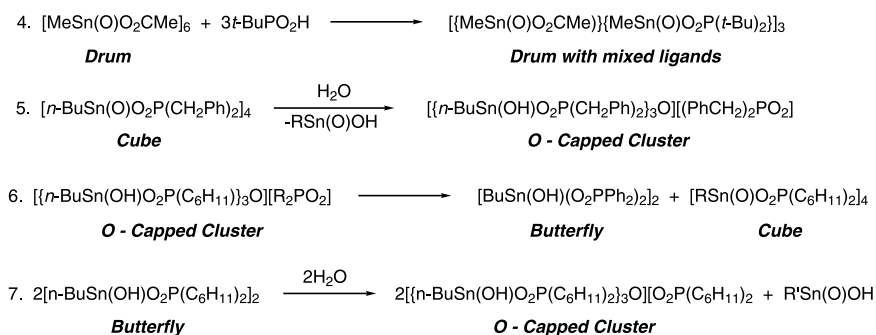


Fig. 81. The formation of an *O*-capped cluster from the dearylation reaction of PhMeSnCl_2 with thiamine diphosphate hydrochloride [178].



Scheme 13.



Scheme 14.

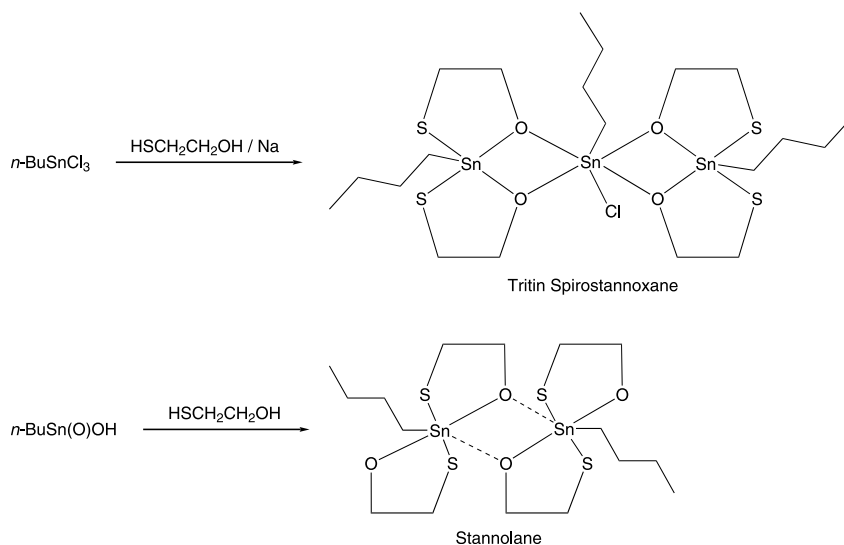


Fig. 82. Formation of spirostannoxane and stannolane from the reaction of monoorganotin precursors [179].

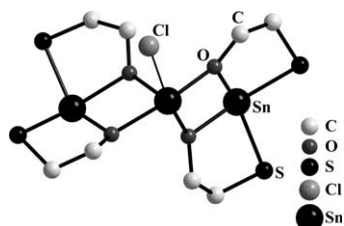


Fig. 83. The X-ray structure of $[n\text{-BuSn(Cl)}]\{(\text{OCH}_2\text{CH}_2\text{S})_2\text{Sn}(n\text{-Bu})\}_2$ showing the spirostannoxane structure (the alkyl groups on tin have been omitted) [179].

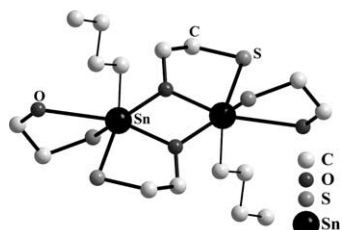


Fig. 84. The X-ray structure of the stannolane, $n\text{-BuSn}(\text{SCH}_2\text{CH}_2\text{O})(\text{SCH}_2\text{CH}_2\text{OH})$. The formation of the distannoxane ring as a result of intermolecular Sn–O interaction is shown [179].

References

- [1] Y. Arakawa, in: P.J. Smith (Ed.), *Chemistry of Tin*, Blackie Academic and Professional, London, 1998, p. 388.
- [2] F. Novelli, M. Recine, F. Sparatore, C. Juliano, *II Farmaco* 54 (1999) 237.
- [3] J.M. Barnes, L. Magos, *Organomet. Chem. Rev.* 3 (1968) 137.
- [4] C.J. Evans, in: P.J. Smith (Ed.), *Chemistry of Tin*, Blackie Academic and Professional, London, 1998, p. 442.
- [5] M. Gielen, *Coord. Chem. Rev.* 151 (1996) 41.
- [6] R. Willem, H. Dalil, P. Broekaert, M. Biesemans, L. Ghys, K. Nooter, D. de Vos, F. Ribot, M. Gielen, *Main Group Met. Chem.* 20 (1997) 535.
- [7] D. de Vos, R. Willem, M. Gielen, K.E. van Wingerden, K. Nooter, *Met. Based Drugs* 5 (1998) 179.
- [8] M. Kemmer, M. Gielen, M. Biesemans, D. de Vos, R. Willem, *Met. Based Drugs* 5 (1998) 189.
- [9] B. Jousseume, M. Pereyre, in: P.J. Smith (Ed.), *Chemistry of Tin*, Blackie Academic and Professional, London, 1998, p. 290.
- [10] A. Orita, A. Mitsutome, J. Otera, *J. Org. Chem.* 63 (1998) 2420.
- [11] Y. Hori, T. Hagiwara, *Int. J. Biol. Macromol.* 25 (1999) 237.
- [12] A. Orita, K. Sakamoto, Y. Hamada, A. Mitsutome, J. Otera, *Tetrahedron* 55 (1999) 2899.
- [13] J. Otera, *Chem. Rev.* 93 (1993) 1449.
- [14] S. Durand, K. Sakamoto, T. Fukuyama, A. Orita, J. Otera, A. Duthie, D. Dakternieks, M. Schulte, K. Jurkschat, *Organometallics* 19 (2000) 3220.
- [15] A. Orita, Y. Hamada, T. Nakano, S. Toyoshima, J. Otera, *Chem. Eur. J.* 7 (2001) 3321.
- [16] R.R. Holmes, *Acc. Chem. Res.* 22 (1989) 190.
- [17] J. Beckmann, K. Jurkschat, *Coord. Chem. Rev.* 215 (2001) 267.
- [18] V.K. Jain, *Coord. Chem. Rev.* 135/136 (1994) 809.
- [19] V. Chandrasekhar, M.G. Muralidhara, *Curr. Sci.* 60 (1991) 158.
- [20] E.R.T. Tiekink, *Appl. Organomet. Chem.* 5 (1991) 1.
- [21] E.R.T. Tiekink, *Trends Organomet. Chem.* 1 (1994) 71.
- [22] R.R. Holmes, *Phosphorus Sulfur Silicon Relat. Elem.* 150–151 (1991) 1.
- [23] R.R. Holmes, R.O. Day, V. Chandrasekhar, C.G. Schmid, K.C. Kumara Swamy, J.M. Holmes, in: M. Zeldin, K.J. Wynne, H.R. Allcock (Eds.), *Inorganic and Organometallic Polymers*, American Chemical Society, Washington DC, 1988, p. 469.
- [24] R.C. Poller, *The Chemistry of Organotin Compounds*, Logos Press Ltd, London, 1970, p. 272.
- [25] P.J. Smith, *Chemistry of Tin*, Blackie Academic and Professional, London, 1998.
- [26] P.G. Harrison, *Chemistry of Tin*, Blackie and Son Ltd, Glasgow, 1989.
- [27] A.G. Davies, *Organotin Chemistry*, Wiley VCH, Weinheim, 1997.
- [28] K. Brandenburg, *Diamond version 2.1c*, Crystal Impact GbR, 1999.
- [29] Cambridge Crystallographic Data Centre, 12 Union Road, Cambridge CB2 1EZ, UK (fax: (+44) 1223-336-033; e-mail: deposit@ccdc.cam.ac.uk).
- [30] K.C. Molloy, in: P.J. Smith (Ed.), *Chemistry of Tin*, Blackie Academic and Professional, London, 1998, p. 138.
- [31] J.B. Hall, D. Britton, *Acta Crystallogr. Sect. B* 28 (1972) 2133.
- [32] C. Glidewell, D.C. Liles, *Acta Crystallogr. Sect. B* 34 (1978) 129.

- [33] A.G. Domingos, G.M. Sheldrick, *Acta Crystallogr. Sect. B* 30 (1974) 519.
- [34] H. Reuter, D. Schröder, *Acta Crystallogr. Sect. C* 49 (1993) 83.
- [35] M. Gielen, K. Jurkschat, *J. Organomet. Chem.* 273 (1984) 303.
- [36] J. Beckmann, K. Jurkschat, M. Schürmann, *J. Organomet. Chem.* 626 (2001) 49.
- [37] B. Rake, P. Müller, H.W. Roesky, I. Usón, *Angew. Chem. Int. Ed. Engl.* 38 (1999) 2050.
- [38] L. Angiolini, M. Biesemans, D. Caretti, E. Salatelli, R. Willem, *Polymer* 41 (2000) 3913.
- [39] V. Chandrasekhar, M.G. Muralidhara, K.R. Justin Thomas, E.R.T. Tiekink, *Inorg. Chem.* 31 (1992) 4707.
- [40] P.J. Smith, R.O. Day, V. Chandrasekhar, J.M. Holmes, R.R. Holmes, *Inorg. Chem.* 25 (1986) 2495.
- [41] B.Y.K. Ho, K.C. Molloy, J.J. Zuckerman, *J. Organomet. Chem.* 187 (1980) 213.
- [42] S.W. Ng, K.L. Chin, C. Wei, V.G. Kumar Das, T.C.W. Mak, *J. Organomet. Chem.* 365 (1989) 207.
- [43] M. Gielen, A.E. Khloufi, M. Biesemans, F. Kayser, R. Willem, B. Mahieu, D. Maes, J.N. Lisgarten, L. Wyns, A. Moreira, T.K. Chattopadhyay, R.A. Palmer, *Organometallics* 13 (1994) 2849.
- [44] S.W. Ng, V.G.K. Das, G. Pelizzi, F. Vitali, *Heteroat. Chem.* 1 (1990) 433.
- [45] K.C. Molloy, F.A.K. Nasser, C.L. Barnes, D. van der Helm, J.J. Zuckerman, *Inorg. Chem.* 21 (1982) 960.
- [46] R. Willem, I. Verbruggen, M. Gielen, M. Biesemans, B. Mahieu, T.S.B. Baul, E.R.T. Tiekink, *Organometallics* 17 (1998) 5758.
- [47] M.J. Begley, D.B. Sowerby, P. Kapoor, R. Kapoor, *Polyhedron* 14 (1995) 1937.
- [48] R. Willem, A. Bouhdid, M. Biesemans, J.C. Martins, D. de Vos, E.R.T. Tiekink, M. Gielen, *J. Organomet. Chem.* 514 (1996) 203.
- [49] R. Willem, A. Bouhdid, B. Mahieu, L. Ghys, M. Biesemans, E.R.T. Tiekink, D. de Vos, M. Gielen, *J. Organomet. Chem.* 531 (1997) 151.
- [50] P.G. Harrison, K. Lambert, T.J. King, B. Majee, *J. Chem. Soc. Dalton Trans.* (1983) 363.
- [51] R.G. Swisher, J.F. Vollano, V. Chandrasekhar, R.O. Day, R.R. Holmes, *Inorg. Chem.* 23 (1984) 3147.
- [52] J.F. Vollano, R.O. Day, D.N. Rau, V. Chandrasekhar, R.R. Holmes, *Inorg. Chem.* 23 (1984) 3153.
- [53] R.R. Holmes, R.O. Day, V. Chandrasekhar, J.F. Vollano, J.M. Holmes, *Inorg. Chem.* 25 (1986) 2490.
- [54] C. Pettinari, F. Marchetti, R. Pettinari, D. Martini, A. Drozdov, S. Troyanov, *J. Chem. Soc. Dalton Trans.* (2001) 1790.
- [55] S. Calogero, P. Ganis, V. Peruzzo, G. Tagliavini, *J. Organomet. Chem.* 191 (1980) 381.
- [56] M. Kemmer, L. Ghys, M. Gielen, M. Biesemans, E.R.T. Tiekink, R. Willem, *J. Organomet. Chem.* 582 (1999) 195.
- [57] P.G. Harrison, in: P.J. Smith (Ed.), *Chemistry of Tin*, Blackie Academic and Professional, London, 1998, p. 10.
- [58] J.E. Huheey, E.A. Keiter, R.L. Keiter, *Inorganic Chemistry: Principles of Structure and Reactivity*, 4th ed., Harper Collins College Publishers, New York, 1993, p. 292.
- [59] M. Danish, S. Ali, M. Mazhar, A. Badshah, M.I. Choudhary, H.G. Alt, G. Kehr, *Polyhedron* 14 (1995) 3115.
- [60] K.C. Molloy, S.J. Blimden, R. Hill, *J. Chem. Soc. Dalton Trans.* (1988) 1259.
- [61] M. Danish, H.G. Alt, A. Badshah, S. Ali, M. Mazhar, N.U. Islam, *J. Organomet. Chem.* 486 (1995) 51.
- [62] M.G. Muralidhara, V. Chandrasekhar, *Indian J. Chem. Sect. A* 30 (1991) 487.
- [63] C.H. Yoder, R.A. Morreall, C.I. Butoi, W.J. Kowalski, J.N. Spencer, *J. Organomet. Chem.* 448 (1993) 59.
- [64] S.W. Ng, C. Wei, V.G.K. Das, *J. Organomet. Chem.* 345 (1988) 59.
- [65] P.G. Harrison, R.C. Philips, *J. Organomet. Chem.* 182 (1979) 37.
- [66] S.W. Ng, A.J. Kuthubutheen, V.G. Kumar Das, A. Linden, E.R.T. Tiekink, *Appl. Organomet. Chem.* 8 (1994) 37.
- [67] T.S.B. Baul, S.M. Pyke, K.K. Sharma, E.R.T. Tiekink, *Main Group Met. Chem.* 19 (1996) 807.
- [68] N.W. Alcock, S.M. Roe, *J. Chem. Soc. Dalton Trans.* (1989) 1589.
- [69] S.W. Ng, V.G. Kumar Das, *Main Group Met. Chem.* 16 (1993) 81.
- [70] M. Gielen, M. Biesemans, D. de Vos, R. Willem, *J. Inorg. Biochem.* 79 (2000) 139.
- [71] V. Chandrasekhar, S. Nagendran, R. Boomishankar, R.J. Butcher, *Inorg. Chem.* 40 (2001) 940.
- [72] R.K. Harris, A. Sebal, *J. Organomet. Chem.* 331 (1987) C9.
- [73] M.A. Edelman, P.B. Hitchcock, M.F. Lappert, *Chem. Commun.* 1 (1990) 1116.
- [74] V.K. Belsky, N.N. Zemlyansky, I.V. Borisova, N.D. Kolosova, I.P. Beletskaya, *J. Organomet. Chem.* 254 (1983) 189.
- [75] H. Puff, W. Schuh, R. Sievers, R. Zimmer, *Angew. Chem. Int. Ed. Engl.* 20 (1981) 591.
- [76] H. Puff, W. Schuh, R. Sievers, W. Wald, R. Zimmer, *J. Organomet. Chem.* 260 (1984) 271.
- [77] S. Masamune, L.R. Sita, D.J. Williams, *J. Am. Chem. Soc.* 105 (1983) 630.
- [78] U. Weber, N. Pauls, W. Winter, H.B. Stegmann, *Z. Naturforsch. Teil. B* 37 (1982) 1316.
- [79] H. Grützmaier, H. Pritzkow, *Chem. Ber.* 126 (1993) 2409.
- [80] L. King, A.C. Sullivan, *Coord. Chem. Rev.* 189 (1999) 19.
- [81] B. Zobel, M. Schürmann, K. Jurkschat, D. Dakternieks, A. Duthie, *Organometallics* 17 (1998) 4096.
- [82] D.L. Alleston, A.G. Davies, M. Hancock, M.F.R. White, *J. Chem. Soc.* (1963) 5469.
- [83] C.K. Chu, J.D. Murray, *J. Chem. Soc. Sect. A* (1971) 360.
- [84] J.F. Vollano, R.O. Day, R.R. Holmes, *Organometallics* 3 (1984) 745.
- [85] J. Beckmann, M. Biesemans, K. Hassler, K. Jurkschat, J.C. Martins, M. Schürmann, R. Willem, *Inorg. Chem.* 37 (1998) 4891.
- [86] M. Schulte, M. Schürmann, D. Dakternieks, K. Jurkschat, *Chem. Commun.* (1999) 1291.
- [87] H. Puff, I. Bung, E. Friedrichs, A. Jansen, *J. Organomet. Chem.* 254 (1983) 23.
- [88] P.G. Harrison, M.J. Begley, K.C. Molloy, *J. Organomet. Chem.* 186 (1980) 213.
- [89] D.L. Alleston, A.G. Davies, M. Hancock, *J. Chem. Soc.* (1964) 5745.
- [90] Y. Maeda, R. Okawara, *J. Organomet. Chem.* 10 (1967) 247.
- [91] D.C. Gross, *Inorg. Chem.* 28 (1989) 2355.
- [92] D. Dakternieks, K. Jurkschat, S. van Dreumel, E.R.T. Tiekink, *Inorg. Chem.* 36 (1997) 2023.
- [93] O. Primel, M.-F. Llauro, R. Pétiaud, A. Michel, *J. Organomet. Chem.* 558 (1998) 19.
- [94] D.L. Tierney, P.J. Moehs, D.L. Hasha, *J. Organomet. Chem.* 620 (2001) 211.
- [95] D.L. Hasha, *J. Organomet. Chem.* 620 (2001) 296.
- [96] M. Mehring, M. Schürmann, I. Paulus, D. Horn, K. Jurkschat, A. Orita, J. Otera, D. Dakternieks, A. Duthie, *J. Organomet. Chem.* 574 (1999) 176.
- [97] D. Dakternieks, K. Jurkschat, D. Schollmeyer, H. Wu, *Organometallics* 13 (1994) 4121.
- [98] M. Mehring, I. Paulus, B. Zobel, M. Schürmann, K. Jurkschat, A. Duthie, D. Dakternieks, *Eur. J. Inorg. Chem.* (2001) 153.
- [99] M. Mehring, M. Schürmann, H. Reuter, D. Dakternieks, K. Jurkschat, *Angew. Chem. Int. Ed. Engl.* 36 (1997) 1112.
- [100] K. Sakamoto, Y. Hamada, H. Akashi, A. Orita, J. Otera, *Organometallics* 18 (1999) 3555.
- [101] K. Sakamoto, H. Ikeda, H. Akashi, T. Fukuyama, A. Orita, J. Otera, *Organometallics* 19 (2000) 3242.

- [102] A. Orita, J. Xiang, K. Sakamoto, J. Otera, *J. Organomet. Chem.* 624 (2001) 287.
- [103] A. Orita, K. Sakamoto, H. Ikeda, J. Xiang, J. Otera, *Chem. Lett.* (2001) 40.
- [104] H. Puff, H. Hevendehl, K. Höfer, H. Reuter, W. Shuh, *J. Organomet. Chem.* 287 (1985) 163.
- [105] A.M. Domingos, G.M. Sheldrick, *J. Chem. Soc. Dalton Trans.* (1974) 475.
- [106] N. Kourkouvelis, A. Hatzidimitrou, D. Kovala-Demertzi, *J. Organomet. Chem.* 514 (1996) 163.
- [107] S.P. Narula, S. Kaur, R. Shankar, S. Verma, P. Venugopalan, S.K. Sharma, R.K. Chadha, *Inorg. Chem.* 38 (1999) 4777.
- [108] R. Kapoor, A. Gupta, P. Kapoor, P. Venugopalan, *J. Organomet. Chem.* 619 (2001) 157.
- [109] P. Brown, M.F. Mahon, K.C. Molloy, *J. Chem. Soc. Dalton Trans.* (1992) 3503.
- [110] M. Gielen, A. El Khoulfi, M. Biesemans, R. Willem, J. Meunier-Piret, *Polyhedron* 11 (1992) 1861.
- [111] S.G. Teoh, S.H. Ang, J.-P. Declercq, *Polyhedron* 16 (1997) 3729.
- [112] S.G. Teoh, S.H. Ang, E.S. Looi, C.A. Keok, S.B. Teo, J.-P. Declercq, *J. Organomet. Chem.* 523 (1996) 75.
- [113] V. Chandrasekhar, R.O. Day, J.M. Holmes, R.R. Holmes, *Inorg. Chem.* 27 (1988) 958.
- [114] M. Dansih, H.G. Alt, A. Badshah, S. Ali, M. Mazhar, N.U. Islam, *J. Organomet. Chem.* 486 (1995) 51.
- [115] M. Kemmer, H. Dalil, M. Biesemans, J.C. Martins, B. Mahieu, E. Horn, D. de Vos, E.R.T. Tiekink, R. Willem, M. Gielen, *J. Organomet. Chem.* 608 (2000) 63.
- [116] S.W. Ng, *J. Organomet. Chem.* 585 (1999) 12.
- [117] F. Mistry, S.J. Rettig, J. Trotter, F. Aubke, *Acta Crystallogr. Sect. C* 46 (1990) 2091.
- [118] M. Gielen, M. Bouâlam, E.R.T. Tiekink, *Main Group Met. Chem.* 16 (1993) 251.
- [119] T.P. Lockhart, F. Davidson, *Organometallics* 6 (1987) 2471.
- [120] S.W. Ng, W. Chen, A. Zainuddin, V.G. Kumar Das, W.H. Yip, R.J. Wang, T.C.W. Mak, *J. Crystallogr. Spectrosc. Res.* 21 (1991) 39.
- [121] T.P. Lockhart, J.C. Calabrese, F. Davidson, *Organometallics* 6 (1987) 2479.
- [122] S.W. Ng, V.G. Kumar Das, *J. Organomet. Chem.* 409 (1991) 143.
- [123] D. Kovala-Demertzi, N. Kourkouvelis, A. Koutsodimou, A. Moukarika, E. Horn, E.R.T. Tiekink, *J. Organomet. Chem.* 620 (2001) 194.
- [124] C. Vatsa, V.K. Jain, T. Keshavdas, E.R.T. Tiekink, *J. Organomet. Chem.* 408 (1991) 157.
- [125] E.R.T. Tiekink, M. Gielen, A. Bouhddid, M. Biesemans, R. Willem, *J. Organomet. Chem.* 494 (1995) 247.
- [126] M. Gielen, A. Bouhddid, R. Willem, V.I. Bregadze, L.V. Ermanson, E.R.T. Tiekink, *J. Organomet. Chem.* 501 (1995) 277.
- [127] S.P. Narula, S. Kaur, R. Shankar, S.K. Bharadwaj, R.K. Chadha, *J. Organomet. Chem.* 506 (1996) 181.
- [128] F. Ribot, C. Sanchez, A. Meddour, M. Gielen, E.R.T. Tiekink, M. Biesemans, R. Willem, *J. Organomet. Chem.* 552 (1998) 177.
- [129] V. Dokorou, Z. Ciunik, U. Russo, D. Kovala-Demertzi, *J. Organomet. Chem.* 630 (2001) 205.
- [130] S.W. Ng, C. Wei, V.G. Kumar Das, *J. Organomet. Chem.* 412 (1991) 39.
- [131] C. Vatsa, V.K. Jain, T.K. Das, E.R.T. Tiekink, *J. Organomet. Chem.* 418 (1991) 329.
- [132] R.G. Xiong, J.L. Zuo, Z.Z. You, H.K. Fun, S.S.S. Raj, *Organometallics* 19 (2000) 4183.
- [133] T.P. Lockhart, W.F. Manders, E.M. Holt, *J. Am. Chem. Soc.* 108 (1986) 6611.
- [134] S.G. Teoh, S.H. Ang, E.S. Looi, C.A. Keok, S.B. Teo, H.K. Fun, *J. Organomet. Chem.* 527 (1997) 15.
- [135] A.G. Davies, D.C. Kleinschmidt, P.R. Palan, S.C. Vasishta, *J. Chem. Soc.* (1971) 3972.
- [136] M. Gielen, H. Dalil, L. Ghys, B. Boduszek, E.R.T. Tiekink, J.C. Martins, M. Biesemans, R. Willem, *Organometallics* 17 (1998) 4259.
- [137] K.C. Kumara Swamy, M.A. Said, S. Nagabrahmanandachari, Damodara M. Poojary, A. Clearfield, *J. Chem. Soc. Dalton Trans.* (1998) 1645.
- [138] F. Ribot, C. Sanchez, M. Biesemans, F.A.G. Mercier, J.C. Martins, M. Gielen, R. Willem, *Organometallics* 20 (2001) 2593.
- [139] F. Kayser, M. Biesemans, M. Bouâlam, E.R.T. Tiekink, A.E. Khloufi, J.M. Piret, A. Bouhddid, K. Jurkschat, M. Gielen, R. Willem, *Organometallics* 13 (1994) 1098.
- [140] R. Willem, A. Bouhddid, F. Kayser, A. Delmotte, M. Gielen, J.C. Martins, M. Biesemans, B. Mahieu, E.R.T. Tiekink, *Organometallics* 15 (1996) 1920.
- [141] R. Willem, A. Bouhddid, A. Meddour, C. Camacho-Camacho, F. Mercier, M. Gielen, M. Biesemans, F. Ribot, C. Sanchez, E.R.T. Tiekink, *Organometallics* 16 (1997) 4377.
- [142] A. Meddour, F. Mercier, J.C. Martins, M. Gielen, M. Biesemans, R. Willem, *Inorg. Chem.* 36 (1997) 5712.
- [143] F.A.G. Mercier, A. Meddour, M. Gielen, M. Biesemans, R. Willem, E.R.T. Tiekink, *Organometallics* 17 (1998) 5933.
- [144] D.K. Dey, M.K. Saha, S. Mitra, R.K. Bansal, L. Dahlenburg, *Chem. Lett.* (2000) 1190.
- [145] R. Contreras, V.M.J. Perez, C. Camacho-Camacho, M.G. Rodriguez, B. Wrackmeyer, *J. Organomet. Chem.* 604 (2000) 229.
- [146] K.C. Kumara Swamy, S. Nagabrahmanandachari, K. Raghuraman, *J. Organomet. Chem.* 587 (1999) 132.
- [147] R. Murugavel, V. Chandrasekhar, A. Voigt, H.W. Roesky, H.-G. Schmidt, M. Noltemeyer, *Organometallics* 14 (1995) 5298.
- [148] R. Murugavel, V. Chandrasekhar, H.W. Roesky, *Acc. Chem. Res.* 29 (1996) 183.
- [149] G. Cerveau, R.J.P. Corriu, B. Dabiens, J. Le Bideau, *Angew. Chem. Int. Ed. Engl.* 39 (2000) 4533.
- [150] R.R. Holmes, S. Shafieezad, V. Chandrasekhar, J.M. Holmes, R.O. Day, *J. Am. Chem. Soc.* 110 (1988) 1174.
- [151] C. Le comte, C.L.J. Protas, M. Devaud, *Acta Crystallogr. Sect. B* 32 (1976) 923.
- [152] S.E. Johnson, C.B. Knobler, *Organometallics* 13 (1994) 4928.
- [153] H. Puff, H. Reuter, *J. Organomet. Chem.* 364 (1989) 57.
- [154] B. Zobel, A. Duthie, D. Dakternieks, E.R.T. Tiekink, *Organometallics* 20 (2001) 2820.
- [155] H. Puff, H. Reuter, *J. Organomet. Chem.* 368 (1989) 173.
- [156] H. Puff, H. Reuter, *J. Organomet. Chem.* 373 (1989) 173.
- [157] D. Dakternieks, H. Zhu, E.R.T. Tiekink, R. Colton, *J. Organomet. Chem.* 476 (1994) 33.
- [158] F. Banse, F. Ribot, P. Toledano, J. Maquet, C. Sanchez, *Inorg. Chem.* 34 (1995) 6371.
- [159] F. Ribot, C. Sanchez, R. Willem, J.C. Martins, M. Biesemans, *Inorg. Chem.* 37 (1998) 911.
- [160] C.E. Baron, F. Ribot, C. Sanchez, *J. Organomet. Chem.* 567 (1998) 137.
- [161] C.E. Baron, F. Ribot, N. Steunou, C. Sanchez, F. Fayon, M. Biesemans, J.C. Martins, R. Willem, *Organometallics* 19 (2000) 1940.
- [162] F. Ribot, F. Banse, F. Diter, C. Sanchez, *New J. Chem.* 19 (1995) 1145.
- [163] G. Kastner, H. Reuter, *J. Organomet. Chem.* 590 (2000) 381.
- [164] B. Zobel, J. Costin, B.R. Vincent, E.R.T. Tiekink, D. Dakternieks, *J. Chem. Soc. Dalton Trans.* (2000) 4021.
- [165] V. Chandrasekhar, R.O. Day, R.R. Holmes, *Inorg. Chem.* 24 (1985) 1970.
- [166] V. Chandrasekhar, C.G. Schmid, S.D. Burton, J.M. Holmes, R.O. Day, R.R. Holmes, *Inorg. Chem.* 26 (1987) 1050.

- [167] V. Chandrasekhar, S. Nagendran, S. Bansal, M.A. Kozee, D.R. Powell, *Angew. Chem. Int. Ed. Engl.* 39 (2000) 1833.
- [168] R.R. Holmes, C.G. Schmid, V. Chandrasekhar, R.O. Day, J.M. Holmes, *J. Am. Chem. Soc.* 109 (1987) 1408.
- [169] R.O. Day, V. Chandrasekhar, K.C. Kumara Swamy, J.M. Holmes, S.D. Burton, R.R. Holmes, *Inorg. Chem.* 27 (1988) 2887.
- [170] R.O. Day, J.M. Holmes, V. Chandrasekhar, R.R. Holmes, *J. Am. Chem. Soc.* 109 (1987) 940.
- [171] K.C. Kumara Swamy, R.O. Day, R.R. Holmes, *J. Am. Chem. Soc.* 109 (1987) 5546.
- [172] R.R. Holmes, K.C. Kumara Swamy, C.G. Schmid, R.O. Day, *J. Am. Chem. Soc.* 110 (1988) 7060.
- [173] K.C. Kumara Swamy, C.G. Schmid, R.O. Day, R.R. Holmes, *J. Am. Chem. Soc.* 112 (1990) 223.
- [174] K.C. Kumara Swamy, C.G. Schmid, R.O. Day, R.R. Holmes, *J. Am. Chem. Soc.* 110 (1988) 7067.
- [175] K.C. Kumara Swamy, R.O. Day, R.R. Holmes, *J. Am. Chem. Soc.* 110 (1988) 7543.
- [176] K.C. Kumara Swamy, R.O. Day, R.R. Holmes, *Inorg. Chem.* 31 (1992) 4184.
- [177] J. Caruso, M.J. Hampden-Smith, A.L. Rheingold, G. Yap, *Chem. Commun.* (1995) 157.
- [178] J.S. Casas, E.E. Castellano, M.D. Couce, M.S. García-Tasenda, A. Sánchez, J. Sordo, C. Taboada, E.M. Vázquez-López, *Inorg. Chem.* 40 (2001) 946.
- [179] R. Cea-Olivares, L.A. Gomez-Ortiz, V. Garcia-Montalvo, R.L. Gavino-Ramirez, S. Hernandez-Ortega, *Inorg. Chem.* 39 (2000) 2284.
- [180] R.R. Holmes, S. Shafieezad, V. Chandrasekhar, A.C. Sau, J.M. Holmes, R.O. Day, *J. Am. Chem. Soc.* 110 (1988) 1168.
- [181] R.O. Day, J.M. Holmes, S. Shafieezad, V. Chandrasekhar, R.R. Holmes, *J. Am. Chem. Soc.* 110 (1988) 5377.